THE ENDEMIC MARINE FISH FAUNA FROM THE EASTERN PARATETHYS RECONSTRUCTED FROM OTOLITHS FROM THE MIOCENE (MIDDLE SARMATIAN S.L.; BESSARABIAN) OF JURKINE (KERCH PENINSULA, CRIMEA)

ANDRIY BRATISHKO[1, 2], WERNER SCHWARZHANS[3]* & YULIIA VERNYHOROVA[4]

[1]Faculty of Natural Sciences, Luhansk Taras Shevchenko National University, Koval St. 3, Poltava, Ukraine, 36023.
[2]BugWare, Inc., 1615 Village Square Blvd, Ste. 8, Tallahassee, FL 32309, U.S.A.
[3]Zoological Museum, Natural History Museum of Denmark, Universitetsparken 15, 2100 København, Denmark; and Ahrensburger Weg 103, 22359 Hamburg, Germany. http://orcid.org/0000-0003-4842-7989
[4]Department of Stratigraphy and Paleontology of Cenozoic Deposits, Institute of Geological Sciences, National Academy of Sciences of Ukraine, O. Honchar Str. 55-b, Kyiv, Ukraine, 01601.
*Corresponding Author. Email: wwschwarz@aol.com

Associate Editor: Giorgio Carnevale.

Abstract: Reconstructing fossil bony fish faunas using otoliths is a well-established method that allows a diverse and dense record in time and space to be assembled. Here, we report about a rich otolith-based fish fauna from the middle Sarmatian s.l. (middle Bessarabian) from Jurkine, Kerch Peninsula, Crimea. The study is based on more than 5,000 specimens constituting 36 different species, 24 of which are new and two remain in open nomenclature. This assemblage represents the first major otolith association described from the Bessarabian. It also represents a fish fauna from the last continuous restricted marine environment that evolved in the Eastern Paratethys, was recruited from the Badenian/Tarkhanian fauna, and was not affected by the subsequent Khersonian crisis. The association of otoliths is characterized by a high content of endemic fishes that derived from the relatively well-known early Sarmatian s.l. (Volhynian) fish fauna, and it contains certain faunal elements that were trapped in the then-isolated Eastern Paratethys and did not range into younger strata. This forced endemic evolution explains the unusually high percentage of new taxa.

The fish fauna is dominated by stenohaline marine shelf fishes apparently recruited from the Konkian and earlier Sarmatian s.l. (Volhynian) fauna after the Karaganian crisis. The families Gobiidae and Gadidae benefited most in this restricted marine environment, while deep-water fishes disappeared with the Karaganian crisis. In this study, we discuss the further evolution of Eastern Paratethyan fishes as far as can be reconstructed from the relatively limited data from post-Bessarabian strata and also outline targets for future research in the field.

The stratigraphic sequence of the Jurkine section is being revised based on a detailed suite of benthic foraminifera. Implications for the stratigraphy of the middle and upper Sarmatian s.l., their boundary, and the paleoenvironments of this part of the Kerch Peninsula are discussed.
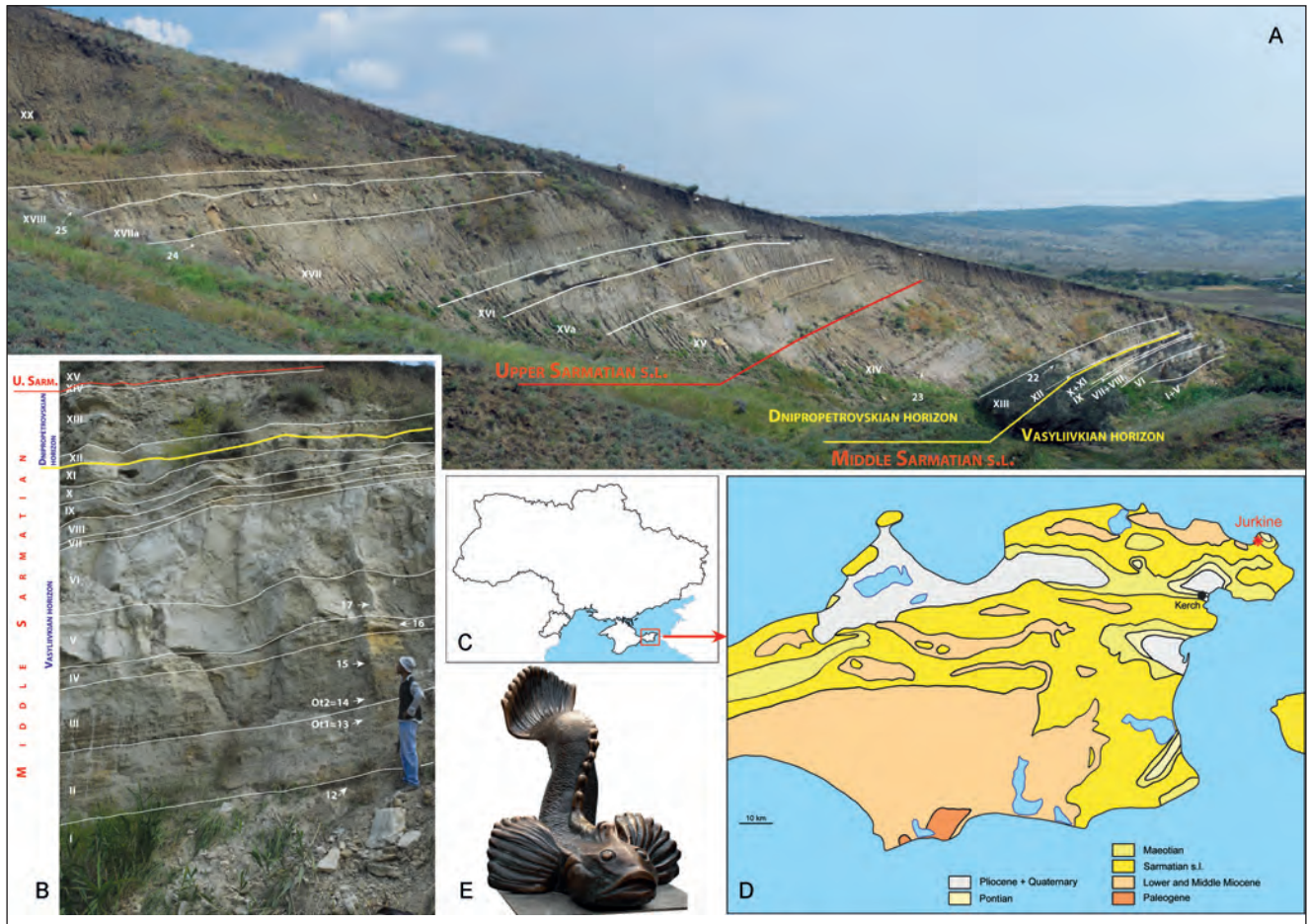
Fig. 1 - Location plate and field photographs. A) Jurkine cliff and outcrop with indication of stratigraphy, lithological levels (Roman numerals) and sample levels (Arabic numerals). B) Detail of middle Sarmatian section with lithological levels (Roman numbers) and sample levels (Arabic numbers); Ot1 and Ot2 indicate levels from which the studied otoliths were obtained. C) Insert map of Ukraine with Kerch Peninsula highlighted. D) Simplified geological map of Kerch Peninsula modified after Andrusov (1893). E) Goby monument in Berdyansk, Ukraine.

INTRODUCTION

The Neogene history of the Paratethys is characterized by rapid environmental changes, as well as changes in the connectivity and separation of its various basins. This development is reflected in a pronounced endemic evolution of its biota, which often differ from basin to basin. Specific stratigraphic schemes with regional stages, sub-stages, and finer stratigraphic units have been established for these basins. For instance, in the Central Paratethys, the Sarmatian stage (Sarmatian s.s.) encompasses only the upper Serravallian to lower Tortonian, while it includes a time interval ranging from the upper Serravallian to near the end of the Tortonian in the Eastern Paratethys (Sarmatian s.l.) (Raffi et al. 2020 in Gradstein et al. 2020). In the Eastern Paratethys, the Sarmatian regional stage (Sarmatian s.l.) is subdivided into a lower regional substage (Volhynian),

middle regional substage (Bessarabian), and upper regional substage (Khersonian) (Fig. 1–2; Nevesskaya et al. 1975; Vernyhorova 2016; and see below). The Eastern Paratethys, which stretched from the Dacian Basin in the west through the Euxinian Basin to the Caspian Basin in the east during the Sarmatian s.l., was characterized by a forced endemic evolution of its biota, the most well-known being the mollusk fauna (e.g., Anistratenko 2004, 2005; Iljina 2006; Lukeneder et al. 2011).

Articulated fish skeletons have commonly been described from the Volhynian in the Eastern Paratethys (e.g., Carnevale et al. 2006; Bannikov 2009, 2010, and literature cited therein). Otoliths from the Sarmatian s.l. of the Eastern Paratethys are less well known and often in need for revision (see Bratishko et al. 2015, 2017; Schwarzhans et al. 2022). Furthermore, the fish fauna from the Bessarabian and Khersonian is much less well known,

both in terms of otoliths and articulated skeletons. Here, we describe a rich assemblage of otoliths from the middle Bessarabian of Jurkine, Kerch Peninsula, Crimea. This assemblage contains 36 teleost species, of which 24 are new, 10 are from older strata and have been previously described, and two remain in open nomenclature. The large number of new species is an expression of the forced endemic evolution of the fish fauna in a restricted marine environment of the Euxinian Basin. A 2011 reconnaissance field trip by one of us (AB) yielded the otoliths from Jurkine (Fig. 1) here described. We planned to follow up this trip with a broader field research trip by AB and WS, but we could not conduct another expedition after 2014. When accessible, the Kerch Peninsula would represent a prime area for sampling otoliths to further unravel the evolution of the eastern Paratethyan fishes due to its excellent and diverse outcrops (Vernyhorova et al. 2012; Popov et al. 2019).

STRATIGRAPHY, GEOLOGICAL SETTING AND LOCATION

The Sarmatian s.l. of the Eastern Paratethys contains three regional substages: lower (Volhynian), middle (Bessarabian), and upper (Khersonian) (Nevesskaya et al. 1975). Details of the mollusk evolution in the Eastern Paratethys and changes in the composition of mollusk associations in the Sarmatian deposits of southern Ukraine led to the recognition of further subdivisions of the Sarmatian s.l. substages. These subdivisions are herein referred to as regional horizons (following e.g., Belokrys 1962, 1963, 1976; Fig. 2a). These horizons of the Sarmatian s.l. were identified and confirmed throughout the Eastern Paratethys using mollusks (e.g., Paramonova & Belokrys 1972; Paramonova 1994) and foraminifers (e.g., Didkovskiy 1964; Maisuradze 1971; Koiava 2006; Maisuradze & Koiava 2011). The base of the Sarmatian s.l. is dated at about 12.65 Ma by magnetostratigraphic data (Ter Borgh et al. 2014; Palcu et al. 2017, 2019), while the base of the Bessarabian has no firm dating yet. It is considered slightly older than the beginning of the Pannonian in the Central Paratethys (11.6–11.3 Ma according to Raffi et al. 2020). Based on the occurrence of oceanic diatoms, the base of the Khersonian is estimated to be younger than 8.9 Ma

(Radionova et al. 2012). Alternatively, the base of the Khersonian has been dated at 9.6 Ma based on magnetostratigraphic evaluation (Palcu et al. 2021; but see Šujan et al. 2022).

Widespread on the Kerch Peninsula, Neogene deposits are folded into anticlines and synclines and represent facies from coastal to relatively deepwater environments (Andrusov 1893; Arkhanguelsky et al. 1930). The Sarmatian s.l. of the Kerch region bears significant data on the development of the Eastern Paratethys and therefore has been an object of intensive paleontological, stratigraphical, and paleoenvironment studies (e.g., Andrusov 1893; Arkhanguelsky et al. 1930; Kolesnikov 1935; Kolesnikov et al. 1940; Paramonova & Belokrys 1972; Belokrys 1976; Paramonova 1994; Vernyhorova et al. 2012). Vernyhorova (2014) presented a comprehensive litho-biostratigraphical summary in which the Jurkine section is located in the North and Central Kerch Peninsula structural/facies subzone (Vernyhorova et al. 2012; Vernyhorova 2014). Within this subzone, the entire Sarmatian sequence is up to 350 m thick according to Arkhanguelsky et al. (1930). It conformably overlays the Petrovske Formation of Konkian age and comprises the Krasnoperekopsk Formation (Volhynian and lower Bessarabian), the Kurortne Formation (middle Bessarabian), the Korenkove Formation (upper Bessarabian and Khersonian), and the Kezey Formation (Khersonian). These formations, in turn, are overlain conformably or with a hiatus comprising the upper Bessarabian by lower Maeotian deposits (Mytridat Beds) (Vernyhorova et al. 2012; Vernyhorova 2014). However, in this study, we clarify the age of the Kezy and Korenkove Formations (see text in the chapter "Biostratigraphic revision of the Jurkine section mainly based on foraminifera," as well as Figs. 2b and 3).

For a description of the lithofacies characteristics of the Sarmatian deposits of the central and northern structural zone (Fig. 2a), we reference previous investigations by, for example, Andrusov (1893), Arkhanguelsky et al. (1930), Kolesnikov (1935), Vernyhorova et al. (2012), and Vernyhorova (2014). The Krasnoperekopsk Formation (up to 220 m) encompasses gray, dark-gray, and black laminated clays with rare intercalation of limestones. The Kurortne Formation (up to 37 m) exhibits stable lithological features and is characterized by interbedded clay deposits with bryozoan limestones (massive, sometimes recrystallized, silicified, clayey). Closer to
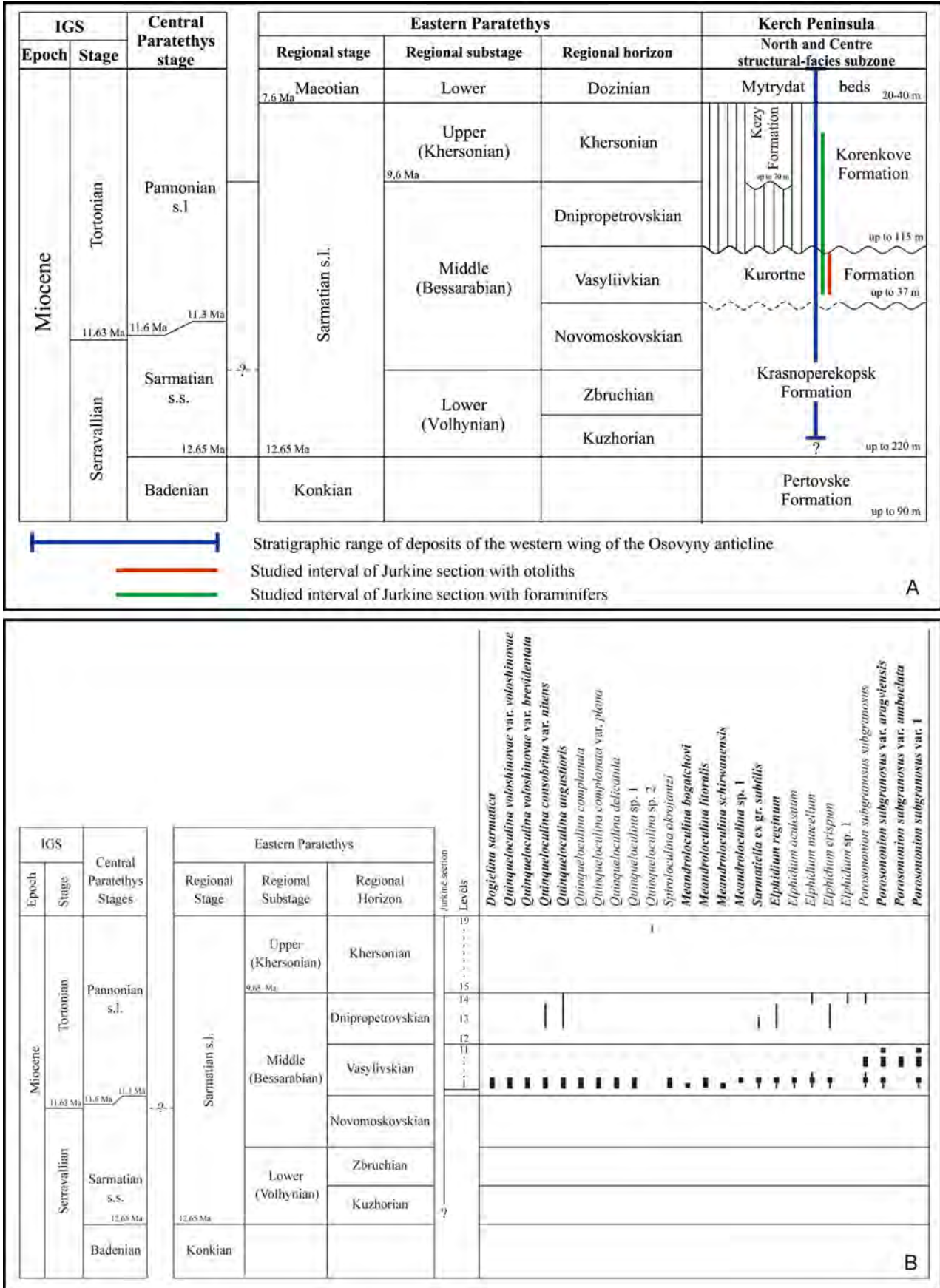
Fig. 2 - Stratigraphic scheme of the Sarmatian s.l. in the Eastern Paratethys. A) Lithostratigraphic formations of the Kerch Peninsula and stratigraphic range of the studied section and sampling. B) Stratigraphic ranges of foraminifers in the Jurkine section; bold printing = index species; broad bars = common species).

Fig. 3 - Stratigraphic column of the Jurkine section with lithology, sedimentological observations and fossil contents; layers are annotated (Arabic numerals) as well as sample levels (Arabic numerals in circles); Sample #1 and #2 indicate levels from which the studied otoliths were obtained.
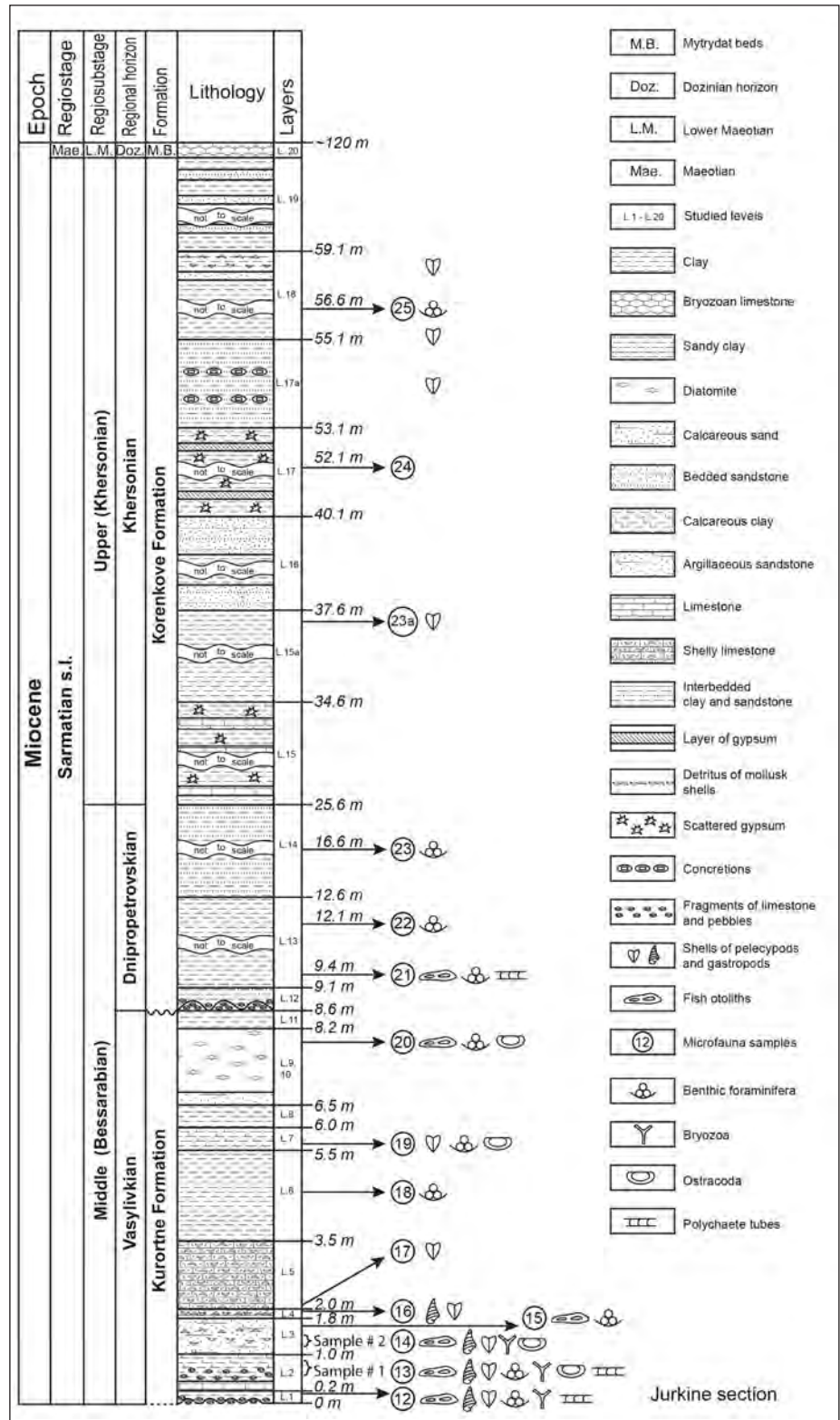
the axial parts of the synclines, the section is dominated by a clay-rich component. A distinctive feature of the Kurortne Formation on the Kerch Peninsula is the presence of bryozoan limestones. The Kezy Formation (up to 70.5 m) is characterized by gray, dark-gray, and light-brown laminated clays that are interbedded at times with fine-grained sands. The Korenkove Formation (up to 115 m) comprises gray laminated clays with thin interlayers of marls, tripoli, and sand. Its top part consists of intercalated layers of clays, marls, and limestones, with volcanic ashes, pebbles, and conglomerates near the top.

Based on the observed foraminifera (see below), mollusks, and lithological data, the studied otoliths from Jurkine originate from the Kurortne Formation. The lithological succession of the western flank of the Osovyny Syncline is exposed with a total thickness of about 120 m at the bluff 200 m northeast from Jurkine (45°2 5'48''N / 36°34'14''E) (Fig. 1). It is described below from bottom to top at 18 m above sea level (Fig. 3).

Kurortne Formation, Vasylivkian regional horizon, middle Sarmatian s.l. (middle Bessarabian)

Level 1. Clay, gray to greenish-gray, crumpled, with diverse mollusks (bivalves and gastropods; see Lukeneder et al. 2011), foraminifera, ostracoda, polychaete tubes, bryozoa (see Veis 1988), and fragments of limestone and pebbles. Visible thickness only 0.2 m. A microfauna sample (#12) was obtained below the first limestone bed.

Level 2. Limestone, gray with brown and black (possibly manganese oxide) stains, solid, brecciated (thickness 0.05–0.20 m.), overlain by clays, greenish-gray, calcareous, crumpled but overall laminated, with limestone fragments. The deposits contain diverse mollusks (bivalves and gastropods; see Lukeneder et al. 2011), foraminifera, ostracoda, polychaete tubes, and bryozoa (see Veis, 1988). Thickness of 0.8 m. Sample #1 for otoliths was obtained at an interval from 0.3–0.5 m below the top of this level, and a microfauna sample (#13) was obtained from the same level as the otoliths.

Level 3. Sand, bright yellow, fine- to medium-grained, calcareous, detrital. Lower in the level, the sand becomes greenish-yellow and argillaceous, containing abundant and diverse mollusks (see Lukeneder et al. 2011) that are randomly distributed. The level also includes foraminifera, ostracoda, and bryozoa (see Veis 1988). Its thickness varies from 0.8–1.5 m. Sample #2 for otoliths was obtained from the upper 0.25 m of this level, and a microfauna sample (#14 from gray sands) was obtained at the same level as the otoliths. A further microfauna sample (#15 from yellow sands) was obtained 0.25 m higher than sample #14.

Level 4. Coquina, light gray, contains three clay interlayers (0.05 cm each) with many cardiids shells, foraminifera, ostracoda, and polychaete tubes, as well as a few fish bones and otoliths. Thickness 0.2–0.3 m. A microfauna sample (#16) was obtained from the top of the level.

Level 5. Shelly limestone, light gray, solid, lithified, composed of nearly 60% of cardiids. Thickness 1.5 m. A microfauna sample (#17) was obtained at the contact plane with the previous level.

Level 6. Clay, light gray to white, silicified, homogeneous, very rich with foramifera of the genus *Nonion*. Thickness 2 m. A microfauna sample (#18) was obtained from the middle part of the level.

Level 7. Clay, light yellow to gray and white, with black (possibly manganese oxide) stains and dots, sandy, laminated, calcareous with rare mollusks (cardiids) and ostracoda. Thickness 0.5 m. A microfauna sample (#19) was obtained from the lower part of the level.

Level 8. Clay, light gray, silicified. Thickness 0.5 m.

Level 9. Sandstone, argillaceous. Thickness 0.2 m.

Level 10. Diatomite, light gray, with interlayers (0.01 m) of brown clay and sand (0.02–0.05 m) containing foraminifera, few fish bones, and otoliths. Thickness 1.5 m. A microfauna sample (#20) was obtained from the top of the level.

Level 11. Clay, light gray, silicified. Thickness 0.4 m.

Korenkove Formation, Dnipropetrovskian regional horizon, middle Sarmatian s.l. (upper Bessarabian)

Level 12. Clay, light gray with variably gray sand grains, gravel and limestone fragments. The basal contact is sharp and undulating, while the contact with the overlying level is poorly discernable. Thickness 0.5 m.

Level 13. Clay, light gray to greenish-, brownish-gray; micro-laminated; soft; containing foraminifera (samples #21, #22), few fish bones, and polychaete tubes (sample #21). Thickness 3.5 m. A microfauna sample (#21) was obtained from the lower part of the level, and a microfauna sample (#22) was obtained from the top of the level.

Level 14. Rhythmically interbedded clays and sandstones. The clays are gray, silicified, and laminated (micro-layers are 0.5–3 mm thick) while the sandstones are fine-grained and flaggy-bedded (partings are up to 0.05 m thick) with black (possibly manganese oxide) dots. The rocks contain fish bones and foraminifera. Thickness 13 m. A microfauna sample (# 23) was obtained from 4.0 m above the bottom of the level.

Korenkove Formation, Upper Sarmatian s.l. (Khersonian)

Level 15. Clay, gray, laminated, contains gypsum and three limestone interlayers (up to 0.5 m thick) containing rare, thin-shelled mollusks of *Mactra* (*Chersonimactra*) *caspia* (Eichwald, 1841). Thickness 9 m. A microfauna sample (#23a) was obtained from the top of the level.

Level 15a. Clay, gray, with yellow (ocher) clay interlayers. Thickness 3 m.

Level 16. Two sandstone layers, gray, flaggy-bedded, 0.4–1.0 m thick each; between sands, interlayer of clay, gray, laminated. Total thickness 2.5 m.

Level 17. Clay, gray, laminated, contains scattered gypsum, and its interlayers contain rare thin-shelled mollusks *Mactra* (*Chersonimactra*) *caspia*, as well as a few fish bones. Thickness 13 m. A microfauna sample (#24) was obtained from the top of the level.

Level 17a. Interbedded clays and sandstones. Sandstones with uneven, convex surfaces, containing concretions. Clays as in the level below with rare, thin-shelled mollusks *Mactra* (*Chersonimactra*) *caspia*. Level interrupted but traceable laterally. Thickness 2 m.

Level 18. Clay, gray to greenish-gray, laminated, containing rare, thin-shelled mollusks *Mactra* (*Chersonimactra*) *caspia*, as well as some tests of foraminifera. Upper part with interlayer of sandstone (0.15 m thick), containing mollusk-shell debris. Thickness 4 m. A microfauna sample (# 25) was obtained from the middle part of the level.

Level 19. Clay, dark gray, laminated, with interlayers of flaggy-bedded sandstone (0.05–0.1 m thick), containing rare, thin-shelled mollusks *Mactra* (*Chersonimactra*) *caspia*. Total thickness up to 60 m.

Mytrydat Beds, Maeotian

Level 20. Bryalgal limestone of the Maeotian. Thickness near 2 m.

MATERIAL AND METHODS

The otolith-bearing samples were collected during a field trip in 2011 by the senior author. In 2013, two of us (YV and AB) studied the western flank of the Osovyny Syncline. The field description of the Jurkine section and its stratigraphic position was analyzed by YV based on mollusk and foraminifer composition. Two otolith samples, #1 (15 kg) and #2 (60 kg), were taken by AB from Levels 2 and 3, respectively, in the Kurortne Formation and processed (wet-screened) through a 0.7-mm sieve in the field. In the laboratory, otoliths were picked from the sieve concentrate, which also contained foraminifera, ostracods, bryozoans, mollusks (pelecypods and gastropods shells), and fish bones. The residue was sorted, and 5685 otoliths were obtained. Sample #2 was much richer than sample #1, and all taxa found in sample #1 were also contained in sample #2. Therefore, the samples were not kept separate.

One of us (YV) studied foraminifera from 15 micro-samples (400 g each) from the Jurkine section. The samples were soaked in water and then washed through a 63-μm sieve. From the resulting dried residue, foraminifera were picked under a stereomicroscope. In addition, 273 otoliths were obtained from micro-samples #12 to #15 that were processed for foraminifers. These otoliths are listed separately in the material annotation of the descriptive part. The species determination of benthic foraminifera was based on Bogdanowich (1952, 1974), Maisuradze (1971), Loeblich & Tappan (1988), and Bugrova et al. (2005). A quantitative ratio of tests of separate species was used (following Boltovskoy & Totah, 1985) to evaluate the changing benthic foraminifera associations during the middle to late Sarmatian s.l.. We interpreted the sea bottom habitat by synthesizing the data of the marine biota (foraminifera, mollusks, and bryozoa), and we classified the epifaunal and infaunal species of benthic foraminifera according to Rosoff and Corliss (1992) and Murray (2006). Additionally, we monitored tendencies of changes in bottom water oxygenation levels based on the ratio of oxic-suboxic-dysoxic benthic foraminiferal indicators according to Kaiho (1994, 1999) and Murray (2006).

The otoliths were photographed with a Leica M 165 FC stereomicroscope in the Department for Earth and Environmental Sciences, Paleontology and Geobiology, Ludwig-Maximilians-Universität München and a Canon EOS 1000D mounted on a Wild M400 photomacroscope that was remotely controlled and captured from a computer at the second author's laboratory in Hamburg. Individual pictures of every view of the objects taken at a ranging field of depth were stacked using the Heliconfocus software from Heliconsoft (Kharkiv, Ukraine). Adjustment of exposure and contrast and retouching were completed in Adobe Photoshop when necessary to impro-

ve the images without altering any morphological features. SEM pictures of some particularly small otoliths were produced at the Zoological State Collection, Munich. All otoliths are shown from the inner face (if not annotated otherwise) of the right side and mirror imaged when necessary. Pleuronectiform otoliths are shown from left and right sides in order to demonstrate potential side dimorphism.

We used the morphological terminology established by Koken (1884) with amendments by Chaine & Duvergier (1934) and Schwarzhans (1978), and we applied the morphometrics for gobies as established in Schwarzhans (2014). The abbreviations used are as follows: OL, otolith length; OH, otolith height; OT, otolith thickness; OsL, ostium length; CaL, cauda length; OCL, length of ostial colliculum; CCL, length of caudal colliculum; SuL, sulcus length; and SL, standard length (in fish).

Depository: The majority of the otoliths, including holotypes, are deposited in the collection of the National Museum of Natural History of the National Academy of Sciences of Ukraine (NMNH), Kyiv, in the Department of Monographic Collection under the collection registrations NMNH ГКН (MBA - main book of acquisition) 5960 001 to 078. Representative paratypes and nontypes are deposited at the Senckenberg Forschunginstitut und Naturmuseum (SMF), Frankfurt/Main under the collection registrations SMF PO 101.152 to 183. A few specimens remain in the comparative collections of the authors of the systematic section.

Systematics
(by A. Bratishko & W. Schwarzhans)

Our classification follows Nelson et al. (2016), with the exception that it does not follow the sequence in all instances. Detailed descriptions are presented only for new species. Updated diagnoses are established for species originally described by Pobedina (1956) and Djafarova (2006) due to relatively indistinct documentation and generalized descriptions. Specimens depicted in Suzin (1968, in Zhizhchenko) are references, but his species names are not used since they are not available according to ICZN article 13.1.1, i.e., "be accompanied by a description or definition that states in words characters that are purported to differentiate the taxon."

Division **Teleostei** Müller, 1846
Order **Clupeiformes** Bleeker, 1859
Family Clupeidae Rafinesque, 1810
Subfamily Alosinae Svetovidov, 1952
Genus *Alosa* Linck, 1790

Alosa grandis (Djafarova, 2006)
Figs. 4A-I

2006   *Engraulis grandis* - Djafarova: pl. 1, fig. 2
2006   *Engraulis* sp. - Djafarova: pl. 1, fig. 4

Material: 20 specimens (figured specimens NMNH ГКН 5960 001 and SMF PO 101.152), Bessarabian, Jurkine, including 1 specimen from micrp-sample #12.

Diagnosis (updated): Elongate, thin otoliths; OL:OH = 1.95–2.1. Rostrum long, 30–35 % of OL, with pointed tip. Excisura wide, deep, nearly rectangular in shape, leading to nearly vertically cut antirostrum. Dorsal rim shallow, postdorsal rim depressed. Ventral rim shallow, with small incision below collum. Ostium about 1.5–2.0 times the length of cauda. Caudal tip broadly rounded, terminating at some distance from posterior rim.

Discussion. The wide and nearly rectangular shape of the excisura is likely one of the most distinctive characteristics of *Alosa grandis*. This feature correlates with Djafarova's drawings (2006) and readily distinguishes *A. grandis* from *A. paulicrenata* Bratishko, Schwarzhans & Reichenbacher, 2015, which is from the Konkian (lower Serravallian) of the Eastern Paratethys. *Alosa grandis* resembles the extant *A. fallax* (Lacepède, 1803) (see Baykina & Schwarzhans 2017 for figures) extant Pontian *A. immaculata* Bennett, 1835, and the extant Caspian species *A. braschnikowi* (Borodin,1904), *A. caspia* (Eichwald, 1838), and *A. kessleri* (Grimm, 1887) (for figures of the otoliths of the Caspian species, see Dizaj et al. 2020). However, these species have a sharper excisura and tend to be more elongate (OL:OH = 2.1–2.3 *vs.* 1.95–2.1, except 1.9–2.0 for *A. kessleri*). Otoliths in situ have been described from *Moldavichthys switshenskae* Baykina & Schwarzhans, 2017 from the lower Sarmatian s.l. (Volhynian), and the extinct genus *Moldavichthys* is considered to be related to *Alosa*. However, the otoliths of *M. switshenskae* are much more compact than those of *Alosa*. *A. grandis* appears to be endemic to the Sarmatian s.l., likely the middle Sarmatian (Bessarabian) of the Eastern Paratethys.

Genus *Maeotichthys* n. gen.

Type species: *Otolithus* (*Osmeridarum*) *wilhelmi* Djafarova, 2006 (fossil, otolith-based species).
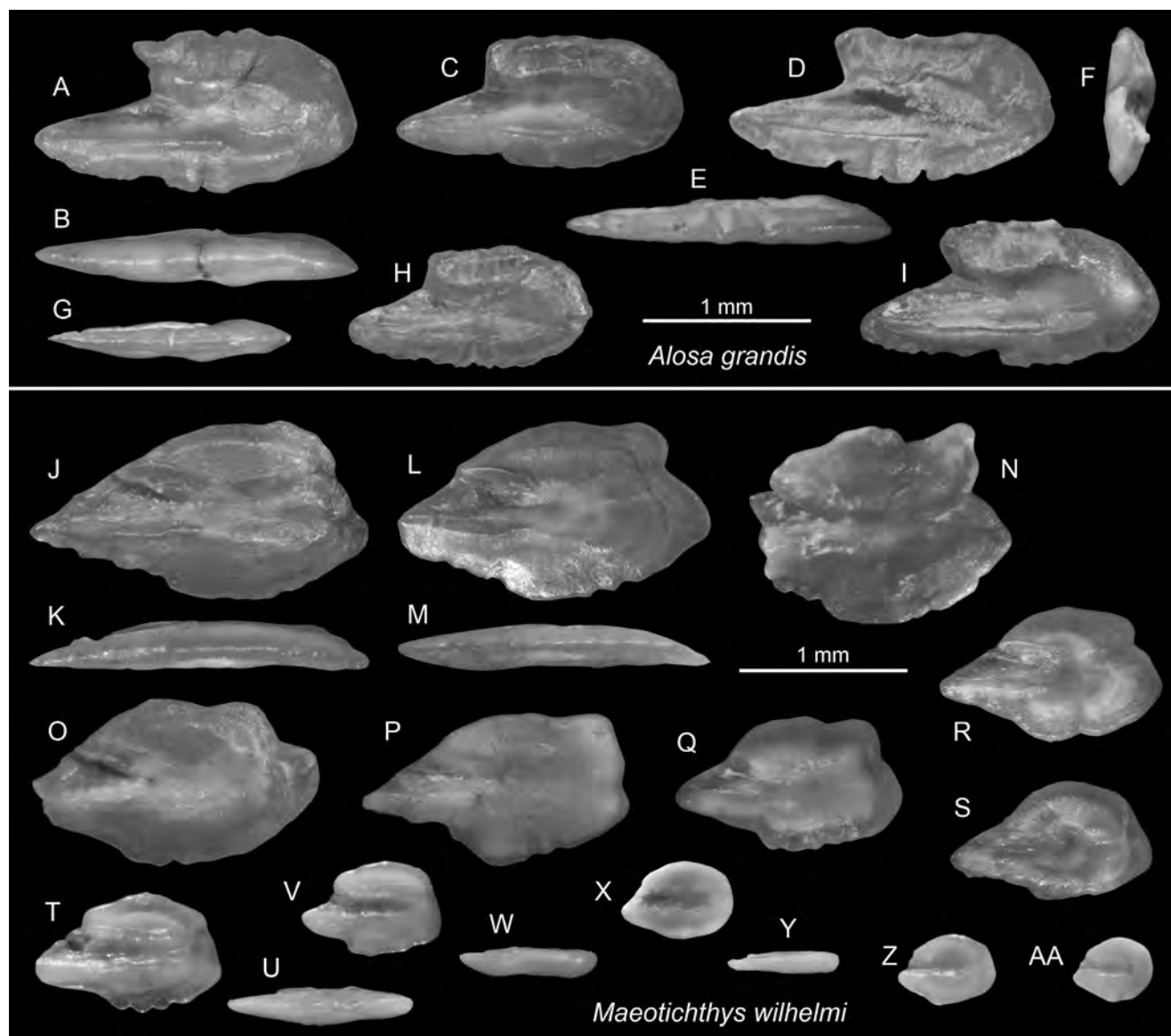
Fig. 4 - Clupeidae. A–I) *Alosa grandis* (Djafarova, 2006), NMNH ГКН 5960 001 (A–C) and SMF PO 101.152 (D–I), B, E, G ventral views, F anterior view, Bessarabian, Jurkine. J–AA) *Maeotichthys wilhelmi* (Djafarova, 2006), NMNH ГКН 5960 002 (L–P) and SMF PO 101.153 (J–K, Q–AA), K, M, U, W, Y ventral views, V–AA juveniles, Bessarabian, Jurkine.

Etymology: Named after Maeotis, the ancient Greek name for the Azov Sea.

Diagnosis: A fossil, otolith-based genus of the family Clupeidae, Alosinae defined by the following combination of characters. Compact and thin otoliths. Ratio OL:OH = 1.5–1.9, usually increasing with size. Rostrum moderately long, 20–25 % of OL, with sharply pointed tip, narrowed by indentation of ventral rim at beginning of rostrum. Excisura and antirostrum absent or feeble. Dorsal rim high with postdorsal angle or rounded. Posterior rim slanted, with inferior tip, rarely rounded. Ventral rim deep, with distinct indentation at beginning of rostrum. Ostium about 0.9–1.3 times the length of cauda. Caudal tip fading.

Discussion. *Maeotichthys* appears to be related to the fossil *Moldavichthys* Baykina & Schwarzhans, 2017 described from articulated fishes with otoliths in situ (Baykina & Schwarzhans 2017), as well as the extant *Clupeonella* Kessler, 1877, a genus now endemic to the Ponto-Caspian Basin. Otoliths of the extant Caspian species *C. cultiventris* (Nordmann, 1840), *C. engrauliformis* (Borodin, 1904), and *C. grimmi* Kessler, 1877 are figured in Dizaj et al. (2020) and of *C. cultiventris* also in Baykina and Schwarzhans (2017). *Maeotichthys* shares with *Clupeonella* the short, compact shape with a low ratio OL:OH; the relatively short rostrum; and a sulcus with an ostium about as long as the cauda or only slightly longer. However, it differs from *Clupeonella* and *Moldavichthys* in its sharply pointed rostrum and lack of a deep excisura. We consider *Maeotichthys* an

endemic genus of the former Paratethys—likely restricted to the Eastern Paratethys—that became extinct at the end of the Sarmatian s.l.

Species. Two species: *Maeotichthys wilhelmi* (Djafarova, 2006) from the Chokrakian (upper Langhian) to Bessarabian (lower Tortonian) of Ukraine and Azerbaidjan, Eastern Paratethys and *Maeotichthys gomotartziensis* (Strashimirov, 1985) (originally described as *Clupea gomotartziensis*) from the Khersonian of Bulgaria, Eastern Paratethys.

Maeotichthys wilhelmi (Djafarova, 2006)
Figs. 4J-AA

?1968   *Otolithus* (*Clupea*) *fimbriosus* - Suzin (in Zhizhchenko): pl. 18, fig. 4 [name not available according to ICZN article 13.1.1].
1984   *Clupea pulchra* Smigielska, 1966 - Strashimirov: pl. 2, figs. 14-15.
2006   *Otolithus* (*Osmeridarum*) *wilhelmi* - Djafarova: pl. 2, fig. 3.
2006   *Otolithus* (*Osmeridarum*) *minimus* - Djafarova: pl. 2, fig. 2.
?2006   *Otolithus* (*Osmeridarum*) *crassa* - Djafarova: pl. 2, fig. 4.

Material: 71 specimens (figured specimens NMNH ГКН 5960 002 and SMF PO 101.153), thereof 45 smaller than 1 mm and probably from juveniles, Bessarabian, Jurkine; 37 specimens from otolith-samples #1 and #2, 20 specimens from micro-sample #14 and 8 specimens from micro-sample #15.

Diagnosis (updated): Compact, thin otoliths; OL:OH = 1.5–1.9, increasing with size. Rostrum moderately long, 20–25 % of OL, with sharply pointed tip. Excisura and antirostrum not or very weak developed. Dorsal rim with distinct postdorsal angle, sometimes developed to massive denticle. Posterior rim slanted, with inferior tip. Ventral rim deep, with distinct indentation at beginning of rostrum. Ostium about 0.95–1.2 times the length of cauda. Caudal tip fading, terminating relatively close to posterior rim.

Discussion. *Maeotichthys wilhelmi* is an easily recognizable clupeid otolith that resembles *Clupeonella* and *Moldavichthys* but differs in its sharp rostrum (see genus diagnosis). Specimens originally described as *Otolithus* (*Osmeridarum*) *crassa* Djafarova, 2006 from the Chokrakian of Azerbaidjan may represent the earliest record, but these are only tentatively assigned to *M. wilhelmi* because of the large stratigraphic difference and limited quality of documentation in Djafarova (2006). A similar species is *M. gomotartziensis* (Strashimirov, 1985), which differs in its even shorter rostrum and regularly rounded dorsal rim. Schwarzhans et al. (2020a) considered otoliths of *Clupeonella* sp. from the latest Messinian, Lago Mare interval, from Italy to be immigrants from the Eastern Paratethys during that time. These otoliths resemble the extant *C. cultiventris*, having a blunt rostrum, and thus clearly represent the genus *Clupeonella*.

Order **Gadiformes** Goodrich, 1909
Family Gadidae Rafinesque, 1810
Genus *Palimphemus* Kner, 1862

Palimphemus cimmerius n. sp.
Fig. 5A-J

1968   *Otolithus* (*Gadidarum*) *chutcievi* - Suzin (in Zhizhchenko): pl. 18, fig. 30 [name not available according to ICZN article 13.1.1].

Holotype: Fig. 5A-B, NMNH ГКН 5960 003, Bessarabian, Jurkine, Crimea.

Paratypes: 9 specimens, NMNH ГКН 5960 004 and SMF PO 101.154, same data as holotype.

Referred specimens: 876 specimens, same data as holotype; in addition 56 juvenile specimens smaller than 1 mm in length; 17 from micro-sample #12, 6 from micro-sample #13, 32 from micro-sample #14 and 1 from micro-sample #15.

Etymology: Named after the Cimmerians, a ancient nation that once lived on the Kerch Peninsula.

Diagnosis: Thin, slender otoliths; OL:OH of 2.15–2.45; OH:OT = 2.9–3.6. Ventral rim shallow, nearly straight, coarsely serrated. Dorsal rim with distinct predorsal angle and nearly straight, inclined pre- and postdorsal rims; predorsal rim inclined at 23–33°, postdorsal rim inclined at 10–15°. Ostium slightly shorter than cauda (OsL:CaL = 0.9–0.97). Colliculi reduced in length, terminating relatively far from anterior and posterior rims of otolith. Collum narrow. Ventral furrow distinct, along middle of ventral field.

Description. Moderately large, slender and thin otoliths, reaching about 6 mm in length (holotype 5.8 mm); OL:OH = 2.15–2.45, increasing with size; OH:OT = 2.9–3.6. Dorsal rim with obtuse but distinct predorsal angle at about 35% of OL measured from anterior tip. Predorsal and postdorsal rims nearly straight, inclined at 23–33° anteriorly and 10–15° posteriorly, relatively smooth and without prominent angles. Ventral rim shallow, nearly straight, very coarsely and irregularly serrated or strongly undulating. Anterior tip blunt or near vertical cut, inferior; posterior tip tapering, median or slightly inferior position.

Inner face slightly bent with slightly supramedian positioned, pseudobiostial sulcus. Ostium only slightly shorter than cauda; OsL:CaL = 0.9–0.97. Colliculi reduced towards the otolith rims and therefore much shorter than ostium and cauda; OCL:CCL = 0.8–1.05. Collum narrow with small and feeble pseudocolliculum. Triangular dorsal field relatively smooth, without distinct dorsal depression. Ventral field with prominent, nearly straight ventral furrow positioned half way between sulcus and ventral otolith rim. Outer face flat to slightly concave, smooth with few vertical furrow.

Discussion. *Palimphemus cimmerius* n. sp. is a common and characteristic otolith in the Bessarabi-
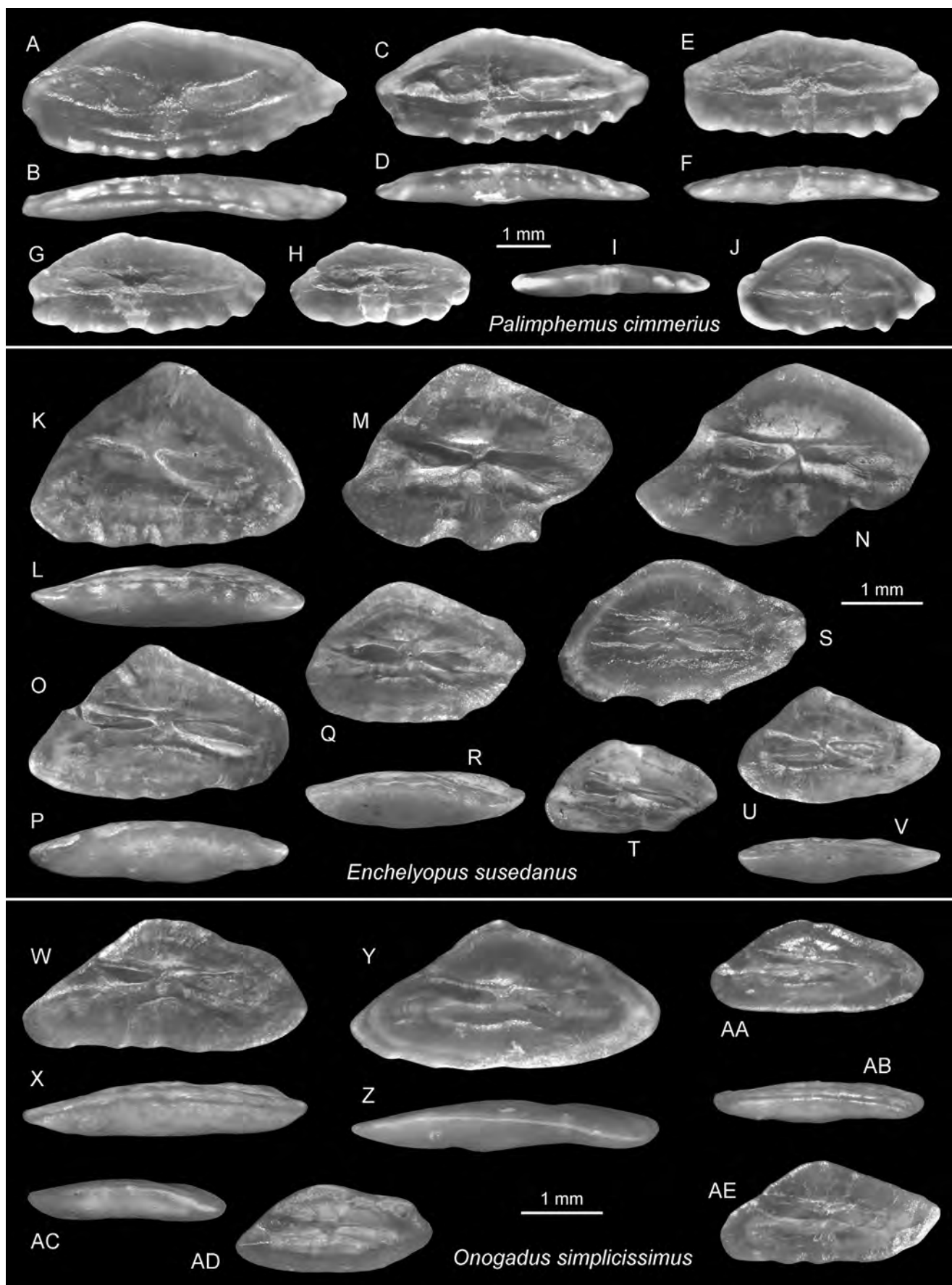
Fig. 5 - Gadiformes. A–J) *Palimphemus cimmerius* n. sp., holotype (A–B) NMNH ГКН 5960 003, paratypes (C–J) NMNH ГКН 5960 004 (G–H) and SMF PO 101.154 (C–F, I–J), B, D, F, I ventral views, Bessarabian, Jurkine. K–V) *Enchelyopus susedanus* (Kner, 1863), NMNH ГКН 5960 005 (K–M, Q–S) and SMF PO 101.155 (N–P, T–V), L, P, R, V ventral views, Bessarabian, Jurkine. W–AE) *Onogadus simplicissimus* (Schubert, 1906), NMNH ГКН 5960 006 (W–X, AE) and SMF PO 101.156 (Y–AD), X, Z, AB, AC ventral views, Bessarabian, Jurkine.

an of Jurkine that has also been identified from Za-
vetnoe nearby (unpublished data). It likely is derived
from *P. macropterygius* (Kramberger, 1883) (syn. *Ga-
didarum minusculoides* Schubert, 1912) (see Bratishko
et al. 2015 for redefinition), and represents an en-
demic species in the Eastern Parathethys. *Palimphe-
mus cimmerius* n. sp. differs from *P. macropterygius* in
several characteristics, the most notable being the
shape of the dorsal and ventral rims, the propor-
tions of ostium and cauda (OCL:CCL = 0.8–1.05
vs 0.5–0.7), and the distinct, nearly straight ventral
furrow positioned along the center of the ventral
field. Overall, *P. cimmerius* n. sp. is a rather unmis-
takable otolith that appears to be restricted strati-
graphically to the Bessarabian.

Family Gaidropsaridae Jordan & Evermann, 1898
Genus *Enchelyopus* Bloch & Schneider, 1801

Enchelyopus susedanus (Kner, 1863)
Figs. 5K–V

2017a   *Enchelyopus susedanus* (Kner, 1863) - Schwarzhans et al.: figs.
     5a-b, 6a-d (6c-d otoliths in situ).

Material: 155 specimens (figured specimens NMNH ГКН
5960 005 and SMF PO 101.155), Bessarabian, Jurkine.

Description. See Schwarzhans et al. 2017a,
which was based on otoliths from Jurkine.

Discussion. *Enchelyopus susedanus* was origi-
nally described based on articulated skeletons by
Kner (1863) from the Volhynian of Dolje, Croa-
tia. Schwarzhans et al. (2017a) found otoliths in situ
in two of the original specimens (paratypes). The
species appears to have been restricted to the Sar-
matian s.s. of the Central Parathethys and the Vol-
hynian, and Bessarabian of the Eastern Parathethys.
Otoliths of *Enchelyopus susedanus* differ from the ex-
tant *E. cimbrius* (Linnaeus, 1766) (see Nolf, 2018: pl.
19) in their straight or nearly straight postdorsal rim,
larger dorsal depression, thicker profile, and flat in-
ner face and convex outer face (vs convex inner face
and flat to concave outer face).

Genus *Onogadus* de Buen, 1934

Onogadus simplicissimus (Schubert, 1906)
Figs. 5W–AE

1906   *Otolithus* (*Crenilabrus*) *simplicissimus* - Schubert: pl. 18, figs. 43,
     44.
2015   *Onogadus simplicissimus* (Schubert, 1906) - Bratishko et al.: figs.
     4.6-12 (see there for further synonymies).

Material: 285 specimens (figured specimens NMNH ГКН
5960 006 and SMF PO 101.156), Bessarabian, Jurkine, including 1
specimen from micro-sample #13.

Description. *Onogadus simplicissimus* was rede-
fined, described in detail and compared to extant
species in Bratishko et al. (2015).

Discussion. *Onogadus simplicissimus* is appar-
ently endemic to the Central and Eastern Parate-
thys, where it occurs from the upper Badenian/
Konkian to the Bessarabian. In the Bessarabian, it is
restricted to the Eastern Parathethys.

Order **Gobiiformes** Günther, 1880
(sensu Thacker, 2009)
Suborder **Gobioidei** Jordan & Evermann, 1896

Remarks. The familial arrangement of the
families of the Gobioidei is still very much in flux.
We have kept here at family level the Gobiidae,
Gobionellidae and Microdesmidae, the latter in-
cluding the subfamily Ptereleotrinae.

Family Gobiidae Cuvier, 1816
Subfamily Gobiinae Cuvier, 1816
Gobius Lineage sensu Agorreta et al. 2013
Genus *Mesogobius* Bleeker, 1874

Mesogobius chersonesus n. sp.
Figs. 6D–R

Holotype: Fig. 6D–F NMNH ГКН 5960 007, Bessarabian,
Jurkine, Crimea.
Paratypes: 18 specimens, NMNH ГКН 5960 079 and SMF
PO 101.157, same data as holotype.
Etymology: Named after Cape Chersonesos and the ancient
Greek settlement on the Crimea.
Diagnosis: OL:OH = 1.2–1.6, increasing with size. Maximal
size 8.4 mm in length. Ventral rim nearly straight. Postdorsal pro-
jection strong; preventral projection distinct, pointed. Sulcus small,
sole-shaped, deepened, slightly inclined at 5-10°; no or very small
subcaudal iugum. Inner face slightly convex; outer face flat to slightly
concave.

Description. One of the largest goby oto-
liths known to date with a maximal size of 8.4 mm
in length (holotype). Thin, slender otolith with
OL:OH = 1.2–1.6, increasing in size resulting from
increasing strength of postdorsal and preventral
projections and increasing depression of predor-
sal region with growth. OH:OT = 3.0–3.5. Ventral
rim shallow, nearly straight and horizontal. Dorsal
rim irregularly undulating, shallow, increasingly

Fig. 6 - Gobiidae, *Mesogobius*. A–C) *Mesogobius batrachocephalus* (Pallas, 1814), ZMUC P2395071-72, B dorsal view, extant, Primorsk, Sea of Azov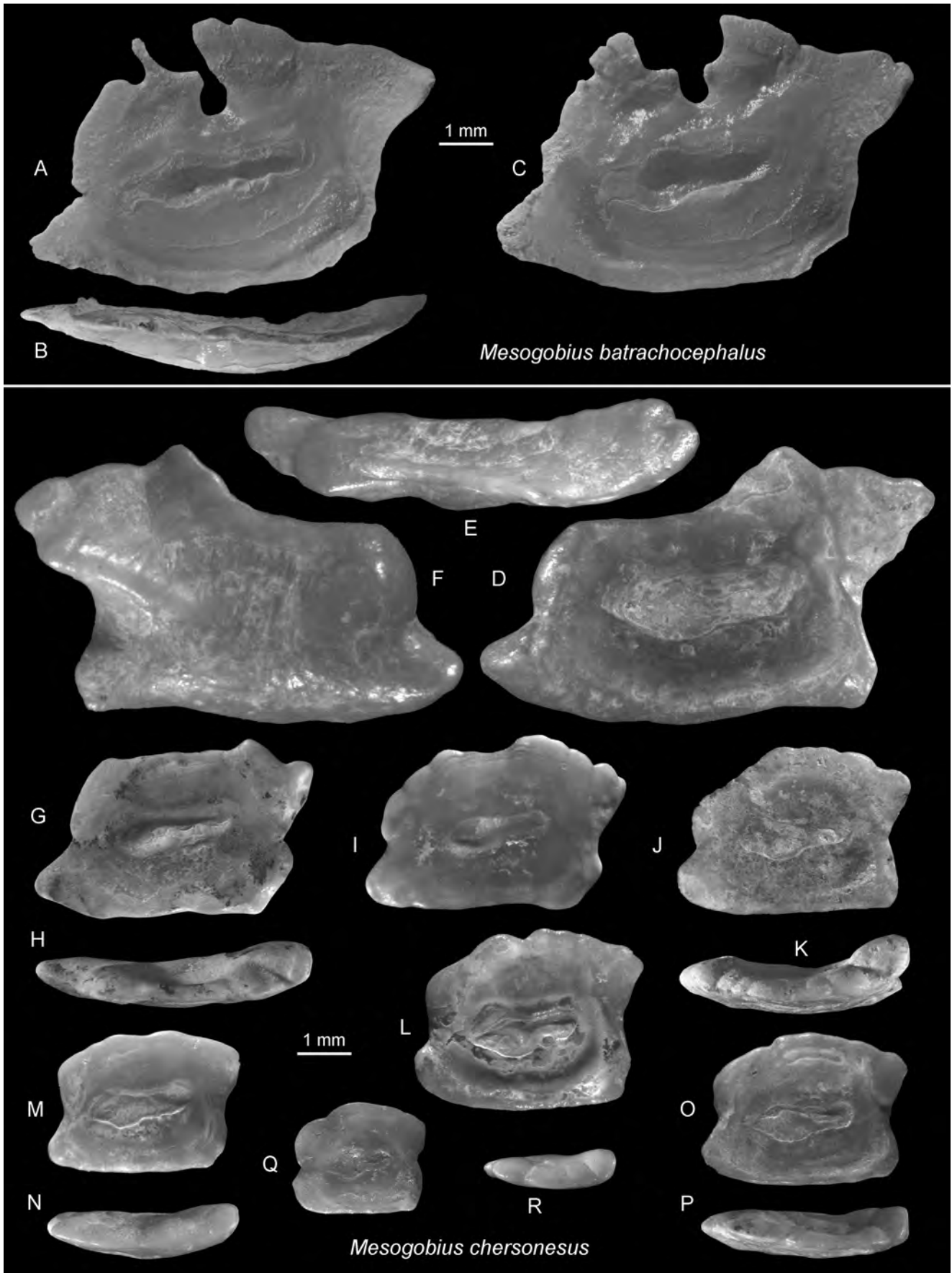. D–R) *Mesogobius chersonesus* n. sp., holotype (D–F) NMNH ГКН 5960 007, paratypes (G–R) NMNH ГКН 5960 079 (J–N) and SMF PO 101.157 (G–I, O–R), F outer face, E, H, K, N, P, R dorsal views, Bessarabian, Jurkine.

depressed anteriorly with size. Postdorsal projection massive, distinctly bent outwards (see dorsal views). Preventral projection pointed, moderately strong to distinct. Predorsal and postventral angles obtuse to orthogonal.

Inner face slightly bent with centrally positioned, small, deepened, sole-shaped and only slightly inclined sulcus (5-10° inclination angle). OL:SuL = 2.0–2.35. No or very small and indistinct subcaudal iugum (Fig. 6L). Ventral furrow leading from anterior to posterior tips of sulcus, often feeble; dorsal depression large and wide, dorsally open when dorsal rim depressed, usually with indistinct margins. Outer face flat to slightly concave, smooth or with few indistinct radial furrows dorsally; postdorsal projection markedly bent outwards.

Discussion. Fully grown *Mesogobius* specimens and their otoliths are among the largest known gobiids (the largest Gobioidei are from the Eleotridae); the extant *M. batrachocephalus* (Pallas, 1814) from the Black Sea reaches 35 cm SL (Froese & Pauly 2021). Two otoliths of specimens just shy of 30 cm SL are figured for comparison (Fig. 6A–C). The otoliths of *M. chersonesus* n. sp. differ from those of *M. batrachocephalus* in their shallower dorsal rim, nearly straight ventral rim, stronger developed postdorsal projection in large specimens, and more elongate shape at comparable sizes. The otoliths of both species share the tendency of a reduced dorsal rim in large specimens, usually seen as a deep indentation in *M. batrachocephalus* and a broad depression of the entire predorsal rim in *M. chersonesus* n. sp. Otoliths of the extant *M. nonultimus* (Iljin, 1936) and *M. nigronotatus* (Kessler, 1877) are unknown. Both of these are endemic to the Caspian Sea and are rare with the latter known only from holotype.

In the fossil record, *Mesogobius* otoliths have occasionally been interpreted in the literature from the Upper Miocene (Messinian and Tortonian) of the Mediterranean, usually in open nomenclature (e.g., Nolf & Cavallo 1994; Caputo et al. 2009; Girone et al. 2010; Lin et al. 2015). These records were reviewed in Schwarzhans et al. (2020a), who found that they pertained to species of *Gobius* Linnaeus, 1758 or *Chromogobius* de Buen, 1930. Thus, *M. chersonesus* n. sp. represents the earliest and, thus far, the only verified fossil record of the genus.

Genus *Neogobius* Iljin, 1927

Neogobius cf. *bettinae* Bratishko, Kovalchuk & Schwarzhans, 2017
Figs. 7A–E

?2017 *Neogobius bettinae* - Bratishko et al.: figs. 4.1-9.

Material: 22 specimens, NMNH ГКН 5960 008 and SMF PO 101.158, Bessarabian, Jurkine, Crimea.

Description. Moderately slender and relatively large otoliths up to about 3.5 mm in length; OL:OH = 1.1–1.3. Thickness variable, OH:OT ranging from 2.8 to 4.0 in specimens from Jurkine, about 2.2 in type specimens figured in Bratishko et al. (2017). Dorsal rim regularly curved anteriorly, with moderately developed postdorsal projection. Ventral rim straight, preventral projection short, pointed or blunt; posterior rim inclined.

Inner face slightly convex with a relatively long and steeply inclined sulcus; OL:SuL = 1.9–2.1; ostial inclination angle 17–20°. Ostium narrow, with small ostial lobe situated nearly above center of sulcus. No or very small and indistinct subcaudal iugum. Ventral furrow distinct, not connected around sulcus to wide dorsal depression. Outer face convex or slightly concave, rather variable.

Discussion. *Neogobius bettinae* has been described from coeval, transitional brackish to freshwater sediments of Mykhailivka, Ukraine (Bratishko et al. 2017). The specimens from Jurkine originate from a normal marine environment and resemble those from Mykhailivka in all morphological aspects, except that they are distinctly less thick. This difference in thickness may have had an ecological cause; therefore, we tentatively associate the specimens from Jurkine with *N. bettinae*. However, the two other otolith-based goby species from Mykhailivka (*Ponticola dorsorostralis* (Weinfurter, 1954) and *Neogobius rhachis* Rückert-Ülkümen, 1993) were not found in Jurkine, indicating that the speciation of the group had already diversified in ecological adaptation during the Bessarabian.

Neogobius ignotus n. sp.
Figs. 7F–L

Holotype: Fig. 7J, NMNH ГКН 5960 009, Bessarabian, Jurkine, Crimea.

Paratypes: 12 specimens, NMNH ГКН 5960 010 and SMF PO 101.159, same data as holotype.

Etymology: From ignotus (Latin) = unfamiliar, obscure, referring to the unspectacular morphology of the otoliths.

Diagnosis: OL:OH = 1.0–1.07. High-bodied and thick otoliths, OH:OT = 2.8–3.0. Postdorsal projection broad, short, only slightly bent outwards; preventral projection short. Anterior and posterior rims inclined, nearly parallel, with concavities at level of sulcal tips anteriorly and posteriorly. Sulcus broad, sole-shaped, with rounded tips and low ostial lobe, inclined at 20–25°; no or very small subcaudal iugum. Outer face more strongly convex than inner face.

Description. Moderately large, high-bodied and relatively thick otoliths with a maximal size of 2.7 mm in length (holotype 2.25 mm). Dorsal rim highest posterior of its midpoint, with low predorsal angle and short, broad postdorsal projection, the latter only slightly bent outwards. Ventral rim flat, horizontal, with short, pointed preventral projection and broadly rounded postventral angle. Anterior and posterior rims inclined, nearly parallel; anterior rim with mild concavity directly above preventral projection at level of ostial tip; posterior rim with mild concavity below postdorsal projection at level of caudal tip. All rims smooth or slightly undulating.

Inner face slightly convex. Sulcus relatively short, with rounded sole-shape and low and rounded ostial lobe, moderately deepened; inclined at 20–25°. OL:SuL = 2.05–2.35. No or very small and indistinct subcaudal iugum. Ventral furrow feeble, not connected around sulcus to small and indistinct dorsal depression. Outer face convex, more strongly than inner face, smooth.

Discussion. *Neogobius ignotus* n. sp. differs from *N.* cf. *bettinae* in that it is more high-bodied (OL:OH = 1.0–1.07 *vs.* 1.1–1.3); has a shorter, wider sulcus (OL:SuL = 2.05–2.35 *vs.* 1.9–2.1) with rounded terminations; and has a less-regularly curved predorsal rim. Furthermore, it has a more compressed outline (OL:OH = 1.0–1.07 *vs.* 1.22–1.45), less-expressed rounded ostial lobe (*vs.* angular), and steeper inclined sulcus than *N. rhachis* Rückert-Ülkümen, 1993, which is known from the time-equivalent freshwater system of Ukraine and Turkey. For further comparison, otoliths were figured from all four extant *Neogobius* species: *N. caspius* (Eichwald, 1831) (Fig. 7W–X), *N. fluviatilis* (Pallas, 1814) (Fig. 7AA–AB), *N. melanostomus* (Pallas, 1814) (Fig. 7AC–AD), and *N. pallasi* (Berg, 1916) (Fig. 7Y–Z).

Neogobius uncinatus n. sp.
Figs. 7M-V

Holotype: Fig. 7M–O, NMNH ГКН 5960 011, Bessarabian, Jurkine, Crimea.

Paratypes: 6 specimens, NMNH ГКН 5960 012 and SMF PO 101.160, same data as holotype.

Etymology: From uncinatus (Latin) = hooked, referring to the strongly outward bent postdorsal projection.

Diagnosis: OL:OH = 0.97–1.15. Thin otoliths, OH:OT = 3.0–4.5, decreasing with size. Postdorsal projection broad, strongly bent outwards. Anterior rim near vertical and posterior rim slightly inclined. Sulcus relatively narrow, sole-shaped, with very low ostial lobe, inclined at 13–17°; no or very small subcaudal iugum. Outer face concave.

Description. Moderately large, high-bodied and relatively thin otoliths with a maximal size of 3.1 mm in length (holotype). Dorsal rim irregularly curved, with middorsal angle in small specimens (Fig. 7S, U) and more gently rounded in large ones. Predorsal angle rounded or obtuse angular; postdorsal projection broad, very strongly bent outwards. Ventral rim flat, horizontal, with variably developed preventral projection either blunt or pointed and nearly orthogonal postventral angle. Anterior and posterior rims nearly vertical or, in case of the latter, slightly inclined. Anterior rim variably without or with mild concavity directly above preventral projection; posterior rim straight or with very weak concavity at about midsection. All rims smooth or slightly undulating.

Inner face slightly convex; strongly convex towards posterior rim. Sulcus relatively short and narrow, sole-shaped, with very low ostial lobe, relatively shallow; inclined at 13–17°. OL:SuL = 2.05–2.1. No or very small and indistinct subcaudal iugum. Ventral furrow feeble, not connected around sulcus to very indistinct dorsal depression. Outer face distinctly concave in large specimens, flat with bent postdorsal projection in small ones, relatively smooth except of a diagonal ridge running to lower portion of postdorsal projection.

Discussion. *Neogobius uncinatus* n. sp. is readily recognized by its significantly outwardly bent postdorsal projection. This feature apparently develops early in the ontogeny and is recognizable even in specimens of only 1.25–1.6 mm in length (Figs. 7T, V). A similar but less significantly bent postdorsal projection is observed in the coeval freshwater to brackish water species *N. rhachis* (see Rückert-Ülkümen et al., 1993 and Bratishko et al., 2017 for figures) and the extant *N. caspius* (Fig. 7W–X).

However, *N. rhachis* is distinguished by a vertical edge on the inner face setting off the postdorsal region and a ridge supporting the postdorsal projection on the outer face. Additionally, *N. rhachis* tends to be less high-bodied, with an OL:OH ratio of 1.1–1.45 (after Rückert-Ülkümen et al. 1993 and Bratishko et al. 2017).

The otoliths of the extant *N. caspius* are more rectangular in outline with a higher predorsal angle and thinner than those of *N. uncinatus* n. sp. *Neogobius ignotus* differs from *N. uncinatus* n. sp. in the wider and more strongly inclined sulcus and the outward-bent postdorsal projection. *Neogobius uncinatus* n. sp. differs from the coeval *N.* cf. *bettinae* in its more high-bodied shape and less-regularly curved predorsal rim. Combined, these three species, as well as *N. rhachis* from the transitional freshwater to brackish water environment, indicate that *Neogobius* was already highly diverse during the Bessarabian, likely as an adaptation to the rapidly changing ecosystems in the Eastern Paratethys.

Genus *Zosterisessor* Whitley, 1935

Zosterisessor pontikapaionensis n. sp.
Figs. 7AE–AL

Holotype: Fig. 7AE–AF, NMNH ГКН 5960 013, Bessarabian, Jurkine, Crimea.

Paratypes: 17 specimens, NMNH ГКН 5960 014 and SMF PO 101.161, same data as holotype.

Etymology: After Pontikapaion, the ancient Greek name for Kerch.

Diagnosis: OL:OH = 1.1–1.2. Rectangular shape with high predorsal and orthogonal pre-and postventral angles. Dorsal rim irregularly undulating. Postdorsal projection short, slightly bent outwards. Anterior rim and posterior rims near vertical to slightly inclined. Sulcus sole-shaped, with low ostial lobe, inclined at 14–17°; no or indistinct subcaudal iugum. Outer face dorsally slightly concave, ventrally flat to slightly convex.

Description. Moderately large, rectangular otoliths with a maximal size of 3.5 mm in length (holotype 3.3 mm). Dorsal rim relatively straight, with high obtuse predorsal angle, irregularly undulating. Postdorsal projection short, broad or angular (Fig. 7AE) or rarely pointed (Fig. 7AI), slightly bent outwards. Ventral rim flat, horizontal, with short, mostly orthogonal preventral projection and nearly orthogonal postventral angle. Anterior and posterior rims nearly vertical or slightly inclined. Anterior rim without or with moderate concavity at level of ostial tip; posterior rim with very weak concavity at about

midsection. Anterior and dorsal rims irregularly undulating, ventral and posterior rims smooth.

Inner face slightly convex. Sulcus moderately long, rounded sole-shaped, with moderate to low ostial lobe, moderately deepened; inclined at 14–17°. OL:SuL = 1.85–2.1. No or very indistinct subcaudal iugum. Ventral furrow feeble, not connected around sulcus to small, relatively distinct dorsal depression. Outer face dorsally slightly concave, ventrally flat to slightly convex, relatively smooth.

Discussion. These otoliths are placed in *Zosterisessor* because of their sulcus with a low ostial lobe, indistinct or nonexistent subcaudal iugum, low inclination angle of the sulcus, and rectangular shape of the otolith. *Zosterisessor pontikapaionensis* n. sp. differs from *Neogobius* cf. *bettinae* in its high predorsal angle (*vs.* rounded predorsal region) and lower sulcus inclination angle (14–17° *vs.* 17–20°). *Zosterisessor pontikapaionensis* n. sp. differs from *Neogobius udovichenkoi* Bratishko, Schwarzhans & Reichenbacher, 2015 from the Konkian in its shorter postdorsal projection, slightly more compact outline, and lower sulcus inclination angle. While it resembles small specimens of *Mesogobius chersonesus*, it has less-pronounced preventral and postdorsal projections, a more rectangular outline, and lower index OL:OH (1.1–1.2 *vs.* 1.3–1.6). The Late Miocene *Z. exsul* Schwarzhans, Agiadi & Carnevale,

Fig. 7 - Gobiidae, *Neogobius* and *Zosterisessor*. A–E) *Neogobius* cf. *bettinae* Bratishko, Kovalchuk & Schwarzhans, 2017, NMNH ГКН 5960 008 (A–B) and SMF PO 101.158 (C–E), B, D dorsal views, Bessarabian, Jurkine. F–L) *Neogobius ignotus* n. sp., holotype (J) NMNH ГКН 5960 009, paratypes (F–I, K–L) NMNH ГКН 5960 010 (K–L) and SMF PO 101.159 (F–I), G, I, L dorsal views, Bessarabian, Jurkine. M–V) *Neogobius uncinatus* n. sp., holotype (M–O) NMNH ГКН 5960 011, paratypes (P–V) NMNH ГКН 5960 012 (R) and SMF PO 101.160 (P–Q, S–V), O outer face, N, Q, T, V dorsal views, Bessarabian, Jurkine. W–X) *Neogobius caspius* (Eichwald, 1831), ZMMU P.22622, X dorsal view, extant, 51°25'N, 46°03'E. Y–Z) *Neogobius pallasi* (Berg, 1916), ZMMU P.23514, Z dorsal view, extant, 43°28'N, 51°18'E. AA–AB) *Neogobius fluviatilis* (Pallas, 1814), ZMMU P.22433, AB dorsal view, extant, 45°20'N, 28°57'E. AC–AD) *Neogobius melanostomus* (Pallas, 1814), ZMMU P.23515, AD dorsal view, extant, 43°38'N, 51°08'E. AE–AL) *Zosterisessor pontipapaionensis* n. sp., holotype (AE–AF) NMNH ГКН 5960 013, paratypes (AG–AL) NMNH ГКН 5960 014 (AK–AL) and SMF PO 101.161 (AG–AJ), AF, AH, AJ, AL dorsal views, Bessarabian, Jurkine.

Neogobius cf. *bettinae*

Neogobius ignotus

Neogobius uncinatus

Neogobius caspius   *Neogobius pallasi*   *Neogobius fluviatilis*   *Neogobius melanostomus*

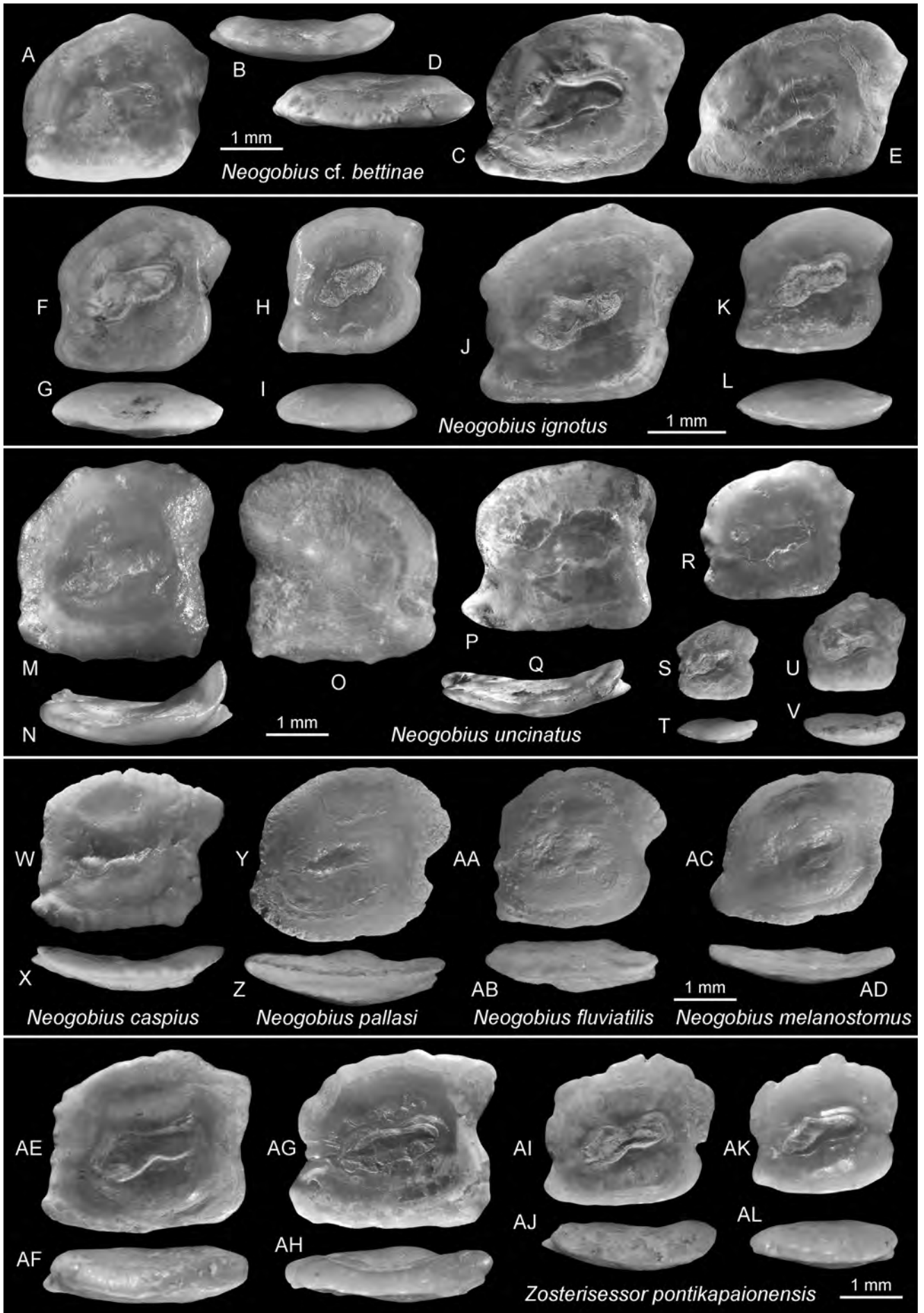*Zosterisessor pontikapaionensis*

FIGURE 7

2020 differs from *Z. pontikapaionensis* n. sp. in being slenderer (OL:OH = 1.25–1.4 *vs.* 1.1–1.2), showing a smaller sulcus and a more strongly developed postdorsal projection, and having a more regularly curved and finely crenulated dorsal rim. The relatively large sulcus in *Z. pontikapaionensis* n. sp. characterizes this species as a plesiomorphic member of the clade, differing from *Gobius* species in its lack or indistinct remnant of a subcaudal iugum and low sulcus inclination angle. *Zosterisessor exsul* is known in the Eastern Paratethys of the Khersonian to Maeotian (Schwarzhans et al. 2020a), as well as the Messinian of the Mediterranean (Schwarzhans et al. 2020a). Pobedina (1956) described *Gobius pricaspicus* Pobedina, 1956 from the Bessarabian of Azerbaidjan, which looks similar to *Z. pontikapaionensis* n. sp. in outline and proportions but differs markedly in its small and anteriorly shifted sulcus. Thus, it could represent a species of *Neogobius*. We have not identified such otolith morphology in Jurkine. *Z. pontikapaionensis* n. sp. differs from the morphologically similar otoliths of the extant *Zosterisessor ophiocepalus* (Pallas, 1814) (for figures, see Schwarzhans et al. 2020a) in terms of a more distinct preventral projection and shorter postdorsal projection.

Benthophilus Group (Benthophilini in Agorreta et al., 2013)

Pontogobius n. gen.

Type species: *Pontogobius ahnelti* n. sp.

Etymology: Named after the Pontian Basin as part of the Eastern Paratethys where Jurkine is located and the genus name *Gobius*. Gender masculine.

Diagnosis: A fossil otolith-based genus of the Gobiidae characterized by the following combination of characters. Otoliths moderately large, reaching sizes of up to 4.7 mm in length. Preventral and postventral angles prominent; postdorsal projection moderately developed, not or only slightly bent outwards. Longest measure of otolith from preventral to postventral tips; ratio OL:OH ranging from 1.03 to 1.35. Inner face nearly flat and noticeably smooth with faint ventral furrow, a dorsal depression with gradual margins, and a shallow sulcus. Sulcus very short, OL:SuL = 2.3–3.0, oval in shape without or with very indistinct ostial lobe and only very indistinct indention at ventral margin characterizing distinction of ostium and cauda; no subcaudal iugum. Outer face convex.

Discussion. Although we have access to an extensive collection of extant gobioid otoliths representing the vast majority of genera, we were unable to identify a morphotype that would sufficiently resemble *Pontogobius*. The smooth inner face and the small, shallow, oval sulcus resemble otoliths found in *Caspiosoma* Iljin, 1927 of the *Benthophilus* Group. Fossil otolith-based *Caspiosoma* species have been recorded as supposed Paratethyan immigrants in the Messinian of the Mediterranean (Schwarzhans et al., 2020a). However, *Pontogobius* otoliths grow to considerably larger sizes than those of *Caspiosoma* (3.3–4.7 mm *vs.* 1.2 mm in length). The otolith outline of *Pontogobius* has its longest distance from the preventral to the postventral tips, which creates a trapezoidal to near rectangular shape. Similar otoliths have been observed in the *Tridentiger* group of the northern Pacific, but these otoliths do not show such a small but more structured sulcus which is not oval in shape. At this stage, we consider a relationships of the highly characteristic otoliths of *Pontogobius* with the *Benthophilus* group to be the most likely.

Species. *Pontogobius ahnelti* n. sp., *Pontogobius trigonus* n. sp. and *Pontogobius zonatus* n. sp., all from the Bessarabian of Jurkine, Crimea.

Pontogobius ahnelti n. sp.
Figs. 8A–K

Holotype: Fig. 8A–B, NMNH ГКН 5960 015, Bessarabian, Jurkine, Crimea.

Paratypes: 8 specimens, NMNH ГКН 5960 016 and SMF PO 101.162, same data as holotype.

Referred specimens: 172 specimens, same data as holotype.

Etymology: Named in honor of Harald Ahnelt (Wien) in recognition of his contribution to the knowledge of Ponto-Caspian gobies.

Diagnosis: OL:OH = 1.03–1.15. Rectangular shape with high predorsal angle and nearly vertical anterior and posterior rims. Postdorsal projection short, not or very slightly bent outwards. Sulcus small, oval, shallow, inclined at 8–13°, OL:SuL = 2.2–2.4; no subcaudal iugum. Inner face nearly flat, outer face convex.

Description: Moderately large, moderately thick, nearly rectangular otoliths with a maximal size of 3.3 mm in length (holotype); OH:OT = 2.5–3.0.

Fig. 8 - Gobiidae, *Pontogobius*. A–K) *Pontogobius ahnelti* n. sp., holotype (A–B) NMNH ГКН 5960 015, paratypes (C–K) NMNH ГКН 5960 016 (G–J) and SMF PO 101.162 (C–F, K), B, F, I dorsal views, Bessarabian, Jurkine. L–W) *Pontogobius trigonus* n. sp., holotype (L–M) NMNH ГКН 5960 017, paratypes (N–W) NMNH ГКН 5960 018 (R–U) and SMF PO 101.163 (N–Q, V–W), M, P, U, W dorsal views, Bessarabian, Jurkine. X–AG) *Pontogobius zonatus* n. sp., holotype (X–Y) NMNH ГКН 5960 019, paratypes (Z–AG) NMNH ГКН 5960 020 (AD–AG) and SMF PO 101.164 (Z–AC), Y, AC, AD dorsal views, Bessarabian, Jurkine.

1mm

Pontogobius ahnelti

1 mm

Pontogobius trigonus

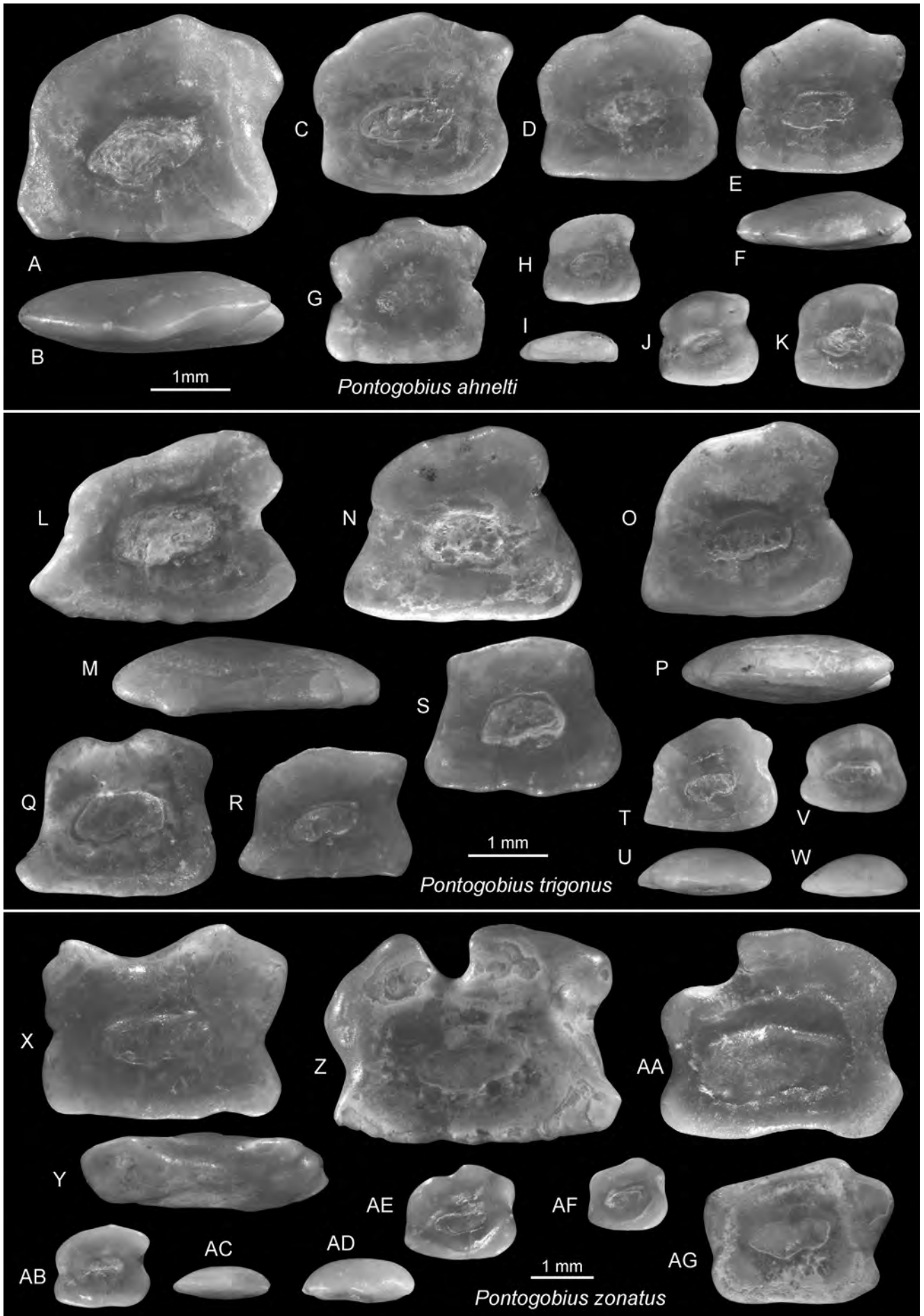1 mm

Pontogobius zonatus

FIGURE 8

Dorsal rim shallow, with high, orthogonal to obtuse predorsal angle and broad postdorsal angle, smooth, sometimes with broad and shallow concavities before and after postdorsal angle (Fig. 8E, G). Postdorsal projection short, not longer than postventral projection, not or very slightly bent outwards. Ventral rim flat, horizontal, with moderate preventral and postventral projections. Anterior and posterior rims nearly vertical. Anterior rim without or with feeble concavity at level of ostial tip; posterior rim with broad concavity above midsection.

Inner face nearly flat and rather smooth. Sulcus very short, oval, shallow, without ostial lobe and ventral indentation. No subcaudal iugum. Ventral furrow feeble, not connected around sulcus to wide dorsal depression with gradual margins. Outer face convex, smooth.

Discussion. *Pontogobius ahnelti* n. sp. is the most common of the three *Pontogobius* species in Jurkine. It differs from *P. trigonus* n. sp. in its rectangular (*vs.* trapezoidal) outline and from *P. zonatus* n. sp. in its more compressed shape (OL:OH = 1.03–1.15 *vs.* 1.2–1.33) and lack of indentations in the dorsal rim. Small specimens below 1.5 mm in length (Figs. 8H–K) tend to be slightly more compressed than larger ones (OL:OH <1.08) and can be well distinguished from small specimens of the other two species.

Pontogobius trigonus n. sp.
Figs. 8L–W

Holotype: Fig. 8L–M, NMNH ГКН 5960 017, Bessarabian, Jurkine, Crimea.

Paratypes: 7 specimens, NMNH ГКН 5960 018 and SMF PO 101.163, same data as holotype.

Referred specimens: 83 specimens, same data as holotype, and 1 specimen from micro-sample #12.

Etymology: From trigonus (Latin) = triangular, referring to the triangular to trapezoidal outline of the otoliths of this species.

Diagnosis: OL:OH = 1.08–1.35. Triangular to trapezoidal shape with high postdorsal angle and inclined anterior and posterior rims. Postdorsal projection short, not bent outwards. Preventral projection long, pointed. Sulcus small, oval, shallow, inclined at 5–10°, OL:SuL = 2.2–3.0; no subcaudal iugum. Inner face nearly flat, outer face convex.

Description. Moderately large, relatively thick, triangular to trapezoidal otoliths with a maximal size of 3.35 mm in length (holotype); OL:OH = 1.08–1.35, increasing with size; OH:OT = 2.1–2.45, decreasing with size. Dorsal rim shortened, with rounded or obtuse predorsal angle and highest

at short postdorsal projection, smooth. Ventral rim straight, horizontal, with long and pointed preventral projection and shorter postventral projection. Anterior rim inclined at 65–78°, usually broadly concave; posterior rim inclined at 73–83°, with concavity below postdorsal projection.

Inner face nearly flat and rather smooth. Sulcus very short, oval, shallow, without ostial lobe and without or very faint ventral indentation. No subcaudal iugum. Ventral furrow feeble, not connected around sulcus to wide dorsal depression with gradual margins. Outer face convex, smooth.

Discussion. *Pontogobius trigonus* n. sp. differs from the other two species in the genus through its long, pointed preventral projection and triangular to trapezoidal otolith outline. This characteristic is stable also in small specimens (Figs. 8T–W) although they are usually less elongate but thicker. The expression and height of the predorsal angle is relatively variable and thus of limited use for species differentiation.

Pontogobius zonatus n. sp.
Figs. 8X–AG

Holotype: Fig. 8X–Y, NMNH ГКН 5960 019, Bessarabian, Jurkine, Crimea.

Paratypes: 6 specimens, NMNH ГКН 5960 020 and SMF PO 101.164, same data as holotype.

Referred specimens: 88 specimens, same data as holotype.

Etymology: From zona (Latin) = belt, girdle, referring to indentation or concavity of the dorsal rim.

Diagnosis: OL:OH = 1.2–1.35. Rectangular shape with high predorsal angle and nearly vertical anterior and posterior rims. Dorsal rim with broad central concavity or indentation or anteriorly depressed. Postdorsal projection short, not or very slightly bent outwards. Sulcus small, oval, shallow, inclined at 5–10°, OL:SuL = 2.3–2.7; no subcaudal iugum. Inner face nearly flat, outer face convex.

Description. Relatively large, moderately thick, nearly rectangular otoliths with a maximal size of 4.7 mm in length (holotype 3.85 mm); OH:OT = 2.1–2.6. Dorsal rim shallow, with orthogonal to obtuse predorsal angle, with broad central concavity, or more narrow indentation or depressed predorsal section. Postdorsal projection short, not or rarely slightly longer than postventral projection, not or very slightly bent outwards. Ventral rim straight, horizontal, with moderate preventral and postventral projections. Anterior and posterior rims nearly vertical, both with variably developed concavities at midsection.

Inner face nearly flat and rather smooth. Sulcus very short, oval, shallow, without ostial lobe

and ventral indentation. No subcaudal iugum. Ventral furrow feeble, not connected around sulcus to wide dorsal depression with gradual margins. Outer face convex, smooth.

Discussion. *Pontogobius zonatus* n. sp. resembles *P. ahnelti* in shape but is more elongate (OL:OH = 1.2–1.33 *vs.* 1.03–1.15), a stable characteristic even in small specimens (Figs. 8AB–AF). The indentation of the dorsal rim or the predorsal depression is a further distinctive characteristic of *P. zonatus* n. sp., but it is typically not well developed in small specimens.

Aphia Lineage sensu Agorreta et al., 2013
Globogobius n. gen.

Type species: *Globogobius globulosus* n. sp.
Etymology: Named after the globular, bulbous subcaudal iugum and the genus name *Gobius*. Gender masculine.
Diagnosis: A fossil otolith-based genus of the Gobiidae characterized by the following combination of characters. Otoliths relatively small, barely exceeding 2.0 mm in length. Ventral rim straight, its preventral and postventral angles distinct; dorsal rim high, or with predorsal depression. Longest measure of otolith from preventral to postventral tips; ratio OL:OH ranging from 0.9 to 1.08. Inner face nearly flat; ventral furrow close to ventral rim of otolith, dorsal depression broad, deep. Sulcus short, OL:SuL = 1.8–2.4, moderately deepened, with low ostial lobe and very distinct, globular, bulbous, short subcaudal iugum. Outer face convex.

Discussion. *Globogobius* resembles otoliths of the extant *Lesueurigobius* Whitley, 1950 but differs in its small sulcus, bulbous subcaudal iugum, and slightly more high-bodied shape. A number of fossil genera have been recently described that may pertain to the *Aphia* Lineage and may be related to *Lesueurigobius* and *Globogobius*. These are *Hoeseichthys* Schwarzhans, Brzobohatý & Radwanska, 2020 in the Middle and Late Miocene and the genera with otoliths in situ recently described by Reichenbacher and Bannikov (2021) from the upper Sarmatian s.l. (Volhynian) of Moldova: *Katyagobius, Pseudolesueurigobius, Sarmatigobius*, and *Yarigobius*. These genera share a relatively small sulcus, smaller than the extant *Lesueurigobius*, and in the case of *Hoeseichthys*, are also characterized by a nearly oval sulcus outline. *Globogobius* differs from all of these genera in its bulbous, albeit rather small, subcaudal iugum. It further differs from the four Volhynian genera described by Reichenbacher & Bannikov (2021) in its straight, horizontal ventral rim (*vs.* curved, convex). We believe that *Golobogobius* represents another endemic evolution of the *Aphia* Lineage during the

Bessarabian of the Eastern Paratethys. Another similar morphotype has been described as *Knipowitschia suavis* Schwarzhans 2014, which has now been placed in the fossil genus *Moldavigobius* Reichenbacher & Bannikov, 2022 based on otoliths found in situ in a related species (Reichenbacher & Bannikov 2022). This species was originally described from the Serravallian of southeastern Turkey and was also later recorded from the coeval Konkian of the Eastern Paratethys by Bratishko et al. (2015). *Moldavigobius suavis* resembles *Globogobius* in the outline but have a larger sulcus and a longer, less elevated subcaudal iugum that characteristically bends around the posterior tip of the cauda. *Moldavigobius* has also been interpreted to belong to the *Aphia* Lineage by Reichenbacher & Bannikov (2022). Finally, the outline of *Globogobius* also resembles that of otoliths of the fossil genus *Hesperichthys* Schwarzhans, Ahnelt, Carnevale & Japundžić, 2017 of the *Pomatoschistus* Lineage, particularly *H. gironeae* Schwarzhans, Agiadi & Carnevale, 2020 from the Tortonian of Italy. However, it differs from this genus because it is characterized by a globular subcaudal iugum (*vs.* no subcaudal iugum) and a sulcus shape with a low ostial lobe (*vs.* oval without ostial lobe).

Species. Two species, both from the Bessarabian of Jurkine, Crimea: *Globogobius globulosus* n. sp. and *Globogobius depressus* n. sp.

Globogobius globulosus n. sp.
Figs. 9A–K

?1956 *Otolithus* (*Gobius*) *pretiosus* Prochaska, 1893 - Pobedina: pl. 23, fig. 6.

Holotype: Fig. 9E–F, NMNH ГКН 5960 021, Bessarabian, Jurkine, Crimea.
Paratypes: 7 specimens, NMNH ГКН 5960 022 and SMF PO 101.165, same data as holotype.
Referred specimens: 836 specimens, same data as holotype, and 1 specimen from micro-sample #12 and 1 specimen from micro-sample #14.
Etymology: From globulosus (Latin) = globular, referring to the bulbous nature of the small subcaudal iugum.
Diagnosis: Dorsal rim high, convex. Otolith higher than long, OL:OH = 0.9–1.0; OL:SuL = 2.0–2.4. Dorsal depression closed towards dorsal rim (rarely opening).

Description. Relatively small, moderately thick, high-bodied otoliths with a maximal size of 2.05 mm in length (holotype 2.03 mm); OH:OT = 2.5–3.3. Dorsal rim high, regularly curved, highest at its middle or slightly before or behind, smooth. Postdorsal projection very weak, not bent outwards.
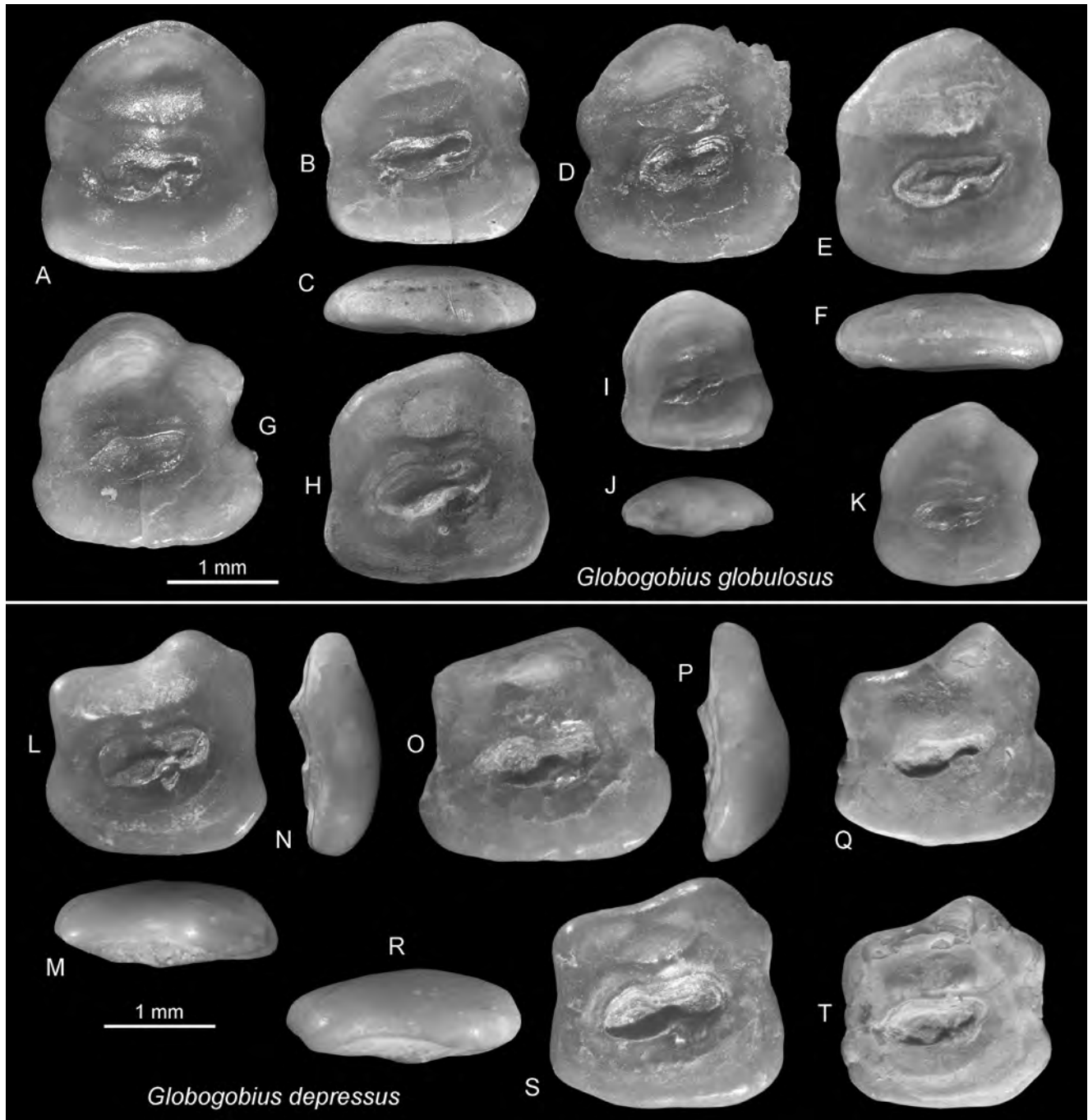
Fig. 9 - Gobiidae, *Globogobius*. A-K) *Globogobius globulosus* n. sp., holotype (E–F) NMNH ГКН 5960 021, paratypes (A–D, G–K) NMNH ГКН 5960 022 (B–D) and SMF PO 101.165 (A, G–K), C, F, J dorsal views, Bessarabian, Jurkine. L–T) *Globogobius depressus* n. sp., holotype (L–N) NMNH ГКН 5960 023, paratypes (O–T) NMNH ГКН 5960 024 (T) and SMF PO 101.166 (O–S), M, R dorsal views, N, P posterior views, Bessarabian, Jurkine.

Ventral rim straight, horizontal, with moderate preventral and postventral angles. Anterior and posterior rims nearly vertical or slightly inclined towards dorsal. Anterior rim with very feeble concavity at midsection; posterior rim with more distinct concavity at midsection.

Inner face nearly flat with centrally positioned sulcus. Sulcus short, deepened, with low and rounded ostial lobe and weak ventral indentation. OL:SuL = 2.0–2.4; sulcus inclination angle 8–14°. Distinct, small, but well exposed globular, bulbous subcaudal iugum. Ventral furrow mostly feeble, close to ventral rim of otolith, not connected around sulcus to wide dorsal depression. Dorsal depression with gradual margins, deep, usually closed to dorsal rim. Outer face convex, smooth.

Discussion. This characteristic otolith is among the three most common otolith-based species in Jurkine, along with *Palimphemus cimmerius* and *Hyrcanogobius eccentricus* n. sp. Its characteristic globular, bulbous subcaudal iugum is easily affected by erosion since it sticks out from the inner face. Therefore, only well-preserved specimens show this trait in its typical expression (compare Figs. 9A, E, H with 9B, D, K).

An otolith figured by Probedina (1956) from the middle Sarmatian s.l. (Bessarabian) of Azerbaijan as *Gobius pretiosus* Prochazka, 1893 is tentatively placed in *G. globulosus* n. sp. It resembles the specimens from Jurkine in all aspects except that Pobedina did not depict a subcaudal iugum. However, the subcaudal iugum was not generally recognized at that time, and Pobedina may have overlooked this feature for her drawing. Alternatively, it may have been eroded. If really absent, the otolith could represent a species of *Hesperichthys*. The specimen should eventually be restudied, or comparative otoliths might be recovered from coeval sediments of the Caspian Basin for a more certain identification.

Globogobius depressus n. sp.
Figs. 9L–T

Holotype: Fig. 9L–N, NMNH ГКН 5960 023, Bessarabian, Jurkine, Crimea.

Paratypes: 21 specimens, NMNH ГКН 5960 024 and SMF PO 101.166, same data as holotype.

Etymology: From depressus (Latin) = depressed, referring to the broadly concave dorsal rim.

Diagnosis: Dorsal rim with broad concavity or depression. Otolith about as high as long, OL:OH = 1.0–1.08; OL:SuL = 1.8–2.0. Dorsal depression opens towards depressed dorsal rim.

Description. Relatively small, moderately thick, and moderately high-bodied otoliths with a maximal size of 2.2 mm in length (holotype 1.98 mm); OH:OT about 2.5. Dorsal rim moderately high, with broad and distinct depression and only the postdorsal angle being elevated, smooth. Postdorsal projection very weak, not bent outwards. Ventral rim straight, horizontal, with moderate preventral and postventral angles. Anterior and posterior rims slightly inclined towards dorsal. Anterior rim with very feeble concavity at midsection; posterior rim with more distinct concavity at midsection.

Inner face nearly flat with centrally positioned sulcus. Sulcus moderately long and wide, deepened, with low and rounded ostial lobe and weak ventral indentation. OL:SuL = 1.8–2.0; sulcus inclination angle 8–12°. Distinct, small, but well-exposed globular, bulbous subcaudal iugum. Ventral furrow mostly feeble, close to ventral rim of otolith, not connected around sulcus to wide dorsal depression. Dorsal depression with gradual margins, deep, opening to concavity of dorsal rim. Outer face convex, smooth.

Discussion. *Globogobius depressus* n. sp. differs from the coeval *G. globulosus* in the broad concavity of the dorsal rim, dorsally open dorsal depression, and slightly larger sulcus, as reflected in a lower OL:SuL ratio (1.8–2.0 *vs.* 2.0–2.4). *Globogobius depressus* n. sp. is much less common at Jurkine than *G. globulosus*, but the key diagnostic character (the dorsal depression) may not be fully developed in small specimens below 1.5 mm in length. Therefore, small specimens may not be fully distinguishable from *G. globulosus*.

Asterropteryx Lineage sensu Agorreta et al., 2013
Genus *Amblyeleotris* Bleeker, 1874

Amblyeleotris robusta n. sp.
Figs. 10A–I

Holotype: Fig. 10A–C, NMNH ГКН 5960 025, Bessarabian, Jurkine, Crimea.

Paratypes: 2 specimens (Fig. 10D–G), NMNH ГКН 5960 026 and SMF PO 101.167, same data as holotype.

Tentatively assigned specimens: 2 specimens (Fig. 10H–I), NMNH ГКН 5960 064, same data as holotype

Etymology: From robustus (Latin) = robust, referring to the massive appearance of the otoliths.

Diagnosis: OL:OH = 0.85–0.95; OH:OT = 2.2–2.8. High-bodied shape, with irregular undulation of dorsal rim. Postdorsal projection broad, moderately long, not or slightly bent outwards. Sulcus small, nearly oval with low and rounded ostial lobe, inclined at 20–26°, OL:SuL = 1.7–2.1; no subcaudal iugum. Inner face nearly flat, outer face distinctly convex.

Description. Relatively small, moderately thick, high-bodied otoliths with a maximal size of 1.6 mm in length (holotype). Dorsal rim high, ascending from slightly projecting, rounded predorsal angle to postdorsal angle, irregularly undulating. Postdorsal projection weak, not or slightly bent outwards. Ventral rim straight, horizontal, with rounded preventral and postventral angles. Anterior and posterior rims nearly vertical. Anterior rim with broad very feeble concavity at level of ostial tip; posterior rim with more distinct concavity at level of caudal tip.

Inner face slightly bent in horizontal direction, not bent in vertical direction, with centrally to

slightly inframedian positioned sulcus. Sulcus short, variably deepened but mostly rather shallow, with low and rounded ostial lobe and without or with indistinct ventral indentation. Sulcus steeply inclined at 20–26°. No subcaudal iugum. Ventral furrow very feeble, at some distance from ventral rim of otolith, not connected around sulcus to moderately wide dorsal depression with indistinct margins. Outer face convex, smooth, with some irregular furrows along dorsal margin.

Discussion. *Amblyeleotris robusta* n. sp. is the last record of the group known thus far from the European seas. It differs from *A. radwanskaae* Schwarzans, 2010 from the early and late Badenian of the Central Paratethys in that is it less compressed (OL:OH = 0.85–0.95 *vs.* 0.75–0.87), has a less strongly curved dorsal rim, and lacks a subcaudal iugum (*vs.* large and distinct subcaudal iugum). Among recent species of *Amblyeleotris*, a similar outline has been observed in otoliths of *A. fontanesii* (Bleeker, 1853) (see Schwarzans et al., 2020b for figure), but *A. robusta* n. sp. differs in terms of its less-curved dorsal rim, greater thickness, and convex outer face (*vs.* concave).

Amblyeleotris robusta n. sp. is a relative rare species in Jurkine, and the best preserved specimen was selected as holotype. One paratype (Fig. 10D, E) has a damaged postventral section but is otherwise well preserved. The second paratype (Fig. 10F, G) differs in the highest point of the dorsal rim, which was shifted forward of the middle of the rim, likely reflecting variability. Two further non-type specimens are rather eroded with a smoothened inner face (Fig. 10H, I as example). These specimens show a relatively strong postdorsal projection. Therefore, we allocate them only tentatively to the species.

Subfamily Gobionellinae Bleeker, 1874
Pomatoschistus Lineage sensu Agorreta et al. 2013
Genus *Hyrcanogobius* Iljin, 1928

Hyrcanogobius eccentricus n. sp.
Figs. 10J-S

Holotype: Fig. 10L–M, NMNH ГКН 5960 027, Bessarabian, Jurkine, Crimea.
Paratypes: 7 specimens, NMNH ГКН 5960 028 and SMF PO 101.168, same data as holotype.
Referred specimens: 877 specimens, same data as holotype; in addition 11 specimens from micro-samples #12 (1), #13 (3) and #14 (7).

Etymology: From eccentricus (Latin) = eccentric, referring to the eccentric position of the sulcus.
Diagnosis: OL:OH = 0.92–1.07; OH:OT = 2.0–2.7. Rounded tetragonal shape, with rounded dorsal rim and rather straight anterior, ventral and posterior rims. Postdorsal projection indistinct, not bent outwards. Sulcus small, shallow, forward positioned nearly oval with low and rounded ostial lobe, narrowed cauda, inclined at 14–21°, OL:SuL = 2.2–2.4; subcaudal iugum wide, below entire cauda, shallow. Inner face slightly bent with edge separating postdorsal region from rest of inner face, inclined at 70–75°; outer face convex.

Description. Small, thick otoliths with nearly tetragonal shape reaching a maximal size of 1.25 mm in length (holotype). Dorsal rim regularly rounded, smooth. Postdorsal projection broad, indistinct, not bent outwards. Ventral rim straight, horizontal, with rounded orthogonal preventral and postventral angles. Anterior and posterior rims nearly vertical. Anterior rim without concavity, smooth; posterior rim with weak, broad concavity at midsection.

Inner face nearly flat, smooth, with eccentrically, forward positioned sulcus. Sulcus short, shallow, anteriorly oval with low and rounded ostial lobe and posteriorly with narrowed, tapering, short cauda. Sulcus moderately inclined at 14–21°. Subcaudal iugum, large, wide, extending below entire cauda, but shallow and often not very well marked. Steeply inclined edge separates postdorsal region from remainder of inner face at angle of 70–75°. Ventral furrow feeble, moderately close to ventral rim of otolith, connected around cauda to wide dorsal depression with gradual margins. Outer face convex, smooth.

Discussion. *Hyrcanogobius eccentricus* n. sp. is similar to otoliths of the extant *H. bergi* Iljin, 1928 (Figs. 10T–V), which is endemic in the Caspian Sea. The differences between the two species are all subtle, the most significant being the presence of the edge on the inner face that separates the postdorsal region from the rest of the inner face; this feature is not seen in the extant species. The sulcus tends to be slightly larger in *H. eccentricus* n. sp., and the subcaudal iugum is larger in *H. bergi*. *Hyrcanogobius eccentricus* n. sp. clearly belongs to the lineage leading to the extant *H. bergi* and represents the first fossil record in this hitherto monotypic genus.

Gobiidae indet. juv.
Figs. 10W–AC

Material: 153 specimens of sizes from 0.1 to 0.7 mm in length, including 16 specimens from micro-sample #12, 5 specimens from micro-sample #13, 55 specimens from micro-sample #14 and 6 specimens from micro-sample #15.
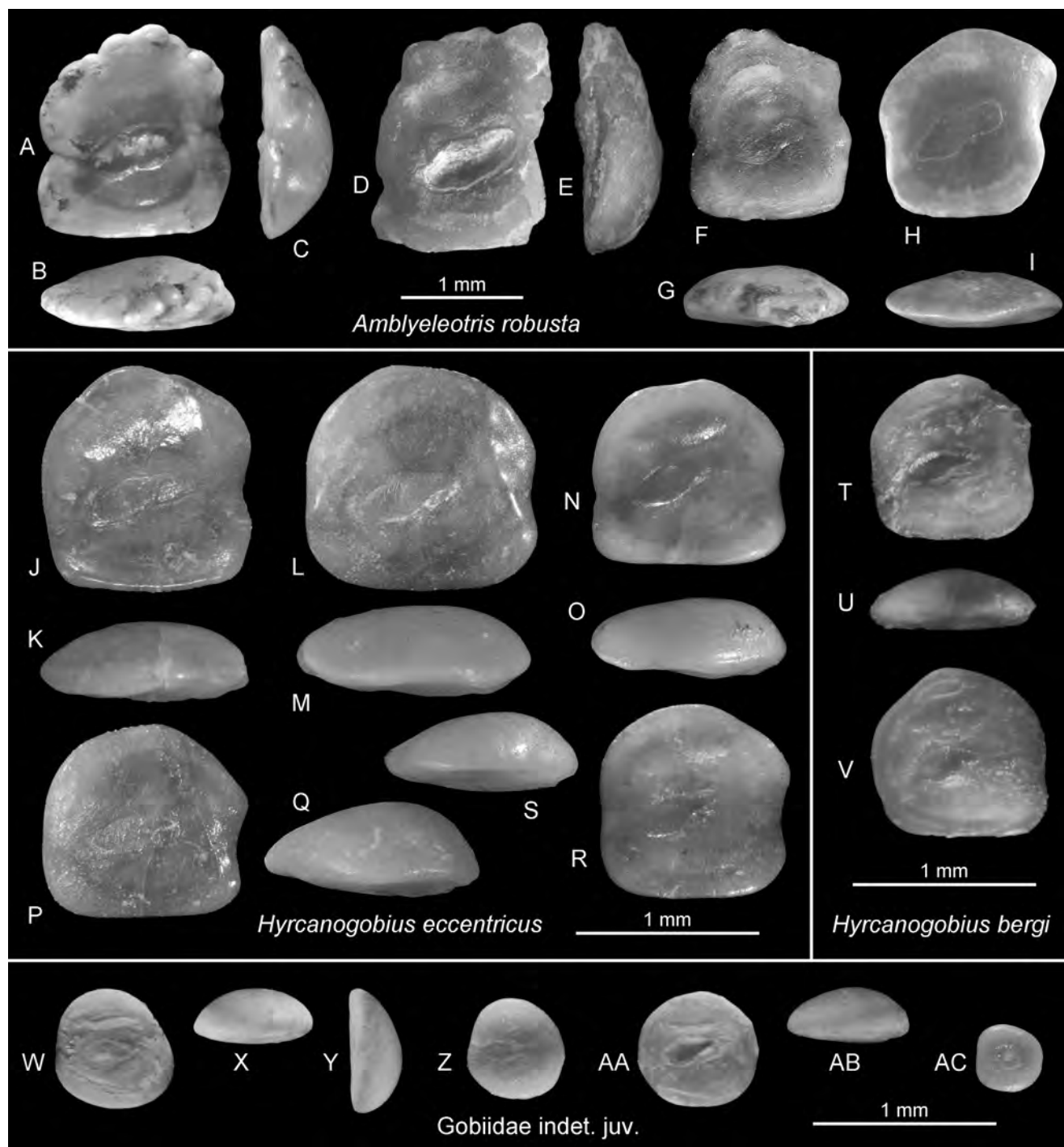
Fig. 10 - Gobiidae, *Amblyeleotris* and *Hyrcanogobius*. A–I) *Amblyeleotris robusta* n. sp., holotype (A–C) NMNH ГКН 5960 025, paratypes (D–G) NMNH ГКН 5960 026 (F–G) and SMF PO 101.167 (D–E), tentatively assigned specimen (H–I) NMNH ГКН 5960 064, B, G, I dorsal views, C, E posterior views, Bessarabian, Jurkine. J–S) *Hyrcanogobius eccentricus* n. sp., holotype (L–M) NMNH ГКН 5960 027, paratypes (J–K, N–S) NMNH ГКН 5960 028 (R–S) and SMF PO 101.168 (J–K, N–Q), K, M, O, Q, S dorsal views, Bessarabian, Jurkine. T–V) *Hyrcanogobius bergi* Iljin, 1928, ZMMU P.4658, U dorsal view, extant, northern Caspian Sea. W–AC) Unidentifiable juvenile Gobiidae, X, AB, dorsal views, Y posterior view, Bessarabian, Jurkine.

Discussion. A subsample processed to mesh sizes of 0.3 and 0.55 mm yielded abundant small gobiid otoliths that can not be identified in detail. They are more or less round with a flat inner and convex outer face and a small, oval sulcus. They most likely represent juveniles of one or several goby taxa. Some show a long subcaudal iugum (Fig. 10AA) and could represent juveniles of *Hyrcanogobius eccentricus*.

Family Microdesmidae Regan, 1912
Subfamily Ptereleotrinae Bleeker, 1875
Genus *Paroxymetopon* n. gen.

Type species: *Paroxymetopon alienus* n. sp.

Etymology: Combination of para (Greek) = similar and the genus name *Oxymetopon* indicating the presumed phylogenetic relationship.

Diagnosis: A fossil otolith-based genus of the Microdesmidae, subfamily Ptereleotrinae, characterized by the following combination of characters. Otolith small, <1.5 mm in length. Outline of otolith very characteristically formed by broad dorsal field and narrow ventral field at a relation of about 4:3. OL:OH = 0.87; OH:OT = 2.7. Inner face flat; outer face convex. Sulcus shallow, short, inframedian, oval in shape with small central ventral indentation, no subcaudal iugum; OL:SuL = 3.0. Ventral furrow distinct, half-moon shape, very close to sulcus and well connected behind sulcus with narrow, half-moon-shaped dorsal depression giving the impression of a circular furrow around the sulcus.

Discussion. *Paroxymetopon* is a highly diagnostic otolith characterized by the combination of a ventral field that is narrower than the dorsal field and a circumsulcal furrow close to the sulcus. This otolith morphotype is shared only with *Oxymetopon* Bleeker, 1860 (see Figs. 10A–I) and is unique amongst gobioids. *Paroxymetopon* differs from *Oxymetopon* in its flat inner and convex outer face (*vs.* slightly bent inner and flat outer face) and oval sulcus (*vs.* bent sole-shaped). In fact, the sulcus morphology appears more derived in *Paroxymetopon* than in *Oxymetopon*, and both genera are clearly related. Since extant ptereleotrine otoliths have rarely been figured, we show otoliths of several genera in the subfamily for comparison: *Aioliops megastigma* Rennis & Hoese, 1987 (Figs. 10J-M), *Ioglossus* sp. (Fig. 10Q–R), *Nemateleotris decora* Randall & Allen, 1973 (Fig. 10V–W), *Nemateleotris magnifica* Fowler, 1938 (Fig. 10S–U), *Oxymetopon compressus* Chan, 1966 (Fig. 10G–I), *Oxymetopon cyanoctenosum* Klausewitz & Condé, 1981 (Fig. 10D–F), *Parioglossus formosus* (Smith, 1931) (Fig. 10N–P), *Ptereleotris evides* (Jordan & Hubbs, 1925) (Fig. 10X–Z), *Ptereleotris hanae* (Jordan & Snyder, 1901) (Fig. 10AC–AE), *Ptereleotris microlepis* (Bleeker, 1856) (Fig. 10AF–AH), and *Ptereleotris uroditaenia* Randall & Hoese, 1985 (Fig. 10AA–AB). Otoliths from *Navigobius* Hoese & Motomura, 2009 and the monotypic *Zagadkogobius* Prokofiev, 2017 are unknown. Our comparison shows that three otolith morphotypes exist in the Ptereleotrinae. One, which was apparently the most derived, comprises only *Oxymetopon* and the fossil *Paroxymetopon*. The second comprises the small fishes of the genera *Aioliops* Rennis & Hoese, 1987 and *Parioglossus* Re-

gan, 1912, and the third comprises *Ioglossus* Bean, 1882, *Nemateleotris* Fowler, 1938, and *Ptereleotris* Gill, 1863. To the best of our knowledge, *Paroxymetopon* is the first fossil record of the subfamily and furthermore documents that some Indo-Pacific faunal influence existed in the Eastern Paratethys as late as the Bessarabian (early Tortonian).

Species. Monospecific genus, *Paroxymetopon alienus* n. sp. from the Bessarabian of Jurkine, Crimea.

Paroxymetopon alienus n. sp.
Fig. 11A–C

Holotype (and unique specimen): Fig. 11A–C, NMNH ГКН 5960 029, Bessarabian, Jurkine, Crimea.

Etymology: From alienus (Latin) = alien, strange, referring to the unusual otolith morphotype.

Diagnosis: See generic diagnosis (monospecific genus).

Description. Small, thick otolith of 1.35 mm in length (holotype). Otolith shape characterized by wide dorsal field and narrow ventral field at ratio of about 4:3. Dorsal rim regularly rounded, its predorsal and postdorsal projection broadly and distinctly protruding, slightly undulating. Ventral rim deep, rounded, much shorter than dorsal rim. Anterior and posterior rims inclined towards ventral at 75–80°, both with broad, shallow concavities at midsection.

Inner face flat, with distinctly inframedian, slightly forward positioned sulcus. Sulcus short, shallow, regularly oval in shape without ostial lobe but

Fig. 11 - Microdesmidae, Ptereleotrinae. A–C) *Paroxymetopon alienus* n. sp., holotype NMNH ГКН 5960 029, B anterior view, C dorsal view, Bessarabian, Jurkine. D–F) *Oxymetopon cyanoctenosum* Klausewitz & Condé, 1981, SMF P.17582, E anterior view, F dorsal view, extant, off Manila, Philippines. G–I) *Oxymetopon compressus* Chan, 1966, SMF P.22084, H anterior view, I dorsal view, extant, Philippines. J–M) *Aioliops megastigma* Rennis & Hoese, 1987, WAM 30810-004, K anterior view, L dorsal view, extant, 05°36'S, 106°32'E. N–P) *Parioglossus formosus* (Smith, 1931), WAM 32977-008, O anterior view, P dorsal view, extant, 01°41'N, 127°32'E. Q–R) *Ioglossus* sp., USNM 348994, R anterior view, extant, Sea of Cortez. S–U) *Nemateleotris magnifica* Fowler, 1938, SMF P.21775, T anterior view, U dorsal view, extant, Philippines. V–W) *Nemateleotris decora* Randall & Allen, 1973, SMF P.19608, W anterior view, extant, Philippines. X–Z) *Ptereleotris evides* (Jordan & Hubbs, 1925), SMF P.17892, Y anterior view, Z dorsal view, extant, Philippines. AA–AB) *Ptereleotris uroditaenia* Randall & Hoese, 1985, BSKU 110752, AB posterior view, extant, Philippines. AC–AE) *Ptereleotris hanae* (Jordan & Snyder, 1901), SMF P.19977, AD anterior view, AE dorsal view, extant, Philippines. AF–AH) *Ptereleotris microlepis* (Bleeker, 1856), BSKU 67982, AG anterior view, AH dorsal view, extant, Philippines.

Paroxymetopon alienus

Oxymetopon cyanoctenosum

Oxymetopon compressus

Aioliops megastigma

Parioglossus formosus

Ioglossus sp.

Nemateleotris magnifica

Nemateleotris decora

Ptereleotris evides

Ptereleotris uroditaenia

Ptereleotris hanae
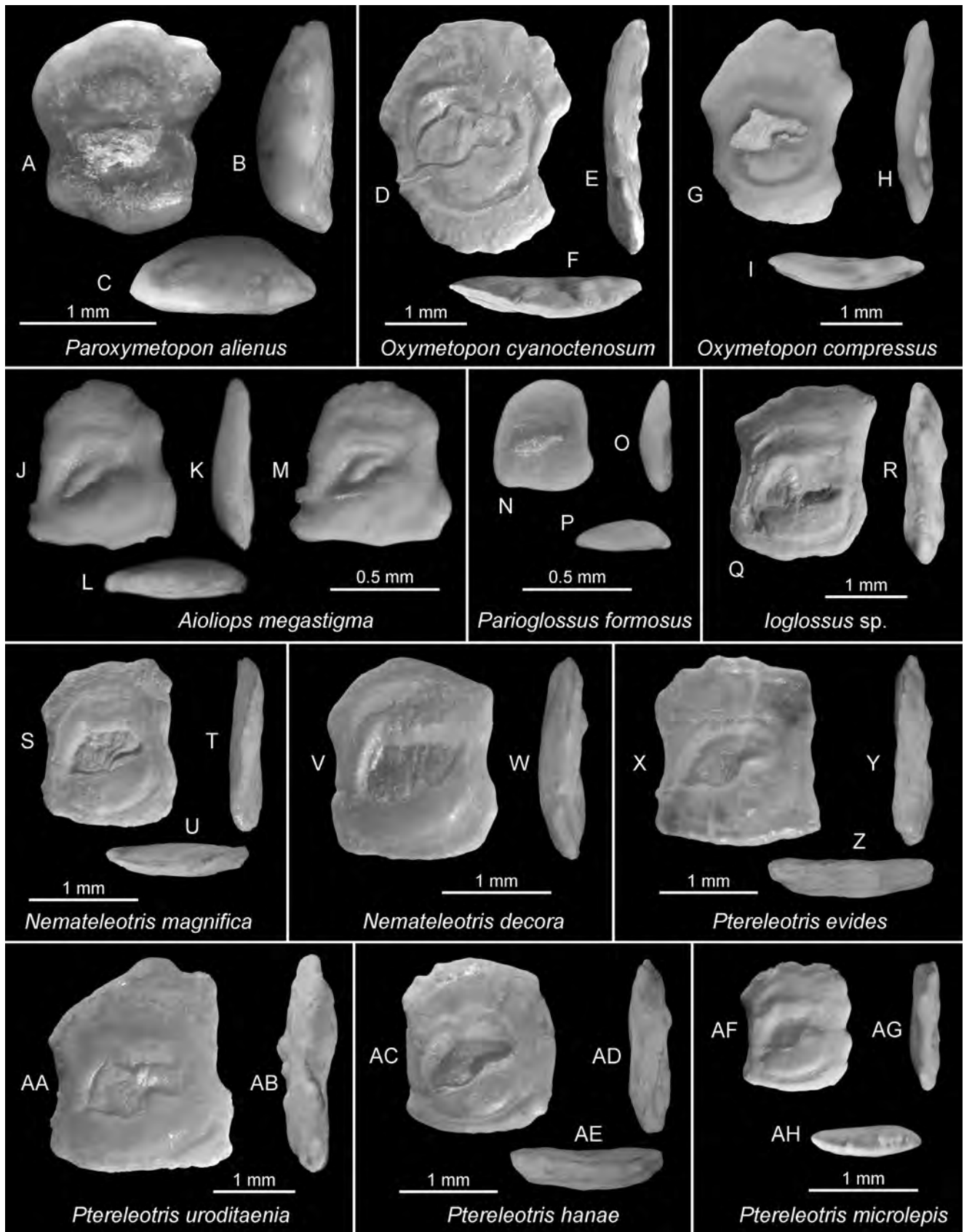
Ptereleotris microlepis

FIGURE 11

small indentation of ventral margin at about mid-section. Sulcus slightly inclined at 5°. No subcaudal iugum. Ventral furrow distinct, regularly half-moon shape, very close to sulcus and connecting around sulcus with narrow, half-moon-shaped dorsal depression resulting in a circumsulcal furrow. Outer face convex, smooth.

Order **Mugiliformes** Regan, 1909
Family Mugilidae Risso, 1827
Genus *Chelon* Artedi in Röse, 1793

Chelon jurkinensis n. sp.
Figs. 12A-G

Holotype: Fig. 12C–D, NMNH ГКН 5960 030, Bessarabian, Jurkine, Crimea.
Paratypes: 3 specimens, NMNH ГКН 5960 031 and SMF PO 101.169, same data as holotype.
Referred specimens: 39 specimens, same data as holotype.
Etymology: Named after the type location Jurkine on the Kerch Peninsula, Crimea.
Diagnosis: OL:OH = 2.15–2.25. All rims intensely crenulated. Dorsal and ventral rims shallow; predorsal region with obtuse angle, postdorsal region not depressed. Otolith mildly bent along long axis, thin (OH:OT = 3.2–3.5). Ostium short; cauda narrow, upward oriented, with short, moderately bent tip.

Description. Slender, elongate and thin otoliths, which are often broken, up to at least 4 mm in length (holotype 3.6 mm). Dorsal rim low, with obtuse predorsal angle above anterior part of cauda; postdorsal region shallow but not depressed. Ventral rim shallow, more or less regularly curved. Rostrum distinct, length 15–20% of OL; excisura and antirostrum small, variable. Posterior tip pointed or blunt, variable. All rims intensely crenulated.

Inner face moderately strongly bent in horizontal direction with slightly supramedian positioned sulcus. Ostium moderately widened and short; cauda long, narrow, upward oriented at angle of 3–6°, with short, moderately downturned tip. CaL:OsL = 1.85–2.45. Dorsal depression relatively distinct, long, narrow; ventral furrow distinct, distant from ventral rim and almost straight, terminating well deeper than tip of cauda. Indistinct furrows reaching from marginal crenulation to dorsal depression and ventral furrow respectively. Outer face slightly concave to almost flat with irregular ornamentation.

Discussion. Two fossil otolith-based *Chelon* species have been described thus far: *C. gibbosus* Reichenbacher & Weidmann, 1992 from the upper

Oligocene and Lower Miocene of the Upper Rhine Valley and *C. reichenbacherae* Schwarzhans & Wienrich, 2009 from the Lower and Middle Miocene of the North Sea Basin. Further *Chelon* sp. otoliths were described by Bratishko et al. (2015) from the Konkian of Kazakhstan, which are rather compressed with a short rostrum. *Chelon jurkinensis* n. sp. differs from all of these species in its slenderer shape (OL:OH = 2.15–2.25 *vs.* 1.7–2.0), its thin and only mildly bent appearance, and its lower, more angular predorsal rim. The absence of a postdorsal depression and the rather mildly bent caudal tip (*vs.* postdorsal rim depressed and caudal tip bent at about 90°) distinguishes *Chelon* otoliths from those of *Liza* Jordan & Swain, 1884, from which a total of five species have been described from the Lower to Upper Miocene of several European Basins. The more or less coeval *Liza voesendorfensis* (Weinfurter, 1953) from the Pannonian of Austria clearly differs in its strongly depressed entire dorsal rim (as opposed to the deeply curved ventral rim), the short rostrum, and strong curvature along the horizontal axis.

Order **Atheriniformes** Rosen, 1964
Family Atherinidae Risso, 1821
Genus *Atherina* Linnaeus, 1758

Atherina gidjakensis (Pobedina, 1956)
Figs. 12H–O

1956   Ot. (*Clupea*) *gidjakensis* - Pobedina: pl. 27, fig. 4.
2015   *Atherina gidjakensis* (Pobedina, 1956) - Bratishko et al.: figs. 5-4, 5-5, 5-7, 5-8 (see there for further synonymies).

Material: 88 specimens, figured specimens NMNH ГКН 5960 032 and SMF PO 101.170, Bessarabian, Jurkine, Crimea.

Discussion. *Atherina gidjakensis* has been identified from the Konkian to Maeotian (Serravallian to lower Messinian) of the Eastern Paratethys. For a detailed description and discussions, see Bratishko et al. (2015). In their study on Konkian otoliths from Kazakhstan, Bratishko et al. (2015) considered *Atherina kalinoraensis* Rückert-Ülkümen, 1993 from the Khersonian and Pannonian of Turkey as a junior synonym. *Atherina kalinoraensis*, however, was considered valid in Schwarzhans, Agiadi & Carnevale (2020a) from Turkey, the Lake Pannon from Slovakia, and the Messinian Lago Mare sediments of Italy. The species differs from *A. gidjakensis* due to its shallow dorsal rim and deep ventral rim

(*A. gidjakensis* has more symmetrically developed rims). *A. gidjakensis* likely lived in a marine environment, and *A. kalinoraensis* may have preferred brackish to freshwater environments.

Order **Syngnathiformes** Rafinesque, 1810
Family Macroramphosidae Bleeker, 1859
Genus *Paramacroramphosus* n. gen.

Type species: *Paramacroramphosus pumilis* n. sp.
Etymology: Combination of para (Greek) = similar and the genus name *Macroramphosus* indicating the presumed phylogenetic relationship.
Diagnosis: A fossil otolith-based genus of the Macroramphosidae characterized regularly curved, deep ventral rim with a thin edge ("velum") extending from the rostrum to a position below the tip of the cauda, a strongly bulged ventral field, and sharp crista superior with a broad and deep dorsal depression above, and a long and narrow cauda reaching close to the posterior rim of the otolith but not opened. Differing from all extant macroramphosid and centriscid otoliths, the outer face is not flat but distinctly bulged and convex.

Discussion. Their regularly curved, deep ventral rim, the posteriorly closed cauda, and bulged outer face distinguish otoliths of *Paramacroramphosus* from all extant genera of the family. The velum along the ventral rim of the otoliths is a characteristic feature of macroramphosid otoliths and is developed more narrowly in *Paramacroramphosus* than in extant macroramphosid otoliths. We, therefore, interpret the otolith morphology of *Paramacroramphosus* as a plesiomorphic status compared to extant taxa.

For comparison, we figure otoliths of the extant *Macroramphosus gracilis* (Lowe, 1839) (Fig. 12Z–AB), *Macroramphosus scolopax* (Linnaeus, 1758) (Fig. 12AC–AE), and *Aeoliscus punctulatus* (Bianconi, 1854) of the related Centriscidae (Fig. 12AF–AH). Otoliths from *Centriscops humerosus* (Richardson, 1846) were figured by Nolf (2013), while those from *Notopogon fernandezianus* (Delfin, 1899) were figured by Conversani et al. (2017). Otoliths of *Aeoliscus* Jordan & Starks, 1902 are remarkable for their extremely extruding, pointed ventral field that is best visible from both the ventral (Fig. 12AE) and lateral view (Fig. 12AF). This feature could be a response of the fish's swimming in a vertical position with the head down.

Macroramphosid and centriscid otoliths, as well as syngnathiform otoliths, are generally very small, usually well below 1 mm in size and often smaller than 0.5 mm. Hence, they are rarely discovered in the fossil record. Therefore, this record and a few aligned unidentified records in earlier publications (see below) from the Eastern Paratethys, as well as a putative macroramphosid from the middle Eocene (Schwarzhans 2007), represent the only fossil records of such otoliths.

In contrast, rich knowledge exists on fossil macroramphosid and centriscid fish from articulated skeletons since Cretaceous times (Bannikov, 2010). Skeleton-based species of *Aeoliscus* have been described from the lower Oligocene to Middle Miocene of eastern Paratethys (Bannikov, 2010). Due to the differences between the morphology of *Paramacroramphosus* otoliths and those of extant *Aeoliscus* species, the fossil skeleton-based species of *Aeoliscus* are unlikely to represent the otolith-based species described here.

Species. Two species: *Paramacroramphosus pumilis* n. sp. from the Bessarabian to Maeotian of the Eastern Paratethys and *Paramacroramphosus platessaeformis* (Pobedina, 1956; as Ot. (inc. sedis) *platessaeformis*) from the Maeotian of Azerbaidjan.

Paramacroramphosus pumilis n. sp.
Figs. 12P–Y

1968 *Otolithus (Berycidarum) latirostratus* - Suzin (in Zhizhchenko): pl. 18, fig. 9 [name not available according to ICZN article 13.1.1].
2006 *Smerdis*? sp. - Djafarova: pl. 13, figs. 3–4.

Holotype: Fig. 12P–S, NMNH ГКН 5960 033, Bessarabian, Jurkine, Crimea.
Paratypes: 4 specimens, NMNH ГКН 5960 034 and SMF PO 101.171, same data as holotype.
Referred specimens: 60 specimens, same data as holotype; in addition 41 specimens from micro-samples: 1 specimen from micro-sample #12, 1 specimen from micro-sample #13 and 39 specimens from micro-sample #14.
Etymology: From pumilus (Latin) = dwarf, referring to the small size of the otoliths.
Diagnosis: OL:OH = 0.95–1.02. Very small size not exceeding 0.8 mm in length. Rostrum long, massive, 20–30% of OL. Ventral rim deeply and regularly curved with narrow velum extending from tip of rostrum to below termination of cauda. Cauda narrow, reaching close to posterior rim of otolith. Outer face as convex and bulged as inner face.

Description. Small, compact, thick and high bodied otoliths not exceeding 0.8 mm in length (holotype 0.78 mm). OH:OT = 1.8–2.2. Dorsal rim high, rounded, highest at its middle, without postdorsal angle. Ventral rim deep, regularly curved, with thin velum along margin from rostrum to position below tip of cauda, terminating with distinct notch before posterior rim, finally crenulated in

largest specimens (Fig. 12P, R). Anterior rim with large, massive, long rostrum, broad excisura and very broad but short, not protruding antirostrum. Posterior rim broadly and regularly rounded.

Inner face strongly convex; ventral field strongly bulged above ventral velum; dorsal field with strong crista superior above sulcus and broad dorsal depression occupying almost entire dorsal field. Crista inferior often present below cauda, but never as strong as crista superior. Sulcus distinctly supramedian, deep; its ostium deeper and wider than cauda, anteriorly broadly opened; its cauda narrow and reaching close to posterior rim of otoliths but closed. CaL:OsL = 1.05–1.45; OsH:CaH = 1.35–1.65. Outer face strongly convex with massive central umbo, smooth except for multiple short radial furrows on the ventral field connected to the fine crenulation of the ventral velum, particularly in larger specimens.

Discussion. These small otoliths are common and easy to recognize in the fraction below 1 mm in mesh size. Their occurrence shows that sampling from screen sizes of 0.8 and 0.5 mm can result in the recognition of species that otherwise would have been missed. At first sight, similar otoliths are juvenile otoliths of *Capros crudus* n. sp. (see below), which occur in the same size range but are much less common. They differ from *P. pumilis* n. sp. in their pronounced postdorsal angle, dorsally pronounced posterior rim, and absence of a velum along the ventral rim (which is nevertheless sharper than other rims) of the otolith. *Paramacroramphosus platessaeformis* is difficult to compare using Pobedina's somewhat schematic drawing, but it at least differs from *P. pumilis* n. sp. in terms of a short rostrum (9% of OL *vs.* 20–30%), less well-developed ventral velum, and seemingly widened caudal tip.

Order **Pleuronectiformes** Bleeker, 1859

Remarks. Pleuronectiform otoliths are known for their side dimorphism, which varies between groups (Schwarzhans 1999). Typically, otoliths from one side reflect diagnostic characteristics better than those from the other side, which are often more modified. Therefore, the following diagnoses and descriptions are based on otoliths from the side with the higher diagnostic value.

When observed, aspects of side dimorphism, ontogenetic changes, and variability are discussed separately for each species.

Family Bothidae Regan, 1910
Genus *Arnoglossus* Bleeker, 1862

Arnoglossus kerichensis n. sp.
Figs. 13A–W

Holotype: Fig. 13A–B (left otolith), NMNH ГКН 5960 035, Bessarabian, Jurkine, Crimea.
Paratypes: 12 specimens (6 specimens left otoliths, 6 specimens right otoliths), NMNH ГКН 5960 036 and SMF PO 101.172, same data as holotype.
Referred specimens: 330 specimens, same data as holotype; in addition 3 specimens from micro-sample #14 and 1 specimen from micro-sample #15.
Etymology: Referring to the city of Kerch (*Keriç*) in Tatar language.
Diagnosis (left otolith): Ratio otolith length minus rostrum length : otolith height ("altered" OL:OH in the following) = 1.1–1.25. Rostrum pointed, long in specimens larger than approximately 1.8–2.0 mm in length, 15–25% OL. Ventral rim deep, regularly curved. OsL:CaL = 1.35–1.65.

Description (left otolith). Roundish otoliths with sharp and long rostrum developed in large specimens of 1.8–2.0 of length; total length up to about 2.85 mm (holotype). OL:OH = 1.2–1.45, increasing with size and strength of rostrum; altered OL:OH = 1.1–1.25. OH:OT = 2.55–2.95. Dorsal rim rounded to somewhat flattened; ventral rim deep, regularly curved or with rounded postventral angle. Rostrum weak in specimens smaller than

Fig. 12 - Mugilidae, Atherinidae and Macroramphosidae. A–G) *Chelon jurkinensis* n. sp., holotype (C–D) NMNH ГКН 5960 030, paratypes (A–B, E–G) NMNH ГКН 5960 031 (F–G) and SMF PO 101.169 (A–B, E), B, D, G ventral views, Bessarabian, Jurkine. H–O) *Atherina gidjakensis* (Pobedina, 1956), NMNH ГКН 5960 032 (J–M) and SMF PO 101.170 (A–B, N–O), I, K ventral views, Bessarabian, Jurkine. P–Y) *Paramacroramphosus pumilis* n. sp., holotype (P–S) NMNH ГКН 5960 033, paratypes (Т–Y) NMNH ГКН 5960 034 (X) and SMF PO 101.171 (Т–W, Y), R outer face, Q, V ventral views, S, U anterior views. Z–AB) *Macroramphosus gracilis* (Lowe, 1839), coll. Schwarzhans, AA ventral view, AB anterior view extant, Mimase fish market, Kochi, Japan. AC–AE) *Macroramphosus scolopax* (Linnaeus, 1758), coll. Schwarzhans, AD ventral view, AE anterior view, extant, Agadir fish market, Morocco. AF–AH) *Aeoliscus punctulatus* (Bianconi, 1854), coll. Schwarzhans, AG ventral view, AH anterior view, extant, aquarium specimen.

Chelon jurkinensis

Atherina gidjakensis

Paramacroramphosus pumilis

Macroramphosus gracilis

Macroramphosus scolopax
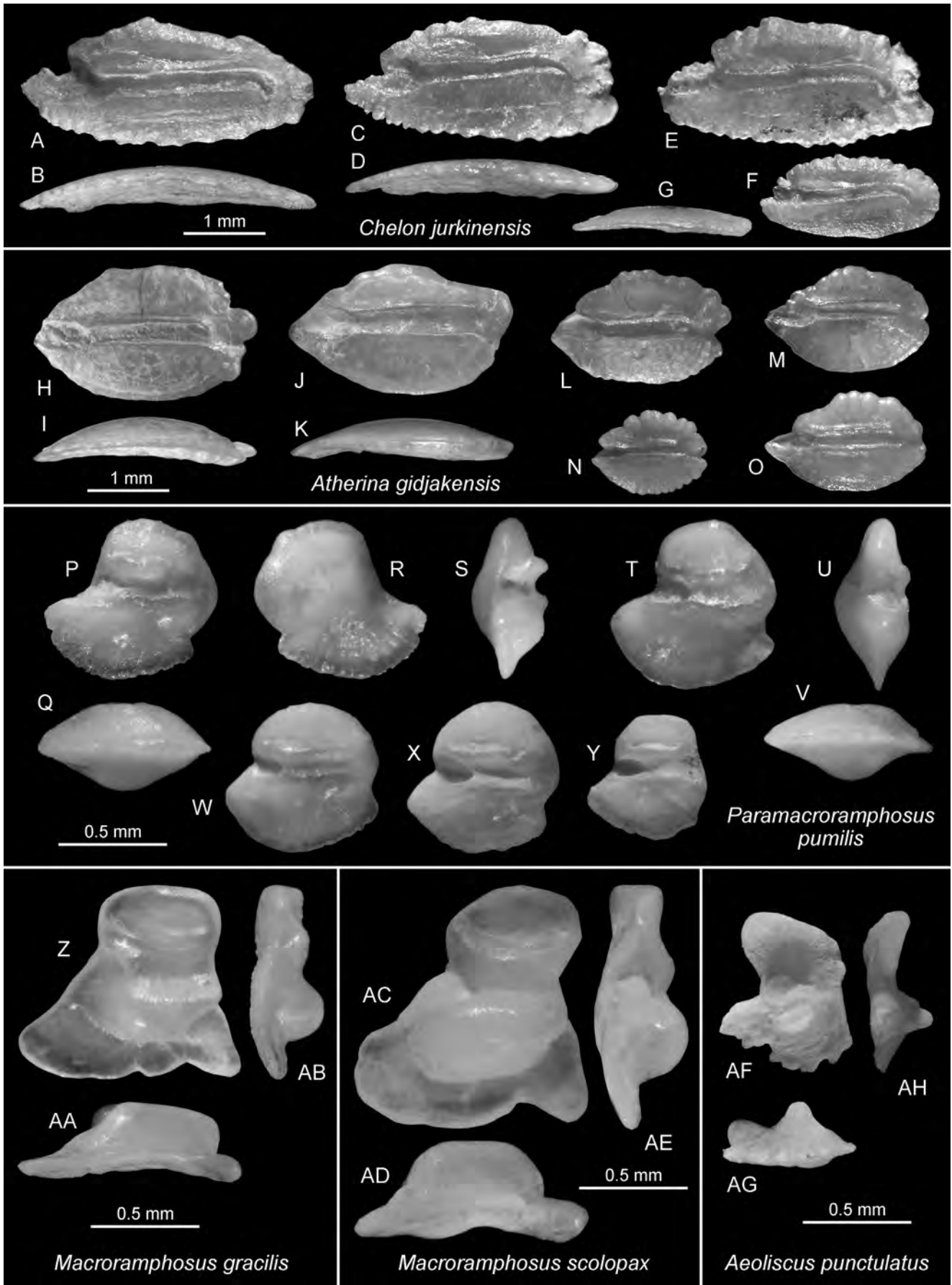
Aeoliscus punctulatus

FIGURE 12

1.5 mm of length, long and pointed in large specimens; excisura a broad concavity; antirostrum not or only slightly protruding.

Inner face moderately convex with slightly supramedian, anteriorly open and moderately deep sulcus. Ostium wider and longer than cauda; OsL:CaL = 1.35–1.65. Sulcus narrowing at collum, with distinct crista surrounding entire sulcus except on rostrum. Circumsulcal depression distinct, wide, with sharp margin towards crista. Outer face flat to slightly convex, smooth.

Side dimorphism. Otoliths from the right side differ from those of the left side by a flatter inner face, shorter rostrum that does not exceed 17% of OL (Fig. 13E), and more convex outer face. Additionally, they tend to be slightly more elongate than the otoliths of the left side, as shown in their OL:OH ratio of 1.3–1.55 (*vs.* 1.2–1.45) and the altered OL:OH ratio of 1.2–1.3 (*vs.* 1.1–1.25). The elevation of the crista is stronger in otoliths of the right side, and the circumsulcal depression wider and deeper. However, the distinction of ostium and cauda is less pronounced.

Ontogeny and variability. The ontogenetic changes and the variability are primarily expressed in the development of the rostrum, which is typically small or even indiscernible in small specimens (Fig. 13T) but becomes a dominant feature in large specimens (Fig. 13A, C). Other characteristics that vary considerably are the shape of the dorsal and ventral rims, which can be well rounded with an obtuse angle at the ventral and posterior rims, or flattened in the case of the dorsal rim. In fact, both of these effects are so substantial that few characteristics remain for diagnosis, and one could be tempted to recognize several further morphotypes. However, in our opinion, subdivision in species or subspecies reflecting such morphotypes would only result in problematic definitions, and we, therefore, refrained from such action. In a recent study by Guenser et al. (2022), the merits of lumping taxa versus the loss of resolution in species with about 80% of morphological intermediate forms between them was discussed. In our case of *A. kerichensis* and the subsequently described *A. scitulus*, we are of the opinion that further taxonomic subdivision would only result in diagnostic ambiguities rather than enhancing resolution.

Discussion. A significant number of bothid otoliths primarily from the Karaganian (early Ser-

ravallian) were described by Chalilov (1946), Pobedina (1954, 1956), and Djafarova (2006). Bratishko et al. (2015) synonymized the majority of these nominal species with *Arnoglossus tenuis* (Schubert, 1906), which was originally described from the early Badenian (Langhian) of the Central Paratethys. Schwarzhans et al. (2017c) described otoliths found in situ in *Arnoglossus bassianus* (Kramberger-Gorjanovic, 1883) from the Sarmatian s.s. (equivalent of the Volhynian), recognizing them as senior synonym of *A. tenuis* sensu Bratishko et al. (2015). However, these otoliths have a regular oval outline without a rostrum, unlike *A. kerichensis* n. sp. For distinction of the second, parallel *A. scitulus* n. sp., see below.

Among extant species of *Arnoglossus*, *A. kessleri* Schmidt, 1915 may be of particular interest because its distribution extends to the Black Sea. A sequence of its otoliths were figured in Lombarte et al. (2006), and they differ clearly from *A. kerichensis* n. sp. in their regular otolith outline and absence of any significant rostrum.

Arnoglossus scitulus n. sp.
Figs. 13X–AQ

Holotype: Fig. 13X–Z (left otolith), NMNH ГКН 5960 037, Bessarabian, Jurkine, Crimea.

Paratypes: 11 specimens (5 specimens left otoliths, 6 specimens right otoliths), NMNH ГКН 5960 038 and SMF PO 101.173, same data as holotype.

Referred specimens: 495 specimens, same data as holotype; in addition 2 specimens from micro-sample #12 and 1 specimen from micro-sample #14.

Etymology: From scitulus (Latin) = elegant, referring to the more delicate, elegant appearance of the otoliths of this species in comparison to the coeval *A. kerichensis*.

Fig. 13 - Bothidae. A–W) *Arnoglossus kerichensis* n. sp., holotype (A–B) NMNH ГКН 5960 035, paratypes (C–W) NMNH ГКН 5960 036 (J–L, Q, U–W) and SMF PO 101.172 D–I, N–P, R–T), B, D, F, H, L, P, S, V ventral views, I, J anterior views, Bessarabian, Jurkine. X–AQ) *Arnoglossus scitulus* n. sp., holotype (X–Z) NMNH ГКН 5960 037, paratypes (AA–AQ) NMNH ГКН 5960 038 (AF–AL) and SMF PO 101.173 (AA–AE, AM–AQ), Z, AD, AI, AL, AN ventral views, X, AE anterior views, Bessarabian, Jurkine. AR–AV) Unidentifiable juvenile Bothidae, NMNH ГКН 5960 070, AT, AU ventral views, AR anterior view, Bessarabian, Jurkine.
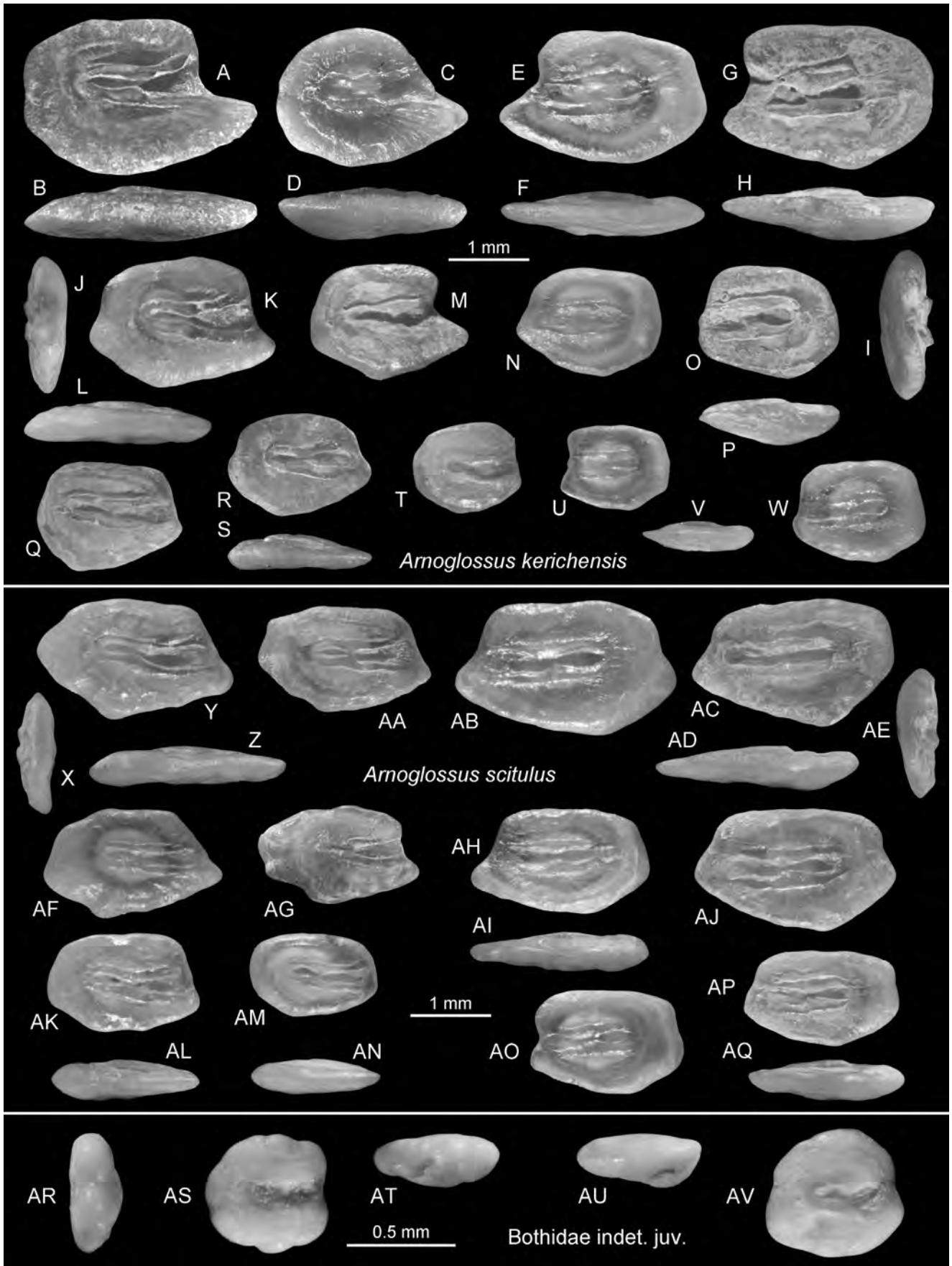
Arnoglossus kerichensis

Arnoglossus scitulus

Bothidae indet. juv.

FIGURE 13

Diagnosis (left otolith): Ratio otolith length minus rostrum length : otolith height ("altered" OL:OH) = 1.4–1.55. Rostrum short, angular, 5–13% OL. Ventral rim deep with distinct postventral angle; dorsal rim shallow; posterior rim angular or undulating. OsL:CaL = 1.55–2.0. Ostial opening indistinct, fading.

Description (left otolith). Slender, elegant and relatively thin otoliths with short rostrum; total length up to about 2.75 mm (holotype 2.45). OL:OH = 1.5–1.75, increasing with size; altered OL:OH = 1.4–1.55. OH:OT = 2.6–3.0. Dorsal rim shallow, sometimes slightly undulating; ventral rim moderately deep with distinct postventral angle and sometimes undulating. Rostrum weak or absent; excisura a broad concavity; antirostrum not or only slightly protruding.

Inner face moderately convex with slightly supramedian, moderately deep, anteriorly fading and not clearly open sulcus. Ostium wider and longer than cauda; OsL:CaL = 1.55–2.0. Sulcus narrowing at collum, with distinct crista surrounding entire sulcus except on most anterior part of ostium. Circumsulcal depression distinct, wide, with sharp margin towards crista. Outer face flat to slightly convex, smooth.

Side dimorphism. Side dimorphism is less strongly expressed in *A. scitulus* when compared to *A. kerichensis*. The primary effects of side dimorphism are that the inner face is flatter in right otoliths and more convex in left otoliths, the marginal undulation is less developed in right otoliths than left otoliths, and right otoliths tend to be thicker than left otoliths, with a slightly convex outer face.

Ontogeny and variability. Ontogenetic changes and variability also appear to be less extensive than in *A. kerichensis*. Small specimens tend to be less slender than large ones (Fig. 13AK, AO) and often show a smoother outline (Fig. 13AM, AP). Aspects of variability resemble ontogenetic changes. In addition, details of the outline, undulations, and expression of the small rostrum can vary.

Discussion. *Arnoglossus scitulus* n. sp. is distinguished from the parallel *A. kerichensis* in terms of its weaker rostrum development in large specimens; more elongate shape (OL:OH = 1.5–1.75 *vs.* 1.2–1.45; altered OL:OH = 1.4–1.55 *vs.* 1.1–1.3); and comparatively longer (OsL:CaL = 1.55–2.0 *vs.* 1.35–1.65), anteriorly fading ostium (*vs.* clearly open ostium). Finally, the marginal undulation and strength of the postventral angle distinguishes *A. scitulus* from *A. kerichensis*. However, multiple mor-

phological transitional forms exist particularly at sizes of less than 2 mm in length, while larger specimens are typically easily discernable. The extant *A. kessleri* from the Black Sea lacks any significant rostrum, while such a rostrum is present, albeit short, in *A. scitulus* n. sp. Another difference of the extant species versus *A. scitulus* n. sp. concerns the smooth, almost regularly oval, otolith outline in the extant species.

Genus indet.
Bothidae indet. juvenile
Figs. 13AR–AV

Material: 28 specimens (figured specimens NMNH ГКН 5960 070), Bessarabian, Jurkine, Crimea, including 2 specimens from micro-sample #13, 19 specimens from micro-sample #14 and 5 specimens from micro-sample #15.

Discussion. 28 small otoliths were found in the small fraction of 0.5-mm mesh size. They are nearly round, with undulating rims, a flat inner and convex outer face, and small axially positioned sulcus composed of equally long ostium and cauda. These finds are interpreted as juveniles of an unknown bothid species, likely not of the genus *Arnoglossus*. Similar in size and roundish outline was an otolith found in situ in *Bothus parvulus* (Kramberger-Gorjanovic, 1883) from the Sarmatian s.s. of the Central Paratethys (Schwarzhans et al. 2017c). However, that otolith was not preserved well enough to perform a detailed analysis.

Family Soleidae Bonaparte, 1835
Genus *Aseraggodes* Kaupp, 1858

***Aseraggodes azovensis* n. sp.**
Figs. 14A–H

Holotype: Fig. 14C–D (left otolith), NMNH ГКН 5960 039, Bessarabian, Jurkine, Crimea.
Paratypes: 4 specimens (3 specimens left otoliths, 1 specimen right otoliths), NMNH ГКН 5960 040 and SMF PO 101.174, same data as holotype.
Referred specimens: 12 specimens, same data as holotype.
Etymology: Referring to the Sea of Azov, which borders the type locality.
Diagnosis (left otolith): OL:OH = 1.05–1.10. Dorsal rim shallow; ventral rim deep, deepest posteriorly. Anterior tip very dorsally positioned. Inner face strongly convex; outer face flat to concave. OsL:CaL = 1.8–2.3. Ostium wider than cauda, and it terminates far from anterior rim of otolith.

Description (left otolith). High bodied, moderately thin otoliths up to about 2.15 mm (holotype 1.9). OL:OH = 1.05–1.10; OH:OT = 2.7–3.1. Dorsal rim shallow, with low, broad and rounded middorsal angle; ventral rim very deep, deepest postventrally, somewhat irregularly curving. Anterior tip projecting high above sulcus near joint with dorsal rim, distinct; posterior rim nearly straight, inclined at 80–95°, with distinct angles at intersections with dorsal and ventral rims.

Inner face strongly convex with distinctly supramedian, moderately deep, anteriorly closed sulcus terminating far from anterior rim of otolith. Sulcus sometimes slightly upward oriented towards anterior. Ostium wider and longer than cauda; OsL:CaL = 1.8–2.3. Sulcus narrowing at collum, with distinct crista surrounding entire sulcus except fading near tip of ostium. Circumsulcal depression distinct, narrow, running close to sulcus. Outer face flat to slightly concave, smooth.

Side dimorphism. Right otoliths do not show the distinction of ostium and cauda that is typically clearly seen in left otoliths. The otolith outline is smoother in right otoliths, not undulating as much as in left otoliths, and the inner face is more strongly convex.

Discussion. *Aseraggodes azovensis* n. sp. is an exotic species from the Miocene of the Paratethys, representing a genus that is currently restricted to the Indo-West Pacific except for a single endemic species off Galapagos (Schwarzhans 1999). It is readily recognized by its low OL:OH ratio of 1.05–1.10, which distinguishes it from otoliths of all extant soleid taxa of Europe. The otolith shape resembles that of otoliths of many extant *Aseraggodes* species (see Schwarzhans 1999, for figures), particularly *A. macleayanus* (Ramsay, 1881) and *A. klunzingeri* (Weber, 1908). Among the known otoliths of extant species, the rather large ostium compared to the small cauda is shared with *A. macleayanus*, but the distance of the ostium from the anterior rim of the otolith is distinctive. The latter characteristic is shared with *A. filiger* Weber, 1913 (see Schwarzhans, 1999 for figures), which, however, has equally long ostium and cauda.

Genus *Dicologlossa* Chabanaud, 1927

Dicologlossa postpatens n. sp.
Figs. 14I–P

Holotype: Fig. 14M–N (right otolith), NMNH ГКН 5960 041, Bessarabian, Jurkine, Crimea.

Paratypes: 5 specimens (2 specimens left otoliths, 3 specimens right otoliths), NMNH ГКН 5960 042 and SMF PO 175, same data as holotype.

Referred specimens: 13 specimens, same data as holotype.

Etymology: Referring to the putative derivation of the species from *Dicologlossa patens* (Bassoli, 1906).

Diagnosis (right otolith): OL:OH = 1.3–1.45. Otolith shape irregularly oval. Inner face strongly convex; outer face flat to concave. OL:SuL = 1.95–2.15; OsL:CaL = 2.5–2.8. Sulcus small; ostium slightly wider than cauda, anteriorly terminating far from anterior rim of otolith.

Description (right otolith). Oval, moderately thin otoliths up to about 2.6 mm (holotype 2.1). OH:OT = 2.3–2.5. Dorsal rim relatively shallow and somewhat irregularly curving with low, broad and rounded pre- to middorsal angle; ventral rim only slightly deeper and more regularly curving. Anterior tip rounded, projecting most at about level of sulcus; posterior rim rounded or blunt, sometimes with slight concavity.

Inner face strongly convex with slightly supramedian, moderately deep, anteriorly closed sulcus terminating far from anterior rim of otolith. Sulcus small, sometimes slightly upward oriented towards posterior; OL:SuL = 1.95–2.15. Ostium slightly wider and considerably longer than cauda but separation indistinct, marked by rounded indentation or step in ventral sulcus margin; OsL:CaL = 2.5–2.8. Circumsulcal depression distinct, wide, running close to sulcus and reaching near to otolith rims. Outer face flat to slightly concave, smooth.

Side dimorphism. Side dimorphism is relatively weak in this species. Left otoliths tend to have a less deepened sulcus than right otoliths, and their OsL:CaL ratio is also considerably less (1.5–2.3 *vs.* 2.5–2.8).

Discussion. Otoliths of *Dicologlossa* are recognized by their elongate, almost oval shape with an OL:OH ratio of 1.30–1.45. *Dicologlossa postpatens* n. sp. differs from *D. patens* in terms of its much smaller sulcus (OL:SuL = 1.95–2.15 *vs.* 1.5–1.7), higher OsL:CaL ratio in right otoliths (2.5–2.8 *vs.* 1.6–1.7), and most obviously, the ostium, which terminates at considerable distance from the anterior rim of the otolith (*vs.* reaching close to the anterior rim in *D. patens*). We postulate that *D. postpatens* n. sp. has evolved as an endemic species from *D. patens* after the separation of the Eastern Paratethys from the world ocean.
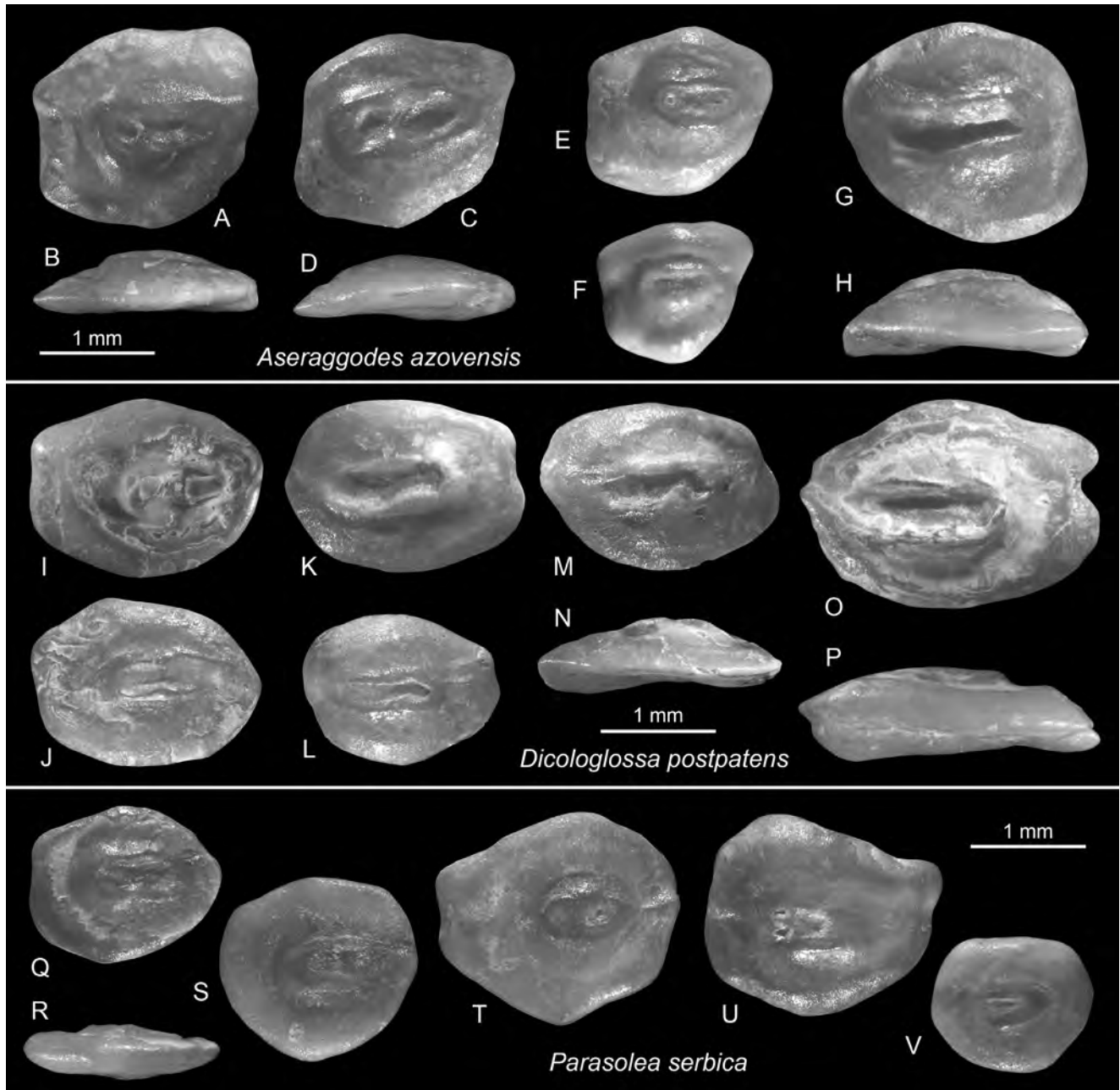
Fig. 14 - Soleidae. A–H) *Aseraggodes azovensis* n. sp., holotype (C–D) NMNH ГКН 5960 039, paratypes (A–B, E–H) NMNH ГКН 5960 040 (E–F) and SMF PO 101.174 (A–B, G–H), B, D, H ventral views, Bessarabian, Jurkine. I–P) *Dicologlossa postpatens* n. sp., holotype (M–N) NMNH ГКН 5960 041, paratypes (I–L, O–P) NMNH ГКН 5960 042 (J–L) and SMF PO 175 (I–K, O–P), N, P ventral views, Bessarabian, Jurkine. Q–V) *Parasolea serbica* (Anđelković, 1966), NMNH ГКН 5960 043 (Q–S, V) and SMF PO 101.176 (T–U), R ventral view, Bessarabian, Jurkine.

Genus *Parasolea* Schwarzhans, Carnevale, Japundžić & Bradić-Milinović, 2017

Parasolea serbica (Anđelković, 1966)
Figs. 14Q–V

2017c *Parasolea serbica* (Anđelković, 1966) - Schwarzhans et al.: figs. 6a-g (6a-c otoliths in situ).

Material: 33 specimens, figured specimens NMNH ГКН 5960 043 and SMF PO 101.176, Bessarabian, Jurkine, Crimea.

Discussion. Otoliths of *Parasolea serbica* were first identified in situ in articulated skeletons from the Sarmatian s.s. of Dolje, Croatia, in the Central Paratethys. The otoliths are characterized by a nearly round, often somewhat irregular shape and an extremely small sulcus. Schwarzhans et al. (2017c) figured otoliths from Jurkine for comparison and placed them in the same species.

Order **Callionymiformes** Berg, 1937
Family Callionymidae Bonaparte, 1831
Genus *Callionymus* Linnaeus, 1758

Callionymus bessarabianus n. sp.
Figs. 15A–F

Holotype: Fig. 15C–D, NMNH ГКН 5960 044, Bessarabian, Jurkine, Crimea.
Paratypes: 2 specimens, SMF PO 101.177, same data as holotype.
Etymology: Named after the Bessarabian, substage of the Sarmatian s.l. (middle Sarmatian), from which the otoliths of Jurkine were collected.
Diagnosis: OL:OH = 2.05–2.35; OH:OT = 1.55–1.95. Inner face relatively flat. Rostrum, antirostrum, and excisura distinct. OsL:CaL = 3.0–3.4.

Description. Elongate, slender and relatively thin small otoliths up to 2 mm in length (holotype 1.9 mm). Dorsal rim triangular, with shallow, obtuse middorsal angle. Ventral rim nearly flat, only slightly bent and smooth. Anterior rim with prominent rostrum, distinct and rather deep excisura, and variable antirostrum, which is shorter than the rostrum. Rostrum sharply pointed, much inferior, its length measured from its tip to deepest point of excisura 15–20% of OL. Posterior tip inferior, symmetrical to rostrum less sharply pointed than rostrum.

Inner face nearly flat to slightly convex. Sulcus narrow, deep, short, anteriorly open, oriented slightly upward towards posterior at angle of about 10° and terminating below middorsal angle. OL:SuL = 1.6–1.85. Separation in slightly wider ostium and cauda indistinct; OsL:CaL = 3.0–3.4. Crista superior distinct, with sharp border towards deep, dorsally fading dorsal depression. Crista inferior variable, usually distinct below cauda and rear part of ostium. Ventral furrow distinct, terminating anteriorly below middle of ostium and curving posteriorly towards tip of cauda, centrally reaching close to ventral rim of otolith. Narrow section of ventral field below central part of ventral furrow sometimes slightly depressed (Fig. 15B). Outer face moderately convex, smooth.

Discussion. *Callionymus bessarabianus* n. sp. differs from the otoliths of the three Konkian callionymid species *Protonymus gontsharovae* Sytchevskaya & Prokofiev, 2007 (known with otolith in situ), *P.?* *primus* (Weiler, 1943), and *P.? miocenicus* (Pobedina, 1954) in that it is much slenderer (OL:OH = 2.05–2.35 *vs.* 1.35–1.9). *Protonymus gontsharovae* was considered a potential junior synonym of *P.? primus* by

Bratishko et al. (2015). Some specimens described as *P.?* aff. *primus* from the Konkian of Mangyshlak are nearly as elongate as *C. bessarabianus* n. sp. (OL:OH = 1.9–2.1), but they lack the clear rostrum and excisura. *Callionymus bessarabianus* n. sp. differs from all *Protonymus* Sytchevskaya & Prokofiev, 2007 species in that its ostium is much longer than the cauda (OsL:CaL = 3.0–3.4 *vs.* 1.3–1.9). Otoliths in situ of *Callionymus* cf. *macrocephalus* Kramberger-Gorjanovic, 1882 from the lower Sarmatian s.l. of Tsurevski in southern Russia have not been published, but specimens investigated courtesy of G. Carnevale (Torino) indicate *Protonymus*-type otoliths with a short rostrum and low OsL:CaL ratio. Thus, they are similar to the otoliths described by Bratishko et al. (2015) as *Protonymus*? aff. *primus*.

Callionymus kalinus n. sp.
Figs. 15G–N

Holotype: Fig. 15G–H, NMNH ГКН 5960 045, Bessarabian, Jurkine, Crimea.
Paratypes: 6 specimens, NMNH ГКН 5960 073 and SMF PO 101.178, same data as holotype.
Tentatively assigned specimens: 5 juvenile specimens: 1 specimen of about 0.9 mm in length (Fig. 15M–N, NMNH ГКН 5960 080), same data as holotype, 4 specimens from micro-sample #14.
Etymology: After kalin (Tatar language) = thick, referring to thick appearance of these otoliths.
Diagnosis: OL:OH = 1.85–2.05; OH:OT = 1.35–1.5. Inner face convex. Rostrum short, antirostrum and excisura indistinct. OsL:CaL = 2.4–2.65.

Description. Elongate, slender, relatively thick, small otoliths up to 1.9 mm in length (holotype). Dorsal rim triangular with shallow, obtuse middorsal angle. Ventral rim nearly flat, only slightly and somewhat irregularly bent and smooth. Anterior rim with short rostrum, indistinct or no excisura and antirostrum. Rostrum much inferior, its length 4–5% of OL. Posterior tip inferior, broad, more or less symmetrical to rostrum.

Inner face markedly convex, particularly section behind cauda. Sulcus narrow, deep, short, anteriorly open but somewhat narrowing, oriented slightly upward towards posterior at angle of 9 to 13° and terminating slightly behind middorsal angle. OL:SuL = 1.5–1.7. Separation of slightly wider ostium and narrower cauda indistinct; OsL:CaL = 2.4–2.65. Crista superior distinct towards dorsally fading dorsal depression. Crista inferior variable, usually indistinct below cauda and rear part of ostium. Ventral furrow
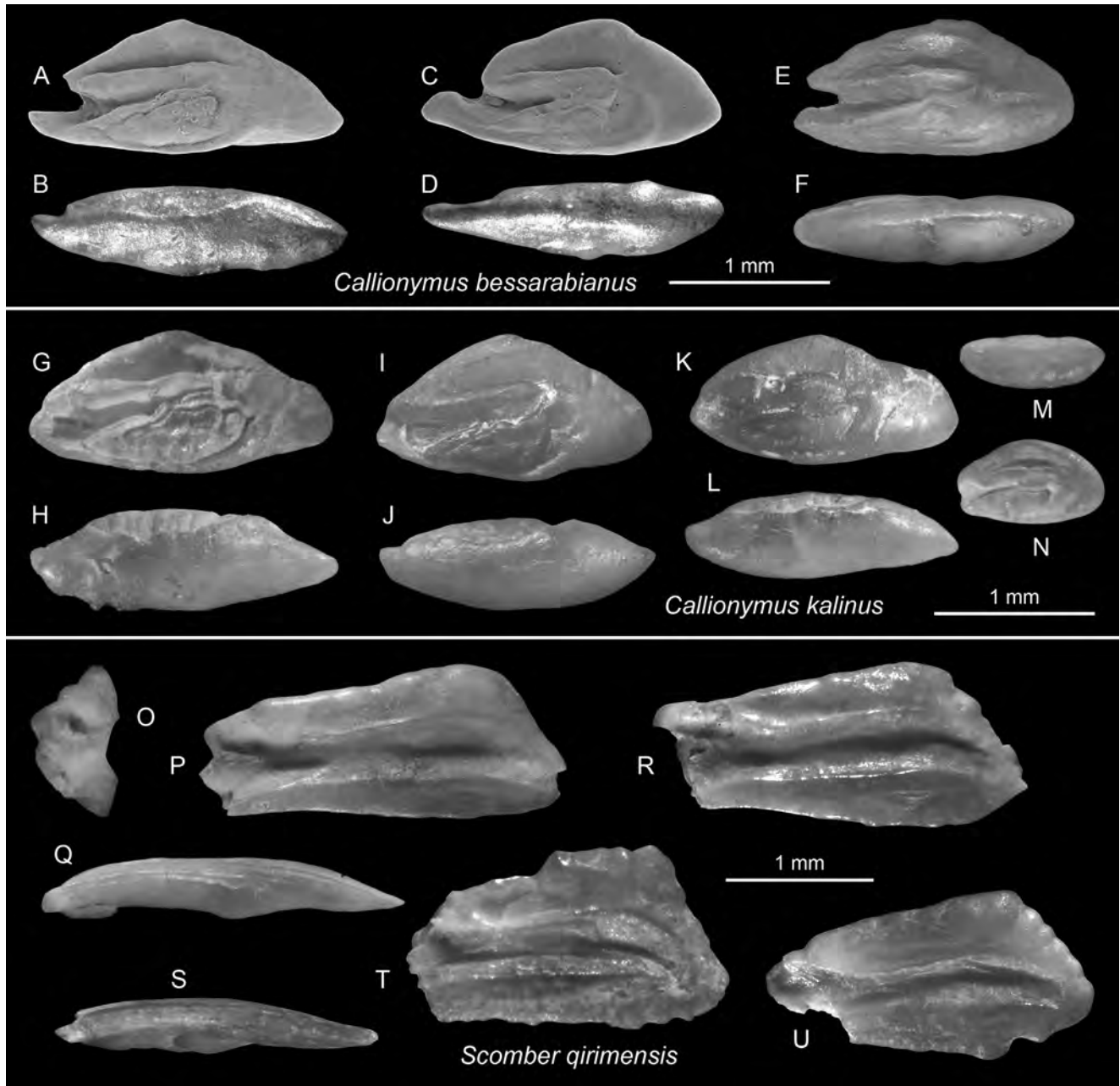
Fig. 15 - Callionymidae and Scombridae. A–F) *Callionymus bessarabianus* n. sp., holotype (C–D) NMNH ГКН 5960 044, paratypes (A–B, E–F) SMF PO 101.177, B, D, F ventral views, Bessarabian, Jurkine. G–N) *Callionymus kalinus* n. sp., holotype (G–H) NMNH ГКН 5960 045, paratypes (I–L) NMNH ГКН 5960 073 (K–L) and SMF PO 101.178 (I–J), tentatively assigned juvenile specimen (M–N) NMNH ГКН 5960 080, H, J, L, M ventral views. O–U) *Scomber qirimensis* n. sp., holotype (O–Q) NMNH ГКН 5960 046, paratypes (R–U) SMF PO 101.179, Q, S ventral views, O anterior view, Bessarabian, Jurkine.

distinct, terminating anteriorly near tip of ostium and curving posteriorly towards tip of cauda, centrally reaching close to ventral rim of otolith. Narrow section of ventral field below central part of ventral furrow strongly depressed as clearly expressed in ventral views (Fig. 15H, J, L). Outer face convex, smooth.

Ontogeny. A single juvenile otolith (Fig. 15M–N) is tentatively assigned to *C. kalinus*. It differs from larger specimens in that its rostrum does not protrude, and its inner face is nearly flat. Its OL:OH ratio is 1.7,

and its OsL:CaL ratio is 2.0. We believe that these differences reflect the ontogenetic effects of juvenile specimens.

Discussion. *Callionymus kalinus* n. sp. differs from *C. bessarabianus* in its thicker appearance (OH:OT = 1.35–1.5 *vs.* 1.55–1.95), short rostrum, weak or absent antirostrum and excisura, slightly less elongate shape (OL:OH = 1.85–2.05 *vs.* 2.05–2.35), and lower OsL:CaL ratio (2.4–2.65 *vs.* 3.0–3.4). The characteristics that distinguish *C. kalinus* from spe-

cies of the genus *Protonymus* and from *C. macrocephalus* from the Konkian and lower Sarmatian s.l. are the same as described above for *C. bessarabianus*. However, the juvenile specimen (Fig. 15M–N) approaches the morphology of these stratigraphically earlier species, which are also known from mostly small specimens. For this tentatively assigned specimen of *C. kalinus* n. sp., the OsL:CaL ratio of 2.0 (*vs.* 1.3–1.9) remains the main distinguishing characteristic, but it also shows the problematic nature of identifying callionymid otolith specimens smaller than 1 mm in length.

Order **Scombriformes** Rafinesque, 1810
Family Scombridae Rafinesque, 1810
Genus *Scomber* Linnaeus, 1758

Scomber qirimensis n. sp.
Figs. 15O–U

Holotype: Fig. 15O–Q, NMNH ГКН 5960 046, Bessarabian, Jurkine, Crimea.
Paratypes: 3 specimens, SMF PO 101.179, same data as holotype.
Referred specimens: 13 fragmentary specimens.
Etymology: From Qirim, Crimea in Tatar language.
Diagnosis: OL from tip of antirostrum: OH = 2.0–2.35. Postdorsal angle shifted far backward. Ostium only slightly widened dorsally. Cauda only slightly bent towards termination, slightly widened at bent.

Description. All specimens lack the presumably thin and fragile rostrum. Otoliths very slender, thin, delicate and fragile reaching up to 2.5 mm in length without rostrum (holotype). OH:OT = 2.5–3.2. Dorsal rim straight along its anterior two thirds, ascending to distinct postdorsal angle at 10–15°; postdorsal rim steeply declining at 50–60°; dorsal rim smooth or irregularly crenulated or undulating. Ventral rim nearly straight, horizontal, smooth or slightly undulating. Posterior tip ventral, close to junction with ventral rim. Antirostrum and excisura short (Fig. 15P) or indistinct (Fig. 15U).

Inner face slightly bent in longitudinal direction with anterior most part apparently being bent most (leading to lacking rostrum). Sulcus long, wide, deep, with distinctly opening ostium and long cauda. Separation of ostium and cauda gradual; ostium only slightly widening dorsally and ventrally. Cauda with nearly horizontal ventral margin except for very slightly bent tip and its dorsal margin being gradually widened towards posterior bent before descending towards tapering tip. Dorsal depression narrow, indistinct; no ventral furrow discernable. Outer face flat with minute umbo behind center, smooth.

Discussion. The genus *Scomber* currently contains four extant species. Three of the extant species—*S. australasicus* Cuvier, 1832, *S. colias* Gmelin, 1789, and *S. japonicus* Houttuyn, 1782—have occasionally been placed in a separate genus (or subgenus), *Pneumatophorus* Jordan & Gilbert, 1883. They differ from the fourth species, *Scomber scomber* Linnaeus, 1758 in, for example, the presence of a swim bladder (*S. scomber* has no swim bladder), which is considered to represent a regression (Chanet & Guintard, 2019). The otoliths of the four species also fall into two categories. First, the otoliths of *Scomber* show a straight, regularly ascending anterior-dorsal rim and a long and thin rostrum (see Nolf, 2018 for figures). Second, the three other species show a broadly concave dorsal rim behind the elevated antirostrum and a strongly reduced rostrum whereby the central part of the ostium projects in a sharp "pseudo-ostium"-like feature beyond the rostrum and antirostrum (see Lombarte et al. 2006 for figures). This latter morphology clearly represents the derived characteristic, but how much it is dependent on the swim bladder development is unclear. In our view, maintaining *Pneumatophorus* as a separate genus or subgenus is still justifiable both from a morphological perspective and a perspective of long stratigraphic persistence of the two lineages (see below).

The fossil record of scombrid otoliths is scarce, likely due to their delicate and fragile nature. The oldest scombrid otolith-based species was described from the Belgian middle Eocene as *Pneumatophorus euodus* Nolf, 1973, and it is characterized by a slight depression of the anterior portion of the dorsal rim and a slightly shortened rostrum (i.e., the perfect match for a plesiomorphic early representative of the *Pneumatophorus* otolith pattern). *Scomber coronatus* Schwarzhans, 1994 from the upper Oligocene and Lower Miocene of the North Sea Basin belongs to the *Scomber* otolith pattern and shares many features with *S. qirimensis* n. sp. The rostrum from either species is unknown, but both have a flat anterior dorsal rim without broad depression or elevated antirostrum. *Scomber qirimensis* n. sp. differs from *S. coronatus* in terms of its smoother dorsal rim and more angular, lower postdorsal angle (*vs.* coarsely-crenulated dorsal rim and projecting post-

dorsal angle), as well as its posterior widening of the dorsal margin of the cauda (*vs.* not widened). These are also features that distinguish *S. qirimensis* n. sp. from the extant *S. scomber*. In addition, *S. qirimensis* shows a gradual sulcus margin transition between ostium and cauda whereby the ostium is only slightly widened dorsally and ventrally. In contrast, the ostium in *S. scomber* is distinctly widened dorsally and ventrally, forming a well-developed collum at the junction with the cauda. Thus, we consider *S. qirimensis* n. sp. an endemic species of the late phase in the Eastern Paratethys.

<div align="center">

Order **Carangiformes** Patterson, 1993
Family Carangidae Rafinesque, 1815
Genus *Trachurus* Rafinesque, 1810

</div>

<div align="center">

***Trachurus* sp.**
Fig. 16A–B

</div>

?2015   *Trachurus* sp. - Bratishko et al.: fig. 6.10.

Material: 1 specimen, NMNH ГКН 5960 047, Bessarabian, Jurkine, Crimea.

Discussion. The single, well-preserved specimen is about 3.85 mm in length and may be considered morphologically mature. It is characterized by a regularly bent, strongly serrated dorsal rim with a relatively weak postdorsal angle; a moderately long, sharply pointed rostrum of about 20% of OL; a distinct ventral furrow; and a moderately bent caudal tip (about 50°). It resembles the single juvenile *Trachurus* otolith of 2.5 mm in length from the Konkian of Mangyshlak, Kazakhstan described by Bratishko et al. (2015) and could represent the same species or a derived form of it. It also resembles *T. elegans* Jonet, 1973 and *T. miosensis* Nolf & Steurbaut, 1979 from the Lower and Middle Miocene of the Mediterranean, Northeast Atlantic, and North Sea Basin. The distinction of fossil and extant *Trachurus* species by means of otoliths has not yet been investigated in sufficient detail; hence, we refrain from identification to the species level.

<div align="center">

Order **Perciformes** Bleeker, 1859
Family Serranidae Swainson, 1839
Genus *Pseudanthias* Bleker, 1871

</div>

<div align="center">

Pseudanthias obrotchishtensis (Strashimirov, 1981)
Figs. 16E–M

</div>

?1968   *Otolithus (Sparidarum) spinosus* - Suzin (in Zhizhchenko): pl. 18, fig. 19 [name not available according to ICZN article 13.1.1].
1981   *Perca obrotchishtensis* - Strashimirov: pl. 2, figs. 3-4.
2006   *Centropristis integer* Schubert, 1906 - Djafarova: pl. 13, fig. 5.
?2015   *Pontinus*? aff. *obrotchishtensis* (Strashimirov, 1981) - Bratishko et al.: figs. 6.1-2.

Material: 526 specimens, figured specimens NMNH ГКН 5960 048 and SMF PO 101.180, Bessarabian, Jurkine, Crimea; in addition 2 specimens from micro-sample #12 and 3 specimens from micro-sample #14.

Remark: The nature of this species has been discussed in Bratishko et al. (2015) but without reaching a definitive conclusion. Abundant new material collected from Jurkine now allows for a detailed investigation and, therefore, diagnosis and description are redefined below.

Diagnosis: Thin, delicate, fusiform shape with pointed rostrum and posterior tip; OL:OH = 1.85–2.15. Dorsal rim coarsely and irregularly crenulated, with obtuse middorsal angle. Rostrum long, pointed, 18–28% of OL. CaL:OsL = 0.85–1.05. Caudal tip very slightly flexed, terminating at some distance from posterior tip of otolith.

Description. Thin, delicate and relatively small otoliths up to 2.7 mm in length. OH:OT = 3.1–3.4. Dorsal rim gently curved and intensely, coarse and irregularly crenulated, with low, obtuse middorsal angle and no postdorsal angle. Ventral rim equally strongly curved but much smoother except some irregular undulating along its posterior most stretch. Rostrum sharp, long, 18–28% of OL; excisura and antirostrum variable, usually not strong. Posterior tip pointed, often sharp, nearly symmetrical to rostrum in expression and position.

Inner face markedly convex. Sulcus long, moderately narrow and deep, its ostium and cauda of nearly same length. Ostium somewhat wider than cauda, particularly ventrally widened and dorsally more gradually bent. Cauda straight for the most part, its tip very slightly flexed and terminating at some distance from posterior rim of otolith. OL:SuL = 1.25–1.3; CaL:OsL = 0.85–1.05. Dorsal depression small, narrow, dorsally fading into broad furrows extending from crenulation of dorsal rim; no ventral furrow discernable. Outer face concave, with some irregular radial ornamentation.

Discussion. *Pseudanthias obrotchishtensis* was originally described from the Konkian of Bulgaria based on a specimen of about 1 mm in length. According to the figure and description by Strashimirov (1981), the small holotype differs from our specimens, which are at least twice the size and in the presence of a small umbo on the center of the outer face. All other characteristics are similar. This small difference may represent an ontogenetic effect that is visible as a hint in the smallest specimens available

from Jurkine (Fig. 16J). A specimen described by Bratishko et al. (2015) as *Pontinus*? aff. *obrotchishtensis* from the Konkian of Mangyshlak, Kazakhstan, differs in terms of its much shorter rostrum than any specimen from Jurkine (12% of OL *vs.* 18–28%); it may indeed represent a different species. A further, very small specimen of 0.6 mm in length from the Tarchanian of Bulgaria cannot reliably be allocated to a species but indicates that this group of fish may have a relatively long history in the Eastern Paratethys.

Bratishko et al. (2015) related these otoliths tentatively to the scorpaenid genus *Pontinus* Poey, 1860. However, after a detailed correlation with serranid otoliths as figured in Lin and Chang (2012) and Lombarte et al. (2006), we consider a serranid genus more likely, particularly the species-rich genus *Pseudanthias*. The main distinguishing characteristic of *P. obrotchishtensis* compared to the otoliths of the extant species figured in Lin and Chang (2012) is the termination of the cauda at a greater distance from the posterior rim of the otoliths than is the case in the extant forms.

The fish of both taxa, *Pontinus* and *Pseudanthias*, are mainly found in the vicinity of reefs. Given the abundance of *P. obrotchishtensis* in Jurkine, the presence of a nearby reef at the time of deposition is likely. Furthermore, the many specimens in Jurkine are all more or less of the same size (between 2.2 and 2.7 mm in length). This is about half the size of most extant *Pseudanthias* otoliths figured in Lin and Chang (2012) and would indicate small fish living in schools.

Order **Scorpaeniformes** Garman, 1899
Family Congiopodidae Gill, 1889
Genus indet.

Congiopodus? *inopinatus* n. sp.
Fig. 16C–D

Holotype: Fig. 16C–D, NMNH ГКН 5960 049, Bessarabian, Jurkine, Crimea.

Etymology: From inopinatus (Latin) = unexpected, referring to the unexpected occurrence of this otolith in the Eastern Paratethys.

Diagnosis: OL:OH = 2.25. Rostrum long, massive with rounded tip, 30% of OL. Excisura broad, orthogonal. Posterior tip mirror image of rostrum including excisura-like incision, 32% of OL. Sulcus short, anteriorly open, dorsally fading. OL:SuL = 1.85; OsL:CaL = 1.45.

Description. The unique holotype is 4.3 mm in length and perfectly preserved. OL:OH = 2.25; OH:OT = 2.35. Dorsal rim subdivided into three nearly equally long sections; anterior section horizontal, forming upper border of rostrum, ending at orthogonal and prominent excisura; posterior section almost exact mirror image of anterior section; middle section elevated by vertical anterior and posterior walls and with flat top reminding a rectangle. Ventral rim very irregularly curved, deepest anterior of its middle, stepping back behind middle. Rostrum long, massive, with rounded tip; posterior rim almost exact mirror image.

Inner face distinctly convex with moderately deep, short, anteriorly open sulcus, posteriorly not quite reaching to posterior end of middorsal section. Sulcus divided in a moderately wide, dorsally open ostium and a straight, short, narrow cauda with fading dorsal margin. OL:SuL = 1.85; OsL:CaL = 1.45; OsH:CaH = 2.0. Dorsal depression only on middorsal section, blending into cauda. Ventral field coarsely sculptured, with ventral furrow only below sulcus until step in ventral rim of otolith. Outer face concave, more or less smooth.

Discussion. *Congiopodus*? *inopinatus* n. sp. is an extraordinary otolith with a prominent and unique morphology. The only vaguely similar morphology we could identify is that of otoliths of the Congiopodidae (see Smale et al. 1995 and Nolf 2013 for figures), but these have considerably longer sulci. The Congiopodidae are a Southern Hemisphere, temperate water fish family, and their occurrence in the Miocene of the Eastern Paratethys is unexpected. Because of the mentioned differences in the otolith morphology and the remoteness of the extant fish of this family, we only tentatively place *Congiopodus*? *inopinatus* n. sp. in this family. If this interpretation could be verified, the species would likely represent an extinct genus, but it could also be the case that it belongs to some other scorpaeniform fish for which no extant otoliths are yet known.

Order **Spariformes** Bleeker, 1876
Family Sparidae Rafinesque, 1810
Genus *Diplodus* Rafinesque, 1810

Diplodus sp.
Fig. 16T–U

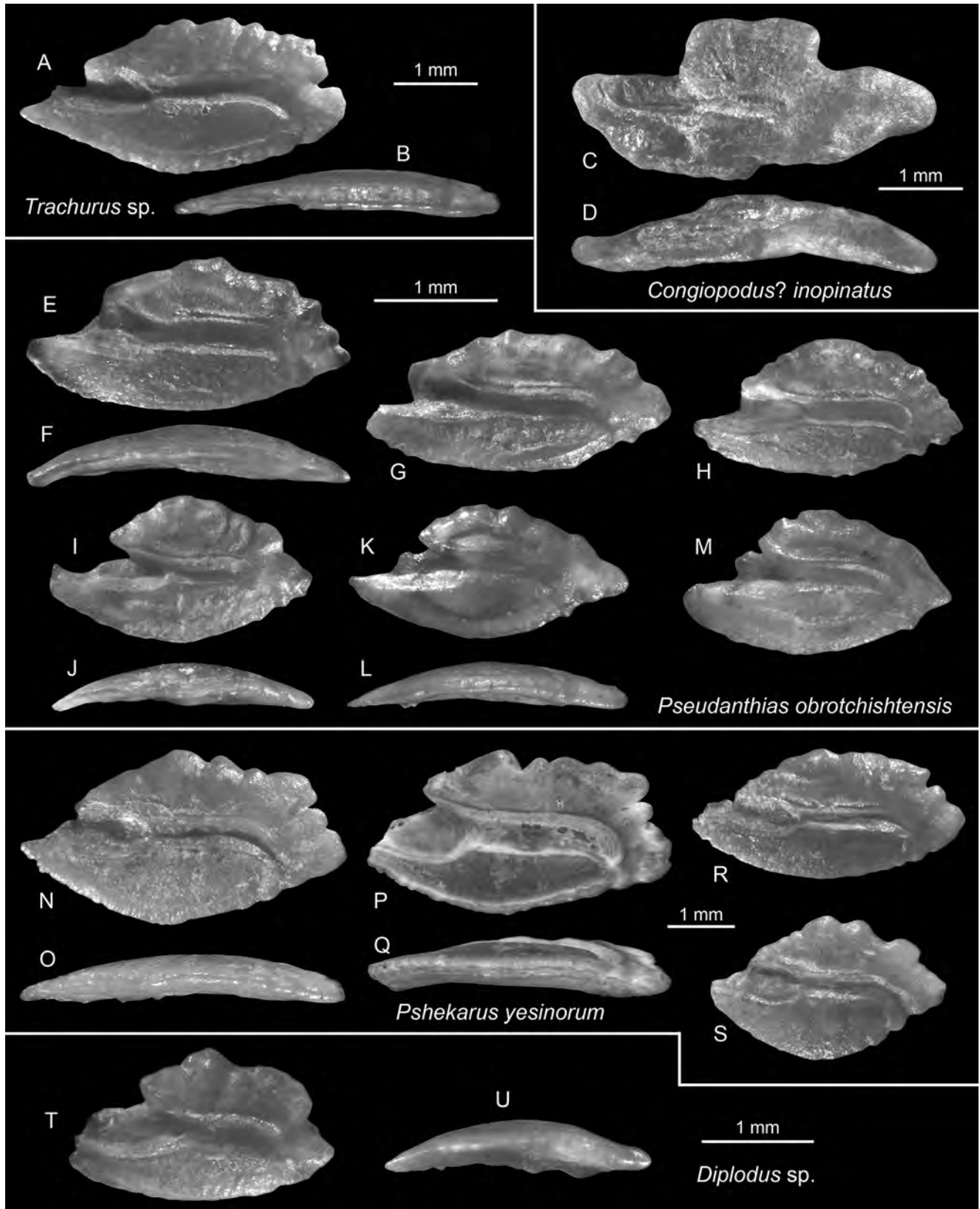**Material**: 1 specimen, NMNH ГКН 5960 050, Bessarabian, Jurkine, Crimea.

Fig. 16 - Carangidae, Congiopodidae, Serranidae, Sparidae. A–B) *Trachurus* sp. NMNH ГКН 5960 047, B ventral view, Bessarabian, Jurkine. C–D) *Congiopodus? inopinatus* n. sp., holotype, NMNH ГКН 5960 049, D ventral view, Bessarabian, Jurkine. E–M) *Pseudanthias obrotch-ishtensis* (Strashimirov, 1981), NMNH ГКН 5960 048 (E–F, I–J) and SMF PO 101.180 (G–H, K–M), F, J, L ventral views, Bessarabian, Jurkine. N–S) *Pshekarus yesinorum* Bannikov & Kotlyar, 2015, NMNH ГКН 5960 051 (N–O, S) and SMF PO 101.181 (P–R), O, Q ventral views, Bessarabian, Jurkine. T–U) *Diplodus* sp., NMNH ГКН 5960 050, U ventral view, Bessarabian, Jurkine.

Discussion. The single specimen of 2.35 mm in length lacks the tip of the rostrum but otherwise is well-preserved. It shares with the extant species of the genus the shallow ventral rim, extensive rostrum, coarsely undulating dorsal rim, and a sulcus with an equally long ostium and cauda (with the latter being only slightly flexed at the tip; see Lombarte et al. 2006 for figures).

Genus *Pshekharus* Bannikov & Kotlyar, 2015

Pshekharus yesinorum Bannikov & Kotlyar, 2015
Figs. 16N–R, 16S?

2015 *Pshekharus yesinorum* - Bannikov & Kotlyar: pl. 10, fig. 1, pl. 11 figs. 1-3 (fig. 2 represents an otolith found in situ).

Material: 37 specimens, thereof one tentatively assigned (Fig. 16S), figured specimens NMNH ГКН 5960 051 and SMF PO 101.181, Bessarabian, Jurkine, Crimea; in addition 1 specimen from micro-sample #12 and 1 specimen from micro-sample #13.

Remark. Bannikov & Kotlyar (2015) figured and described an otolith found in situ in the holotype. A diagnosis of the otolith was not given and is therefore added here, while the description is referred to their article.

Diagnosis: OL:OH = 1.85–2.05. Ventral rim shallow, rather smooth; dorsal rim intensely crenulated with low middorsal and more pronounced postdorsal angle. Rostrum long, 18–28% of OL (rostral tip damaged in holotype). Ostium ventrally widened; cauda slightly flexed at tip. OsL:CaL = 0.95–1.05. Ventral furrow close to ventral rim of otolith.

Discussion. A single otolith is distinctly more compressed (OL:OH = 1.65) and therefore only tentatively assigned to *Pshekharus yesinorum*, which are typical sparid otoliths that would not be distinguishable on the genus level from other sparid genera. However, *Pshekharus yesinorum* is known from an articulated skeleton with otoliths in situ for calibration (Bannikov & Kotlyar 2015). This case exemplifies the limitations of generic diagnosis in otoliths in certain groups. *Pshekharus yesinorum* appears to be an endemic genus and species of the Paratethys in the lower and middle Sarmatian s.l. (Volhynian and Bessarabian).

Order **Acanthuriformes** Berg, 1937
Family Sciaenidae Cuvier, 1828
Genus *Pontosciaena* Bannikov, Schwarzhans & Carnevale, 2018

Pontosciaena acuterostrata (Rückert-Ülkümen, 1996)
Figs. 17A–J

1996 *Serranus acuterostratus* - Rückert-Ülkümen: pl. 2, figs. 4-6.
2017? *Genyonemus?* sp. - Bratishko, Kovalchuk & Schwarzhans: figs. 3.5-8.
2018 *Pontosciaena acuterostrata* (Rückert-Ülkümen, 1996) - Bannikov, Schwarzhans & Carnevale: fig. 7 (see there for further references).

Material: 22 specimens, figured specimens NMNH ГКН 5960 052 and SMF PO 101.182, Bessarabian, Jurkine, Crimea.

Discussion. *Pontosciaena acuterostrata* was redefined by Bannikov et al. (2018) based primarily on the material from Jurkine presented herein. This species is known from the Bessarabian of Ukraine found in marine environments like Jurkine and also estuarine brackish environments like Mykhailivka (Bratishko et al. 2017). It was originally described from undiffereniated Sarmatian deposits of western Turkey deposited in a brackish environment with marine intervals (Rückert-Ülkümen 1996).

Order **Caproiformes** Nelson, 2006
Family Caproidae Bonaparte, 1835
Genus *Capros* Lacepède, 1802

Capros crudus n. sp.
Figs. 17K-X

Holotype: Fig. 17L–M, NMNH ГКН 5960 053, Bessarabian, Jurkine, Crimea.

Paratypes: 7 specimens, NMNH ГКН 5960 054 and SMF PO 101.183, same data as holotype.

Referred specimens: 15 specimens, same data as holotype.

Etymology: From crudus (Latin) = raw, crude, referring to the uneven and irregular features of the otolith.

Diagnosis: OL:OH = 1.2–1.5. Dorsal rim shallow; ventral rim deep, very irregular with postventral indentation. Cauda closed posteriorly or incompletely open. CaL:OsL = 1.05–1.35.

Description (for specimens greater than 1.25 mm in length). Small, compact otoliths with very deep sulcus, up to 2.2 mm in length (holotype 1.9 mm). OL:OH = 1.2–1.5; OH:OT = 2.0–3.0. Dorsal rim shallow, almost horizontal, irregularly undulating, with pronounced postdorsal projection at junction with posterior rim. Ventral rim deep, anteriorly more or less regularly curved, posteriorly with very variable and irregular indentation. Rostrum massive, ventrally steeply curved, dorsally nearly flat, 18–32% of OL. Excisura variably deep and wide; antirostrum mostly distinct, half as long or less than rostrum. Posterior rim irregular, inclined at 95–110° upwards toward projection at intersection with dorsal rim.
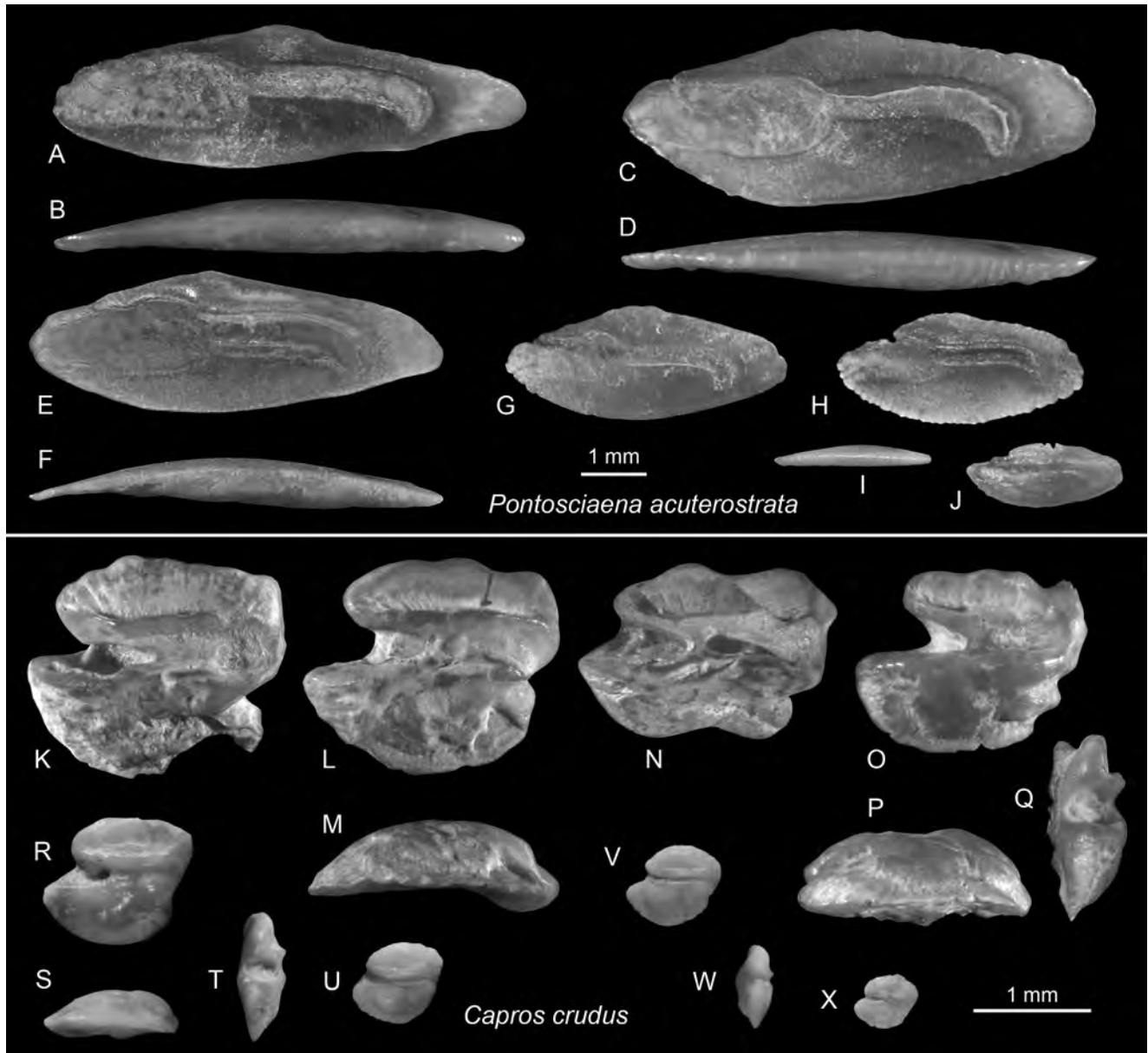
Fig. 17 - Sciaenidae and Caproidae. A–J) *Pontosciaena acuterostrata* (Rückert-Ülkümen, 1996), NMNH ГКН 5960 052 (C–D, H–J) and SMF PO 101.182 (A–B, E–G), B, D, F, I ventral views, Bessarabian, Jurkine. K–X) *Capros crudus* n. sp., holotype (L–M) NMNH ГКН 5960 053, paratypes (K, N–X) NMNH ГКН 5960 054 (N, R–U) and SMF PO 101.183 (K, O–Q, V–X), M, P, S ventral views, Q, T anterior views, U–X juvenile specimens, Bessarabian, Jurkine.

Inner face strongly convex, particularly ventral field strongly bulged. Sulcus very deep, distinctly supramedian, its ostium open and its cauda posteriorly closed or nearly so. Ostium slightly wider, deeper, and shorter than cauda; CaL:OsL = 1.05–1.35. Ostial colliculum usually well marked, caudal colliculum less so. Dorsal field with deep depression across entire length bordered by strong crista superior towards sulcus; ventral field irregularly bulged with small depressions posteriorly adjacent to indentations of postventral otolith rim. Outer face flat to slightly concave sometimes with small, shallow central umbo, irregularly sculptured or smooth.

Ontogenetic changes. A complete ontogenetic series has been found from *Capros crudus*, and further commentary is necessary due to a number of changes. Smaller specimens smaller than 1.25 mm in length (Figs. 17U–X) show a much more regular shape: the dorsal rim is evenly bent, and the ventral rim is deeply but regularly curved without posterior indentation. Furthermore, the sulcus is narrower than in the larger specimens. The excisura

and antirostrum are much weaker, and the rostrum projects less strongly than in large specimens. The cauda is always closed to the posterior rim of the otolith and sometimes even leaves a marked interspace. The outer face is typically convex with a broad umbo (Fig. 17W).

Discussion. The genus *Capros* is monospecific today with *Capros aper* (Linnaeus, 1758), known from the Northeast Atlantic and the Mediterranean. Its unmistakable otoliths are known to occur without much morphological change since the Middle Miocene of the North Sea Basin (Schwarzhans 2010). Recently, a specimen of *C. aper* was found in the late Badenian of western Ukraine (Schwarzhans et al. 2022). *Capros crudus* n. sp. differs from the otoliths of *C. aper* and its putative predecessor *C. siccus* Schwarzhans, 2008 from the late Oligocene of the North Sea Basin first in the higher OL:OH ratio of 1.2–1.5 (*vs.* 0.9–1.05) and second in the shallow dorsal rim. It further differs from *C. aper* in the closure of the caudal tip toward the posterior rim of the otolith (*vs.* open), a characteristic shared with *C. siccus*. Several skeleton-based fossil species of *Capros* are known from the Oligocene of the Paratethys and the North Sea Basin, and one fossil species is known from the Late Miocene of Italy (Baciu et al. 2009; Bannikov 2010). However, *Capros* skeletons have not been recorded from the Miocene of the Paratethys, although four skeleton-based species of the closely related fossil genus *Proantigonia* are known from the Oligocene to lower Sarmatian s.l. in the Paratethys (Baciu et al., 2009). *Capros crudus* n. sp. likely represents an endemic offshoot of the main branch of the lineage with the extant *C. aper* as suggested by the finding of *C. asper* in the late Badenian of western Ukraine (Schwarzhans et al., 2022). Alternatively, the species could be related to the *Proantigonia* lineage. The final allocation of the species can only be resolved when otoliths are found in situ in *Proantigonia*.

FAUNAL EVALUATION AND DISCUSSION

Biostratigraphic revision of the Jurkine section mainly based on foraminifera

The foraminiferal analysis provided tools for re-interpreting the stratigraphic range of the Kurortne and Korenkovo formations (Figs. 2a,b, 3).

- *Kurortne Formation, Vasylivkian regional horizon, middle Sarmatian s.l. (middle Bessarabian).*

Levels 1 and 2 (samples #12 and #13) contained many (514) large and thick-walled tests of benthic foraminifera. The representatives of miliolids (*Dogielina sarmatica* Bogdanovich & Voloshnova, 1949, *Quinqueloculina voloshinovae* var. *voloshinovae* [Bogdanovich, 1947], *Q. voloshinovae* var. *brevidentata* [Voloshinova & Bogdanovich, 1952], *Q. consobrina* var. nitens [Reuss, 1860], *Q. angustioris* [Bogdanovich, 1952], *Quinqueloculina* sp.1, *Q. complanata* [Geerke & Issaeva, 1952], *Q. consobrina* var. *plana* [Voloshinova, 1952], *Q. delicatula* Vella, 1957, *Meandroloculina bogatschovi* Bogdanovich, 1935, *M. litoralis* Bogdanovich, 1952, *M. schirwanensis* Bogdanovich, 1952, *Meandroloculina* sp.1, and *Sarmatiella* ex gr. *subtilis* Bogdanovich, 1952) were dominant (93%). Elphidiids (*Elphidium reginum* d'Orbigny, 1846, *E. aculeatum* [d'Orbigny, 1846], *E. macellum* [Fichtel & Moll, 1798], *E. crispum* [Linnaeus, 1758]) and nonionids (*Porosononion subgranosus* [Egger, 1857], *P. subgranosus* var. *aragviensis* [Dzhanelidze, 1953], *P. subgranosus* var. 1) were less common, accounting for remaining 7%.

A significant change was observed in the quantitative ratio of foraminifera in level 3. Sample #14 with 143 foraminiferal tests showed an equal ratio of milliolids (*Dogielina sarmatica, Quinqueloculina angustioris, Q. delicatula, Spiroloculina okrojantzi* Bogdanovich, 1947, *Meandroloculina litoralis, Meandroloculina* sp.1), elphidiids (*Elphidium reginum* [d'Orbigny, 1846], *E. aculeatum, E. macellum, E. crispum*), and nonionids (*Porosononion subgranosus, Porosononion subgranosus* var. *aragviensis*). Sample #15 is characterized by a predominance of the species *Elphidium reginum* (82%) over other representatives of elphidiids (*Elphidium aculeatum, E. macellum, E. crispum*), nonionids (*Porosononion subgranosus subgranosus*), and milliolids (*Quinqueloculina voloshinovae* var. *voloshinovae, Q. consobrina* var. nitens, *Q. angustioris, Q. complanata* var. *plana, Q. delicatula Q.* sp.1).

In level 4 (sample #16), representatives of milliolids were no longer evident. Only two foraminiferal species were found in this level: *Elphidium macellum* (129 tests, 83%) and *Porosononion subgranosus* var. 1 (26 tests, 17%).

Level 5 (sample #17) did not contain foraminifera.

The sediments from level 6 (sample #18) revealed representatives of nonionids only. The sample did contain a large amount of specimens of *Porosononion subgranosus* and its related varieties: *Porosononion subgranosus* var. *aragviensis, Porosononion*

subgranosus var. *umboelata* Gerke, 1960, and *Porosononion subgranosus* (Egger) var. 1.

Level 7 (sample #19) contained the same nonionid assemblage, but this assemblage based on fewer tests (49).

In level 10 (sample #20), representatives of nonionids (*Porosononion subgranosus* var. *aragviensis, P. subgranosus* var. 1) dominated (94%), accompanied with 13 tests (6%) of *Elphidium macellum*.

Levels 1–10 pertain to the middle Sarmatian s.l. based on foramniferal index species typical of the Bessarabian (all representatives of the genera *Meandroloculina, Sarmatiella, Dogielina*; varieties of *Porosononion subgranosus*; *Quinqueloculina voloshinovae,* and its varieties) (e.g., Bogdanowich 1965; Maissuradze 1980; Maissuradze & Koiava 2011). The benthic foraminifer species composition is typical for the middle part of the Bessarabian (called "deposits with typical Middle Sarmatian fauna" in the cited literature). This fauna is characterized in the Eastern Paratethys by an evolutionary pulse in the diversity of foraminiferal species driven by the appearance of a large number of endemic species and their variations (e.g., Didkovsky 1964; Muratov & Nevesskaya 1986; Maissuradze 1971, 1980; Maissuradze & Koiava 2011). In addition to the specific set of foraminifera, these levels also exhibit a diverse association of mollusks and bryozoans (the so-called "vincular limestones" with clusters of Schizoporellidae; e.g. Andrusov 1893; Arkhanguelsky et al. 1930; Arkhangelsky 1940; Veis 1988). This diversity allows these deposits to be identified as representing the middle part of the Bessrabian—that is, the Vasylivkian regional horizon (e.g. Paramonova & Belokrys 1972; Belokrys 1976; Paramonova 1994). Based on their lithological characteristics, these deposits (Andrusov 1893; Arkhanguelsky et al. 1930; Arkhangelsky 1940; Vernigorova et al. 2012; Vernyhorova 2014) are identified as belonging to the Kurortne Formation of the Kerch Peninsula (Vernyhorova et al. 2012; Vernyhorova 2014).

- *Korenkove Formation (lower part), Dnipropetrovskian regional horizon, middle Sarmatian s.l. (upper Bessarabian).*

A sharp reduction in the diversity of the benthic foraminiferal composition and a change in the morphological characteristics of their tests were observed in deposits of level 13 (samples #21, #22) and 14 (sample #23). Only a few specimens

of the thin-walled, small-test species *Quinqueloculina consobrina* var. *nitens*, *Q. angustioris*, and *Elphidium reginum*, as well as a fragment of *Sarmatiella* ex gr. *subtilis*, were found in samples 21 and 22. *Quinqueloculina angustioris, Elphidium macellum, Elphidium* sp.1., and *Porosononion subgranosus subgranosus* were found in sample #23.

In earlier literature, the clay formations overlying rocks of the middle Sarmatian vincular limestones on the Kerch Peninsula were attributed to the late Sarmatian due to the presence of the mollusk *Mactra (Chersonimactra) caspia* (Eichwald, 1841) (e.g., Andrusov 1893; Arkhanguelsky et al. 1930; Arkhangelsky 1940; Muratov & Nevesskaya 1986; Paramonova 1994). This mollusk species is considered typical of the clayey facies of the late Sarmatian (e.g., Andrusov 1893; Arkhanguelsky et al. 1930; Arkhangelsky 1940). However, *Mactra (Chersonimactra) caspia* is absent from the lower part of this section at Jurkine and it only occurs higher in the section. The boundary between the middle and upper Sarmatian s.l. (Bessarabian and Khersonian) in this part of the Kerch Peninsula was thus determined by a change in lithology from clayey limestones to clays, as well as the presence of a sharp contact with pebbly gravel between them (Andrusov 1893). This contact led Andrusov to suggest a sedimentary hiatus caused by a folding phase on the Kerch Peninsula that occurred at the beginning of the late Sarmatian and resulted in the folding of middle Sarmatian limestones (Andrusov 1893). Previously, we agreed with this concept and considered the clays above the contact to represent the late Sarmatian. The rocks above the contact would then represent the upper part of the Korenkove Formation of the Khersonian (upper Sarmatian s.l.) (Vernyhorova at al. 2012; Vernyhorova 2014). In the Jurkine section, levels 12–19 were consequently assigned to the upper part of the Korenkove Formation of Khersonian age. However, the foraminiferal analysis of the new samples indicates that some of the samples are of middle Sarmatian age. The samples from levels 12–14 contain middle Sarmatian s.l. index species of foramnifera: *Quinqueloculina consobrina* var. *nitens*, *Q. angustioris, Sarmatiella* ex gr. *subtilis, Elphidium reginum.* Thus, based on the foraminifera and in the absence of the index species of mollusks for the Khersonian (*Mactra (Chersonimactra) caspia*), these deposits (levels 12–14) are now placed in the Dnipropetrovskian regional horizon of the Bessarabian

(following Didkovsky, 1964; Maissuradze, 1971, 1980; Maissuradze & Koiava, 2011).

- *Korenkove Formation (upper part), upper Sarmatian s.l. (Khersonian).*

Deposits from levels 15a (sample #23a) and 17 (sample #24) did not contain foraminifera. Only one thin-walled, small test of *Quinqueloculina* sp. 2 was found in level 18 (sample # 25). A sharp depletion of the foraminifer species composition, the absence of index species for the middle Sarmatian in mollusks and foraminifera, and the presence of the upper Sarmatian index mollusk *Mactra* (*Chersonimactra*) *caspia* support the stratigraphic dating of levels 15–19 as representing the upper Sarmatian s.l. (Khersonian) (see, e.g., Bogdanowich 1965; Muratov & Nevesskaya 1986). From a lithological viewpoint, these rocks belong to the upper part of the Korenkove Formation (according to Vernyhorova at al. 2012; Vernyhorova 2014). The boundary between the middle and upper Sarmatian is thus considered to be gradual and defined only by faunal changes within the Korenkove Formation. Regarding the timing of a Sarmatian folding phase on the Kerch Peninsula, the phase most likely occurred at the end of the middle Sarmatian, whereas the transition from the middle to the late Sarmatian s.l. in the area was gradual, without abrupt environmental or tectonic events.

EVALUATION OF OTOLITH DATA

Faunal composition (Tab. 1), diversification level, and comparison with skeleton findings (Tab. 2)

The otolith association of the Bessarabian of Jurkine is rich, unique and diverse, having yielded 36 species representing 29 genera and 18 families (Tab. 1). By far the most diverse family is the Gobiidae, which has 12 species, followed by the Soleidae, with 3 species. All other families are represented by only one or two species. The dominance of gobiid otoliths has been observed in all Paratethyan otolith assemblages of post-Badenian times, as well as in the Eastern Paratethys, since Konkian times (e.g., Bratishko et al. 2015, 2017; Reichenbacher et al. 2018; Schwarzhans et al. 2022). The species diversity observed in Jurkine, however, was significantly larger than that previously observed in any otolith-based faunas in the Paratethys since the Sarmatian, as well as that of the Konkian of Kazakhstan (Bratishko et al. 2015), which was already unusually rich with 30 recognized species (*vs.* 36 in Jurkine). The species richness of Jurkine compares well with that observed from articulated fish skeletons (e.g., Bannikov 2010; Schwarzhans & Carnevale 2017; Reichenbacher & Bannikov 2021, 2022), as discussed in more detail below. One prime difference is observed in the abundance of fish taxa when comparing otolith and skeleton data from the Sarmatian s.l., which is the abundance of clupeids in skeletons and their rarity in otoliths. The reason for this discrepancy is unknown but could possibly be related to the delicate nature of clupeid otoliths, which can break easily into unrecognizable fragments or become decomposed and/or fragmented in the guts of predators (see discussion in Carnevale & Schwarzhans 2022). We also noted that clupeid otolith specimens smaller than 1 mm in length occur relatively common in certain micro-samples (see below).

As described in the Material and Methods section, the majority of otoliths were collected in residue of a mesh size of 0.7 mm. However, smaller fractions of 0.5 and 0.3 mm mesh sizes were also sampled for otoliths in smaller samples, and few samples processed for microfossils (#12 to #15) at 0.063 mm mesh size also yielded small otoliths. These primarily yielded very small gobiid otoliths, likely from juvenile or larval fishes, but also revealed one species (*Paramacroramphosus pumilis* of the Macroramphosidae) that otherwise would have remained undiscovered. *Paramacroramphosus pumilis* was particularly common in micro-sample #14 where it was second only to unidentifiable juvenile gobiid otoliths. The abundance and composition of small otoliths in the micro-samples varies somewhat with juvenile, and mostly unidentifiable gobiid and bothid otoliths as well as those of *Palimphemus, Paramacroramphosus* and *Maeotichthys* being the most common ones. It documents, however, that residue obtained from very small mesh sizes can result in a different picture of the frequency of taxa. A few paleontologists have previously sampled otoliths from foraminiferal screening, which also included very small otoliths (e.g., Pobedina 1954, 1956; Suzin 1968; Strashimirov 1972, 1980, 1981a,b, 1984, 1985; Djafarova 2006). Their finds suggest similar results, including the record of (unrecognized) *Paramacroramphosus* otoliths (Pobedina 1956; Suzin 1968; Djafarova 2006).

Family	Species	Specimens	Percentage
Clupeidae			
	Alosa grandis Djafarova, 2006)	20	0.35
	Maeotichthys wilhelmi (Djafarova, 2006)	71	1.25
	clupeid indet. juv.	3	0.05
Gadidae			
	Palimphemus cimmerius n. sp.	942	16.57
Gaidropsaridae			
	Enchelyopus susedanus (Kner, 1863)	155	2.73
	Onogadus simplicissimus (Schubert, 1906)	285	5.01
Gobiidae			
	Mesogobius chersonesus n. sp.	19	0.33
	Neogobius cf. *bettinae* Bratishko et al., 2017	22	0.39
	Neogobius ignotus n. sp.	13	0.23
	Neogobius uncinatus n. sp.	7	0.12
	Zosterisessor pontikapaionensis n. sp.	18	0.32
	Pontogobius ahnelti n. sp.	181	3.18
	Pontogobius trigonus n. sp.	92	1.62
	Pontogobius zonatus n. sp.	95	1.67
	Globogobius globulosus n. sp.	846	14.88
	Globogobius depressus n. sp.	22	0.39
	Ambyleleotris robusta n. sp.	5	0.09
	Hyrcanogobius eccentricus n. sp.	896	15.76
	gobiid indet. juv.	153	2.69
Microdesmidae			
	Paroxymetopon alienus n. sp.	1	0.02
Mugilidae			
	Chelon jurkinensis n. sp.	43	0.76
Atherinidae			
	Atherina gidjakensis (Pobedina, 1956)	88	1.55
Macroramphosidae			
	Paramacroramphosus pumilis n. sp.	106	1.86
Bothidae			
	Arnoglossus kerichensis n. sp.	347	6.10
	Arnoglossus scitulus n. sp.	508	8.94
	bothid indet. juv.	28	0.49
Soleidae			
	Aseraggodes azovensis n. sp.	17	0.30
	Dicologlossa postpatens n. sp.	19	0.33
	Parasolea serbica (Anđelković, 1966)	33	0.58
Callionymidae			
	Callionymus bessarabianus n. sp.	3	0.05
	Callionymus kalinus n. sp.	12	0.21
Scombridae			
	Scomber qirimensis n. sp.	17	0.30
Carangidae			
	Trachurus sp.	1	0.02
Serranidae			
	Pseudanthias obrotchishtensis (Strashimirov, 1981)	531	9.34
Congiopodidae			
	Congiopodus? *inopinatus* n. sp.	1	0.02
Sparidae			
	Diplodus sp.	1	0.02
	Pshekharus yesinorum Bannikov & Kotlyar, 2015	39	0.69
Sciaenidae			
	Pontosciaena acuterostrata (Rückert-Ülkümen, 1996)	22	0.39
Caproidae			
	Capros crudus n. sp.	23	0.40
Totals	**36 species + 3 indet. juv.**	**5685**	**100.00**

Tab. 1 - Species list of identified otoliths with total counts and percentages.

Also of interest is the presence or absence of small otolith specimens of certain taxa in the samples. We found small otoliths—supposedly stemming from juvenile specimens of small ranges in size—of *Maeotichthys wilhelmi, Palimphemus cim-* *merius, Mesogobius chersonesus, Neogobius uncinatus, Pontogobius ahnelti, Pontogobius trigonus, Pontogobius zonatus, Arnoglossus kerichensis, Arnoglossus scitulus, Pontosciaena acuterostrata*, and *Capros crudus*. All these species can be considered as having lived in the same area

and environment through most of their ontogeny. However, this list may contain more species of the gobiids that cannot be recognized/differentiated at very small sizes. In contrast, we only observed otoliths of a well-defined size class, mostly considered to stem from adult individuals of the following species: *Alosa grandis, Enchelyopus susedanus, Globogobius globulosus, Chelon jurkinensis, Parasolea serbica*, and *Pseudanthias obrotchishtensis* (considering only species with more than 15 specimens recovered). Assuming that these fishes lived in schools of different size classes or migrated between environments during ontogeny is reasonable. The most obvious case is the common *Pseudanthias obrotchishtensis*, for which practically all 500-plus specimens were of the same size (between 2.0 and 2.6 mm in length). This species was originally described based on a unique holotype 1 mm in length from the Konkian of Bulgaria.

The diversity index (adding the most common species up to the 90% threshold) is 13 species, a relatively high diversification level comparable with fully marine otolith-based faunas known from the Miocene of New Zealand (Schwarzhans 2019) or Chile (Schwarzhans & Nielsen 2021). The number of species was also higher than most diversity indices from the Miocene of the North Sea Basin (Schwarzhans 2010) but slightly lower than that of a late Badenian back-reef fauna from western Ukraine (Schwarzhans et al. 2022). The three most common species were *Palimphemus cimmerius* (16.57%), *Hyrcanogobius eccentricus* (15.76%), and *Globogobius globulosus* (14.88%). Other common fish in ranges between 1.25 and 9.34% are found with two species of the Gaidropsaridae, three additional species of the Gobiidae, two species in the Bothidae, and one species each in the Serranidae, Atherinidae, and Macrorhamphosidae. This diversity assessment does not consider unidentifiable juvenile or eroded gobiid otoliths, which make up 2.69% alone, and unidentifiable juvenile bothid otoliths (0.49%).

Articulated fish skeletons are well known from the Middle Miocene of the Central and Eastern Paratethys. Schultz (2013) listed 28 skeleton-based species from the Leitha Limestone of Austria, which amounts to 30 species including new records by Carnevale & Harzhauser (2013) and Carnevale and Collette (2014). According to Harzhauser et al. (2020), the Leitha Limestone is the lateral equivalent of the Baden Formation and corresponds to the latest Langhian (i.e., top early Badenian) accord-

ing to Kovać et al. (2018), which was just prior to the Badenian Salinity Crisis (middle Badenian in the sense of Hohenegger et al. 2014). Additionally, diverse articulated skeleton faunas are known from the Sarmatian s.s. of the Central Paratethys and the early Sarmatian s.l. (Volhynian) of the Eastern Paratethys. Gorjanovic-Kramberger (1891) listed 43 species from the Sarmatian s.s. of Croatia. At least five species were added with otoliths found in situ by Schwarzhans et al. (2017a-c). Bannikov (2010) listed 30 skeleton-based species in the Sarmatian s.l. of the Eastern Paratethys, likely mainly from the Volhynian. Many of these records are in open nomenclature. Reichenbacher & Bannikov (2021 and 2022) added six gobiid taxa with otoliths in situ. More undescribed fish skeletons from Volhynian strata are likely to exist in collections, many of them gobiids with otolith in situ (personal information Reichenbacher, 2022). Thirty-two fish species with otoliths in situ pertaining to 27 genera of 15 families have been recorded from the Volhynian of the Paratethys (Schwarzhans & Carnevale 2017; Reichenbacher & Bannikov 2021) (Table 2). This data set represents the highest degree of calibration of otoliths with in situ finds in articulated skeletons known from any basin and any time interval. Only four families identified by otoliths are unknown from skeletal remains in the Sarmatian s.l. (Microdesmidae, Macroramphosidae, Carangidae, Serranidae), while Centropomidae and Centracanthidae are the only families known by skeletal remains but not by otoliths (Table 2). This correlation shows how skeletal and otolith data merge to form a complementary picture when both data sets are large and comparable. However, in some of the large and diverse groups, particularly of the Gobiidae, more diversity is documented in otoliths on the genus and species level than in articulated skeletons, although studies by Schwarzhans et al. (2017c) and Reichenbacher and Bannikov (2021, 2022) narrowed this gap. In respect to the rich otolith-based Bessarabian fauna from Jurkine, however, the correlation with Volhynian or older skeletal-based taxa is limited, as will be discussed in the section on the endemic fish evolution below.

Environmental assessment (Tab. 3-4)
In a study on the mollusk fauna of the Sarmatian endemic system, Lukeneder et al. (2011) also investigated mollusks from the Bessarabian of

Genus	lower Sarmatian s.l. (Volhynian)			middle Sarmatian s.l. (Bessarabian)
	skeleton	otolith	in situ otol.	otoliths Jurkine (other)
Clupeidae				
Alosa	X	X		X
†*Maeotichthys*				X
†*Moldavichthys*	X	X	X	
†*Sarmatella*	X	X	X	
Gadidae				
†*Palimphemus*	X	X	X	X
†*Paratrisopterus*	X	X	X	(X)
Gaidropsaridae				
Enchelyopus	X	X	X	X
Onogadus		X		X
Gobiidae				
Mesogobius				X
Neogobius		X		X
Ponticola		X		(X)
†*Proneogobius*	X	X	X	
Proterorhinus		X		(X)
Zosterisessor				X
Benthophilus		X		(X)
†*Pontogobius*				X
†*Protobenthophilus*	X	X	X	(X)
Aphia	X	X	X	(X)
†*Globogobius*				X
†*Katyagobius*	X	X	X	
†*Pseudolesueurigobius*	X	X	X	
†*Sarmatigobius*	X	X	X	
†*Yarigobius*	X	X	X	
Amblyeleotris		X		X
Economidichthys	X	X	X	(X)
†*Hesperichthys*	X	X	X	(X)
Hyrcanogobius				X
Knipowitschia		X		(X)
Pomatoschistus		X		
Microdesmidae				
†*Paroxymetopon*				X
Mugilidae				
Chelon				X
Mugil	X			
Atherinidae				
Atherina	X	X	X	X
Clinidae				
†*Clinitrachoides*	X		X	
Gobiesocidae				
Apletodon	X		X	
Macroramphosidae				
†*Paramacroramphosus*				X
Bothidae				
Arnoglossus	X	X	X	X
Bothus	X		X	

Tab. 2a - Summary table of otolith and skeleton-based data from the Sarmatian (Volhynian and Bessarabian) on genus level. Brackets in Bessarabian column indicate finds other than in Jurkine.

Jurkine (Jurkino therein). They concluded a "shallow to moderately deep sublittoral environment" for the interval, "characterized by the *Hydrobia–Venerupis–Pseudamnicola* assemblage" (Lukeneder et al. 2011, p. 775). A warm and carbonate-dominated system was assumed for the Bessarabian in the Eastern Paratethys with microbialitic bryozoan-polychaete bioherms and biostroms in the coastal waters of a shallow, well-aerated, eutrophic sea (Goncharova & Rostovtseva 2009). Lukeneder et al. (2011) found that the mollusk composition of Jurkine (and the nearby Zavetnoe location) was strongly separate from that of the Volhynian from the Central Paratethys.

The foraminiferal data support the above conclusions. The benthic foraminifer association

Tabl. 2b - Summary table of otolith and skeleton-based data from the Sarmatian (Volhynian and Bessarabian) on genus level. Brackets in Bessarabian column indicate finds other than in Jurkine.

Genus	lower Sarmatian s.l. (Volhynian)			middle Sarmatian s.l. (Bessarabian)
	skeleton	otolith	in situ otol.	otoliths Jurkine (other)
Soleidae				
Aseraggodes				X
Dicologlossa		X		X
†Parasolea	X	X	X	X
Callionymidae				
Callionymus	X	X	X	X
Scombridae				
Scomber	X			X
Carangidae				
Trachurus		X		X
Trachinidae				
Trachinus	X		X	
Labridae				
Symphodus	X	X	X	
Polynemidae				
Polydactylus	X	X		
Centropomidae				
Lates	X			
Serranidae				
Pseudanthias		X		X
Mullidae				
Mullus	X	X		
Scorpaenidae				
"Scorpaena"	X		X	
Congiopodidae				
Congiopodus?				X
Centracanthidae				
†Naslavcea	X			
Sparidae				
Diplodus				X
†Pshekharus	X	X	X	X
Sparus	X	X	X	(X)
Moronidae				
Morone	X	X	X	(X)
Sciaenidae				
Argyrosomus	X			
†Croatosciaena	X			
†Leptosciaena				(X)
†Pontosciaena		X		X
†Trewasciaena		X		(X)
Umbrina		X		(X)
Caproidae				
Capros				X
†Proantigonia	X			
Totals		**50**		**44**

from the middle part of the Bessarabian (Vasylivkian regional horizon, Kurortne Formation) consists of shallow-water taxa (*Quinqueloculina*, *Dogielina*, *Meandroloculina*, *Elphidium*, and *Porosononion*), which indicate a photic zone of a middle to inner shelf (upper sublittoral zone after Hedgpeth 1957 and Longhurst 2007) resistant to salinity fluctuations (after Murray 2006; and https://paleobiodb.org; http://www.fossilworks.org). The presence of the herbivorous species *Quinqueloculina*, *Elphidium*, and nonionids in this association indicate a seagrass ecosystem in this part of the sea (e.g., Murray 2006; Trabelsi et al. 2017). Furthermore, the predominance of miliolid representatives among epifaunal species (*Quinqueloculina*, *Dogielina*, *Meandroloculina*, *Sarmatiella*) with large, thick-walled tests (oxic indicators) (Table 3) indicate a high oxygen content in the bottom water (Kaiho 1994, 1999). The changes in foraminiferal associations, including the disappearance of miliolid representatives among the epi-

	Endemic	Epifauna; Infauna	Oxic; Suboxic
1. *Dogielina sarmatica* Bogdanowicz et Voloshinova, 1949	+	epi	O
2. *Quinqueloculina voloshinovae* var. *voloshinovae* (Bogdanowicz)	+	epi	O
3. *Quinqueloculina voloshinovae* var. *brevidentata* (Voloshinova in Bogdanovich, 1952)	+	epi	O
4. *Quinqueloculina consobrina* var. *nitens* (Reuss in Bogdanowicz, 1952)	+	epi	SO
5. *Quinqueloculina angustioris* (Bogdanovich, 1952)	+	epi	O
6. *Quinqueloculina complanata* (Gerke & Isaeva in Bogdanovich, 1952)	+	epi	SO
7. *Quinqueloculina complanata* var. *plana* Gerke & Isaeva in Bogdanovich, 1952	+	epi	SO
8. *Quinqueloculina delicatula* Kolesnikova in Bogdanovich, 1952	+	epi	O
9. *Quinqueloculina* sp.1	?	epi	O
10. *Quinqueloculina* sp. 2	?	epi	O
11. *Spiroloculina okrojantzi* Bogdanovich, 1947	+	epi	O
12. *Meandroloculina bogatchovi* Bogdanowicz, 1937	+	epi	O
13. *Meandroloculina litoralis* Bogdanowicz, 1952	+	epi	O
14. *Meandroloculina schirwanensis* Bogdanowich, 1952	+	epi	O
15. *Meandroloculina* sp.1	+	epi	O
16. *Sarmatiella* ex gr. *subtilis* Bogdanowicz, 1952	+	epi	O
17. *Elphidium reginum* (d'Orbigny, 1846)		epi	SO
18. *Elphidium aculeatum* (d'Orbigny, 1846)		epi	SO
19. *Elphidium macellum* (Fichtel et Moll, 1798)		in	SO
20. *Elphidium crispum* (Linnaeus, 1758)		in	SO
21. *Elphidium* sp. 1	?	in	SO
22. *Porosononion subgranosus* (Egger) *subgranosus* Egger in Bogdanowich, 1960		in	SO
23. *Porosononion subgranosus* (Egger) var. *aragviensis* Djanelidze in Bogdanowich, 1960	+	in	SO
24. *Porosononion subgranosus* (Egger) var. *umboelata* Gerke in Bogdanowich, 1960	+	in	SO
25. *Porosononion subgranosus* (Egger) var. 1	+	in	SO

Tab. 3 - Characterization of benthic foraminifera identified from the Jurkine section in respect to endemicity and environmental indications.

fauna and the formation of monospecies infaunal associations with *Elphidium* and *Porosononion*, indicate a shallowing of the basin toward the end of the Bessarabian (e.g., Maisuradze 1980). These could also indicate a slight decrease in oxygen content in the bottom waters (Suboxic B indicators, according to Kaiho 1994, 1999). Additionally, the middle part of the Bessarabian (Vasylivkian regional horizon) is characterized by a maximal diversity of endemics in foraminifera (Table 3), mollusks (e.g., Muratov & Nevesskaya 1986; Paramonova 1994; Maisuradze 1971, 1980; Maisuradze & Koiava 2011), and, as will be discussed below, fishes (as reconstructed from otoliths).

Despite the predominance of epifaunal species, a sharp decrease in the number of foraminifer species, as well as a decrease in the abundance and size of tests, indicates the onset of oxygen deficiency (Suboxic A) in the bottom water (after Kaiho 1994; Murray 2006) at the end of the Bessarabian (Dnipropetrovskian regional horizon).

The findings of single, small-sized tests of few foraminifer species of *Quinqueloculina*, *Elphidium*, and *Porosononion*, as well as a small number of small-sized mollusk shells of *Mactra* (*Chersonimactra*) *caspia* in layers of a sufficiently thick, clayey stratum (near 95 m, levels 15–19), suggest that there were unfavorable conditions (e.g., oxygen depleted) on

Tab. 4 - Ecological characterization of teleosts identified from otoliths in the Jurkine section on genus level. For extinct genera putative related extant genera are used as place holders.
Extant genera related to and used for fossil genera in table:
X1 from *Clupeonella*
X2 from *Trisopterus*
X3 from *Benthophilus*
X4 from *Lesueurigobius*
X5 from *Oxymetopon*
X6 from *Macroramphosus*
X7 from *Vanstraelenia*
X8 from *Pagellus*

Genus	ecology			
	reef associated	stenohaline marine	marine-brackish	freshwater
Alosa			X	X
†Maeotichthys			X[1]	
†Palimphemus		X[2]		
Enchelyopus		X		
Onogadus		X		
Mesogobius			X	X
Neogobius			X	X
Zosterisessor			X	
†Pontogobius			X[3]	
†Globogobius		X[4]		
Amblyeleotris	X	X		
Hyrcanogobius			X	
†Paroxymetopon	X[5]	X[5]		
Chelon			X	
Atherina			X	
†Paramacroramphosus		X[6]		
Arnoglossus		X		
Aseraggodes		X		
Dicologlossa		X		
†Parasolea		X[7]		
Callionymus		X		
Scomber		X		
Trachurus			X	
Pseudanthias	X	X		
Congiopodus		X		
Diplodus		X		
†Pshekharus		X[8]		
†Pontosciaena			X	
Capros		X		
Totals	**3**	**18**	**11**	**3**
% of specimens		**71.12%**	**28.88%**	

the sea bottom in the study area during the late Sarmatian s.l. These conditions improved only to the extent of allowing a limited faunal assemblage to populate the sea bottom at certain times. The small size of epifaunal species and the thin walls of their tests indicate that even when the seabed was populated, the amount of near-bottom oxygen was insufficient (Suboxic A, after Kaiho 1994, 1999). Such unsuitable environmental conditions for life were typical of the late Sarmatian (Khersonian) throughout the Eastern Paratethys (e.g., Muratov & Nevesskaya 1986; Paramonova 1994; Maisuradze 1971, 1980; Maisuradze & Koiava 2011; see also below).

The environmental assessment of the otoliths from the Bessarabian of Jurkine, however, met certain limitations because of the rather large number of extinct genera in the assemblage (9 of 29; Table 4). An effort was made to select putative-related extant genera for those fossil otolith-based genera, but such an assessment can only be an approximation. Similar effects could potentially hold true for the genera that still exist today; evolving in a secluded endemic environment like the Eastern Paratethys enables endemic lineages to adapt to the changing environmental conditions. Despite these complexities and possible aberrations, certain ecological trends can be clearly recognized in the composition of the fish fauna as reconstructed from their otoliths. First, we observe a high percentage of stenohaline marine fishes in the assemblage (71.12%

of the total identified specimens; Table 4). Eighteen genera (62%) are considered stenohaline marine, including seven extinct ones for which the supposed nearest extant relatives are selected as analogs. Besides those less-certain candidates, the amount of stenohaline marine fishes was still high. Three of the stenohaline genera even show an affinity to reefal habitats, which is feasible considering potential nearby microbialitic bryozoan-polychaete bioherms as described by Goncharova & Rostovtseva (2009).

Eleven genera (58% of the total genera and approximately 28% of the total specimens) were euryhaline marine known to extend into brackish water, and three genera were known to extend into freshwater (*Alosa* of the Clupeidae and the two gobiid genera *Mesogobius* and *Neogobius*). Half of the euryhaline genera were from the family Gobiidae. Apparently, of the specimens, the Gobiidae were the ones most quickly able to adapt to the changing environments and salinities, which would explain their dominance in the assemblage both in terms of total abundance and species diversity.

A discussion of the ecological preferences of some of the other common taxa is also warranted. The most common species (albeit by a small margin) was *Palimphemus cimmerius*, an endemic, likely open-water roaming gadid that may have been able to adapt to slightly lower salinities. The demersal gaidropsarids (*Enchelyopus susedanus* and *Onogadus simplicissimus*) were relatively common as well, and they did not show any further endemic evolution from the status known from the Konkian or Volhynian. They may thus be considered survivors that were less able to adapt to changing environments and were able to thrive only when ecological conditions were supportive. Two species of bothids were common (*Arnoglossus kerichensis* and *A. scitulus*) and had evolved to endemic species from the Volhynian stock (Schwarzhans et al. 2017c). The same may have been true for the three species of soleids, but they were much less common. Finally, the serranid *Pseudanthias obrotchishtensis* needs some specific mentioning. It was considered a scorpaenid possibly related to *Pontinus* by Bratishko et al. (2015). Despite some remaining level of uncertainty in its attribution, these otoliths persistently align with extant taxa associated with reef environments. *Pseudanthias obrotchishtensis* has been very rarely observed in otolith associations of the Paratethys, but in Jurkine, it represents the fourth most-common species.

Time-equivalent otolith assemblages have rarely been recorded from the Paratethys. Bratishko et al. (2017) described a small association from a mixed riverine/marginal marine environment from Mykhailivka, southern Ukraine, containing five putative euryhaline species—three of the Gobiidae and one each of the Moronidae and Sciaenidae. Two of these, *Pontosciaena acuterostrata* (*Genyonemus?* sp. in Bratishko et al. 2017) and *Neogobius bettinae* are shared with Jurkine. Weinfurter (1953) studied otoliths from deposits of the brackish water of Lake Pannon (Central Paratethys) from the locality Brunn-Vösendorf of the substage Pannonian E (Papp 1951; Lueger 1981), which is more or less coeval with the Bessarabian of Jurkine (Fig. 18). Weinfurter (1953) described 14 species (four sciaenid species reviewed by Bannikov et al. 2018), and Schwarzhans (2010) added one additional species from the Pannonian C/D of Wiesen. Of these 15 species, one—namely, *Ponticola dorsorostralis* (Weinfurter, 1953)—is shared with Mykhailivka, and none are shared with Jurkine (Fig. 18). In respect to the families Clupeidae, Gadidae, Mugilidae, and Moronidae, as well as certain genera of the Gobiidae (*Neogobius* and *Ponticola*), different taxa have been found in Lake Pannon and at Jurkine (see below).

In conclusion, we postulate that the otolith-based fish fauna of the Bessarabian of Jurkine stands for a truly marine environment, likely with insignificantly reduced salinity and some elements expected near reefal settlements. The main exception from truly marine fishes are in the Gobiidae, which already contain a certain component of putative euryhaline taxa that foreshadowed their ability to cope with accelerated ecologic stresses that occurred at a later time. Nevertheless, the correlation with the brackish faunas from Mykhailivka and Lake Pannon are low, even for the Gobiidae, indicating that the distinguishing character of the two faunal complexes primarily reflects differences of the salinity levels.

Paleobiogeographic assessment (Fig. 18)
The early Late Miocene (Tortonian) time was characterized by a high degree of segmentation of the European seas. The North Sea Basin formed a cul-de-sac connected northward with the North Atlantic. Faunal exchange may have occurred between the North Sea and Atlantic, but fauna had to pass around the Faroe and Shetland Island pla-

Fig. 18 - Stick diagram showing the number of recorded otolith-based species per region (black) and the number of shared species between regions (red numbers) printed on the paleogeographic reconstruction of Europe during the early Tortonian (= Bessarabian in the Eastern Paratethys), based on Popov et al. (2004).

teau then believed to be contiguous with the British Islands (Popov et al. 2004; Fig. 18). Thus, faunal exchange likely had to overcome at least one step in temperature zones, and a certain part of the fish fauna in the North Sea may have thus evolved endemically (Schwarzhans 2010, 2019). Consequently, the percentage of shared species with the Mediterranean Sea was likely rather low, that is, approximately 20% of the species in the North Sea Basin at the time are also known from the Mediterranean Sea (Fig. 18) during the same period.

Knowledge of otolith assemblages in the rich Aquitaine Basin terminates with the Sallomacian (Serravallian; biozones N12 and NN6 according to Folliot et al. 1993) as studied in the comprehensive monograph by Steurbaut (1984) and only re-commences with the Redonian (latest Miocene/earliest Pliocene) of the Normandy Basin (Lanckneus & Nolf 1979). Presumed Tortonian strata sampled for otoliths from Portugal are actually primarily of Serravallian age (Steurbaut & Jonet 1981; Antunes et al. 2000), and a small fauna collected by one of us (WS) from the Tortonian Cacela Formation of the Algarve Coast has not yet been published. Thus, no Tortonian otolith assemblages from the European Atlantic coast are available for comparison.

In contrast, the Mediterranean Basin has provided an extremely rich Tortonian otolith assemblage from Piedmont, Italy (Bassoli 1906; Lin

et al. 2015, 2017). These assemblages have been described from turbidite-induced rocks that contain both deep water and shelf fish otoliths. With extensive new material currently being studied by one of us (WS), the Tortonian strata of Piedmont contains an otolith-based fish fauna of at least 180 species (Fig. 18). However, no species are shared with the stenohaline marine fauna of Jurkine (Fig. 18). This strongly indicates that no connection existed between the Eastern Paratethys and the Mediterranean during the Bessarabian and likely the entire Sarmatian s.l. (Schwarzhans 2014) (Fig. 18). Furthermore, according to Bialik et al. (2019), Torfstein and Steinberg (2020), and Sun et al. (2021), the Mediterranean Sea was permanently closed from Serravallian toward the Arabian Gulf and Indian Ocean following the Mid-Miocene Climate Transition (MMCT). This transition left the slowly restricting westward connection to the Northeast Atlantic as the only remaining passage from the Mediterranean to the world ocean for a while (Fig. 18).

Endemic fish evolution in the Bessarabian of the Eastern Paratethys (Fig. 19-23)

The lower Badenian deposits of the Central Paratethys have been extensively studied for otoliths since Koken (1891) and Procházka (1893) and have proven to be exceptionally diverse with more than 150 valid taxa (see, e.g., Radwańska 1992; Brzobo-

Fig. 19 - Range chart of teleost families from Middle Miocene to Early Pliocene in the Paratethys based on otolith data from referenced literature. Blue bars indicate taxa of Atlanto-Mediterranean origin and shared with time-equivalent occurrences in other European basins; red bars indicate putative endemic taxa in the Paratethys.
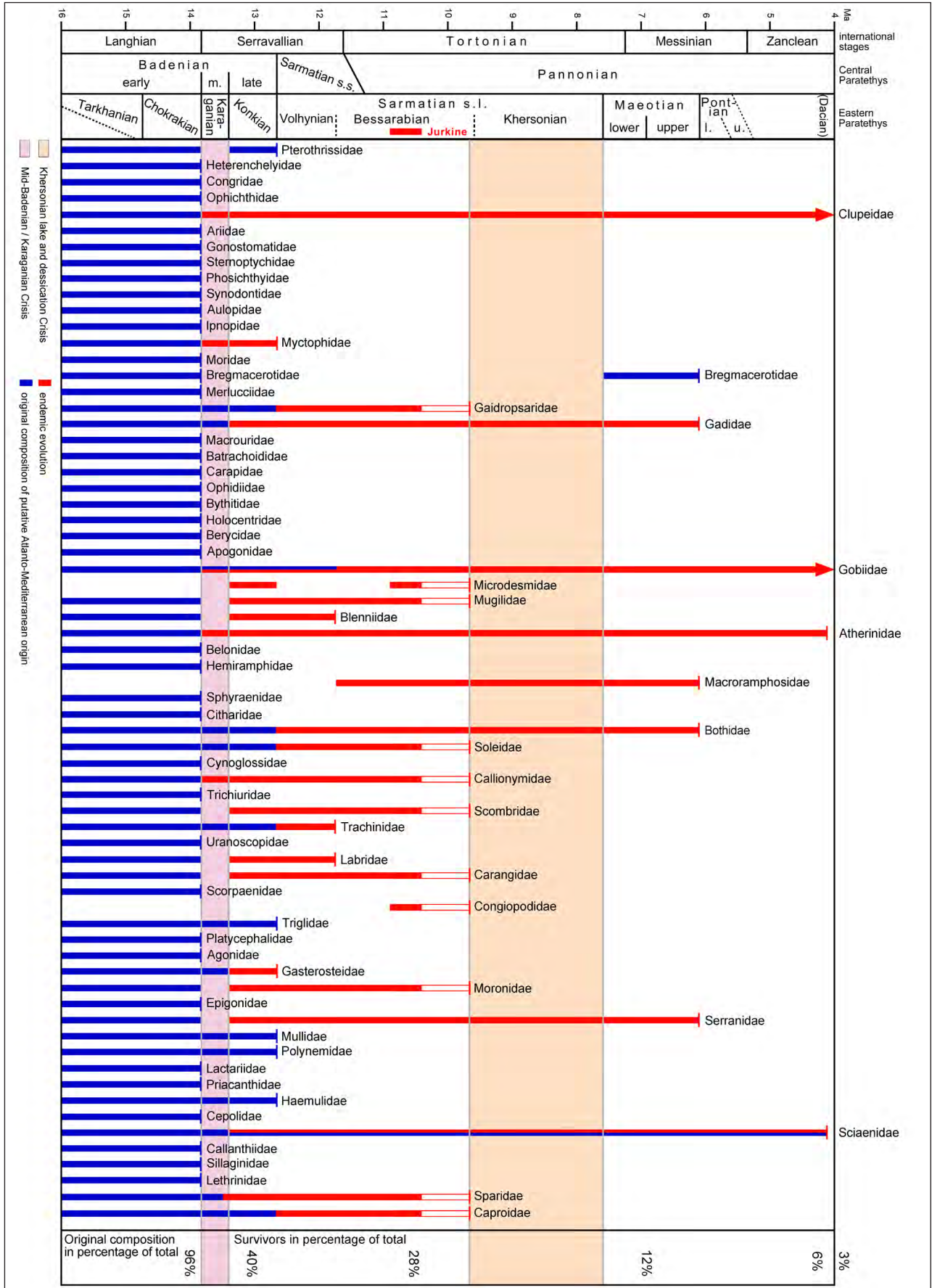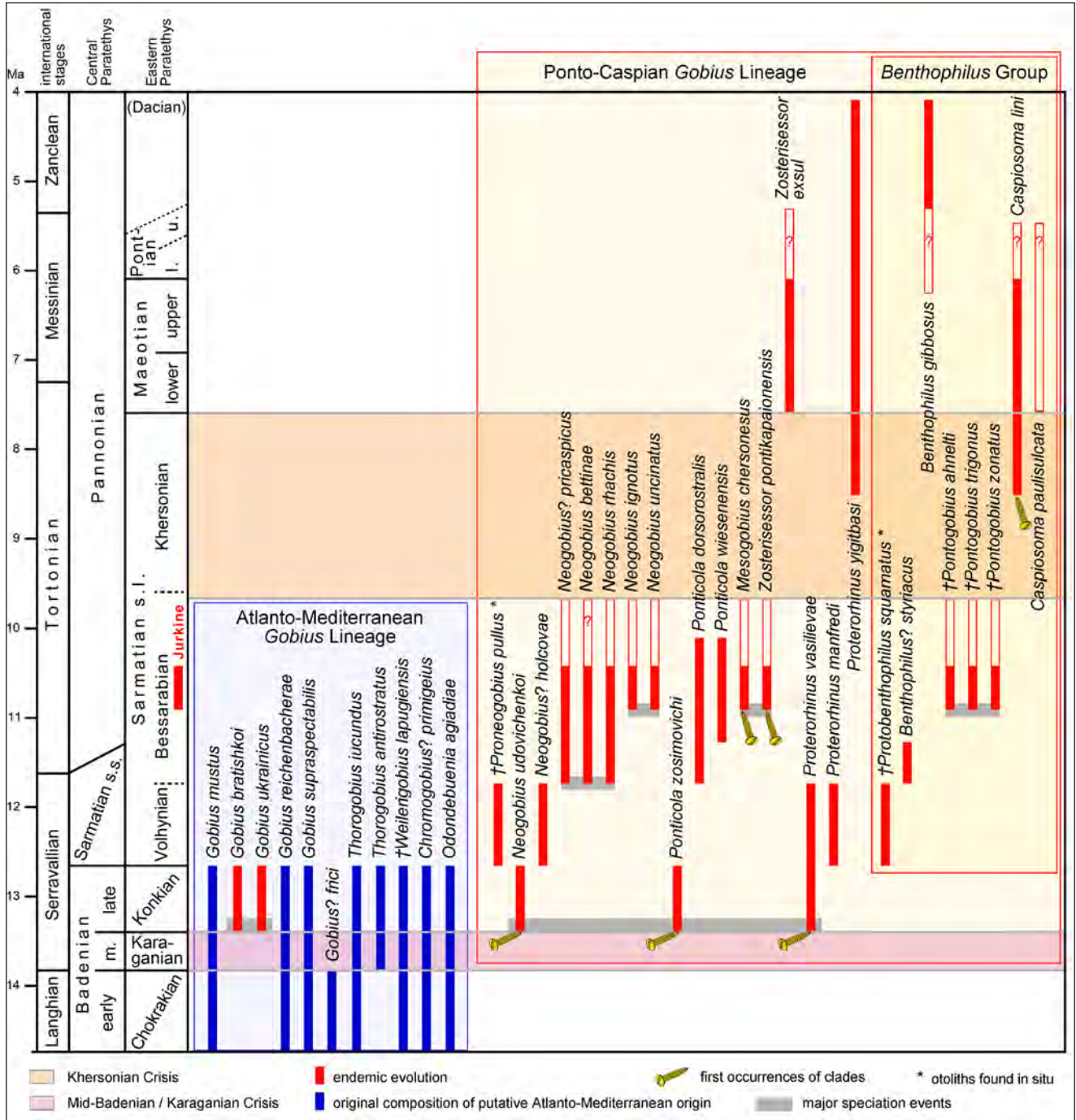
Fig. 20 - Range chart of otolith-based taxa of the *Gobius* Lineage (Gobiidae) in the Paratethys from Middle Miocene to Early Pliocene. Blue bars indicate taxa of Atlanto-Mediterranean origin and shared with time-equivalent occurrences in other European basins; red bars indicate putative endemic taxa in the Paratethys; open bars indicate possible range extensions.

hatý et al. 2007; Nolf & Brzobohatý 2009; Schwarzhans 2017; Brzobohatý & Nolf 2018; Schwarzhans et al. 2020b). This diversity is represented by otoliths of 64 families, which correspond to 96% of all teleost families identified by means of otoliths during the Middle and Upper Miocene (Fig. 19). Only otoliths of three rare families, which have only been found in younger rocks, have not yet been identified

in the lower Badenian: the Microdesmidae, Macroramphosidae, and Congiopodidae. The knowledge of coeval otolith assemblages from the Mediterranean and Eastern Paratethys is not comparable to that of the Central Paratethys; rather, diverse assemblages are known from the Aquitaine Basin in SW France (Steurbaut 1984) and the North Sea Basin (Schwarzhans 2010). Thus, the database outside of
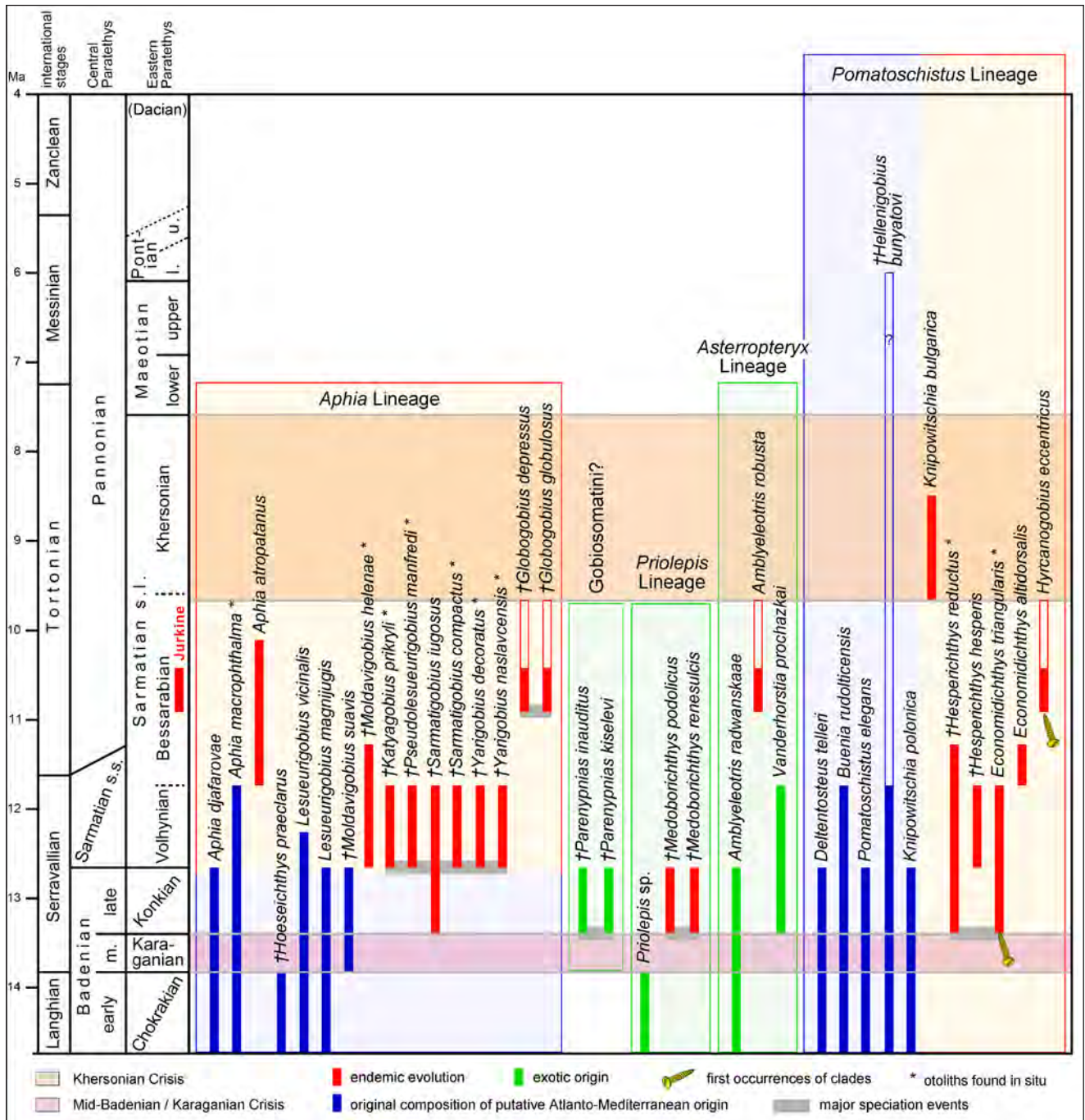
Fig. 21 - Range chart of otolith-based taxa of the *Aphia, Priolepis, Asterropteryx* and *Pomatoschistus* lineages and the Gobiosomatini? in the Parate-
thys from Middle Miocene to Early Pliocene. Blue bars indicate taxa of Atlanto-Mediterranean origin and shared with time-equivalent
occurrences in other European basins; red bars indicate putative endemic taxa in the Parathys; green bars indicate non-indigenous
lineages in European seas; open bars indicate possible range extensions.

Central Paratethys somewhat hampers the compara-
bility, but as far as can be assessed, there appears to
be a high degree of shared taxa between the Europe-
an faunal provinces (see Steurbaut 1984 and Schwar-
zhans 2010). We interpret the good putative compa-
rability as an indication that the Paratethys formed
a more or less contiguous faunal province with the

other seas around western Europe at the time. Such
an interpretation is consistent with geological and pa-
leogeographic considerations (Sant et al. 2017; Palcu
et al. 2019), as well as the assessment of the Miocene
mollusk faunas of the Paratethys by Harzhauser and
Piller (2007). They recognized an extraordinary "ear-
ly Badenian-build-up-event" (EBBE).
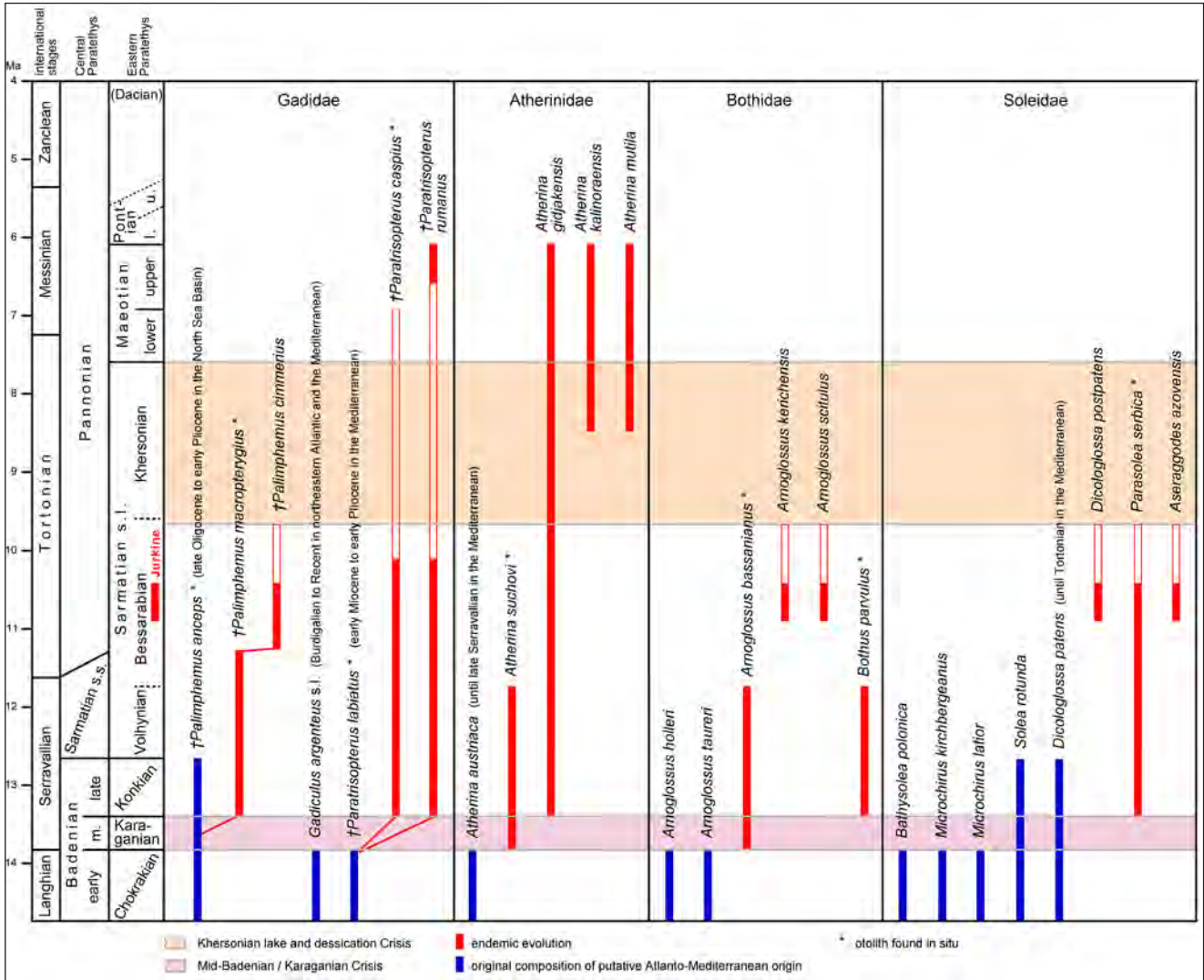
Fig. 22 - Range chart of otolith-based taxa of the Gadidae, Atherinidae, Bothidae and Soleidae in the Parathys from Middle Miocene to Early Pliocene. Blue bars indicate taxa of Atlanto-Mediterranean origin and shared with time-equivalent occurrences in other European basins; red bars indicate putative endemic taxa in the Parathys.

Following the Middle Badenian Salinity Crisis in the Central Parathys and the Karaganian Crisis in the Eastern Parathys, the number of teleost families was drastically reduced in the late Badenian/Konkian to only 27 (equaling 40% of all Middle and Late Miocene teleost families recognized by otoliths in the Parathys). Similarly, Harzhauser and Piller (2007) recognized a middle Badenian-extinction-event (MBBE) in mollusks and related it to the global cooling and sea-level drop during the Middle Miocene Climate Transition (MMCT). We observe that the deepwater mesopelagic and bathydemersal fish families primarily disappeared from the Parathys, never to return. The deepwater fish families that disappeared are the Gonostomatidae, Sternoptychidae, Phosichthyidae,

Ipnopidae, Moridae, Bregmacerotidae, Macrouridae, Ophidiidae, Bythitidae, Berycidae, and most of the Myctophidae. Of the latter, two endemic *Diaphus* species survived/evolved in certain regions of the Central Parathys for a short time (late Badenian) (Schwarzhans & Radwanska 2022). These two species (*Diaphus latirostratus* and *D. "obliquus"*) were likely capable of surviving at reduced oxygen levels. It is known from the exceptionally large and low-oxygen minimum zone in the tropical East Pacific off eastern tropical America that few dwarfed endemic myctophid species are known to be adapted to this specific environment (Froese & Pauly 2021). Many other teleost families disappeared during the MBBE as well, but the near-complete extinction of the deep-water fish points to another mechanism
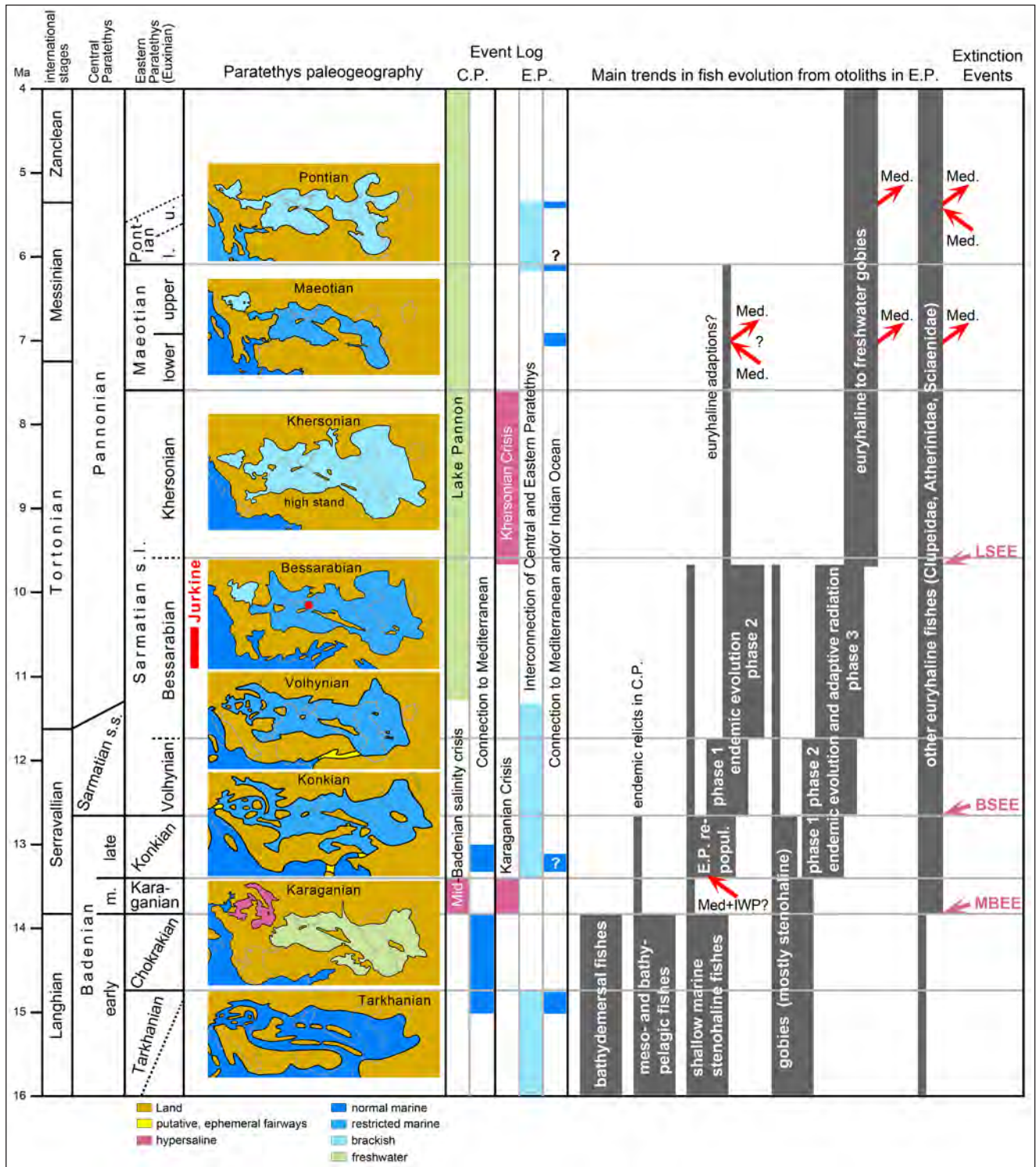
Fig. 23 - Schematic chart summarizing the evolution of bony fishes in the Paratethys from Middle Miocene to Early Pliocene. Major putative faunal exchange events are indicated by red arrows. Abbreviations used are: MBEE = middle Badenian extinction event, BSEE = Badenian/Sarmatian extinction event, LSEE = late Sarmatian extinction event, Med. = Mediterranean, IWP = Indo-West Pacific. The paleogeographic reconstructions are based on: Tarkhanian after Rögl (1999), Karaganian after Palcu et al. (2017), Konkian, Volhynian, Bessarabian, Pontian after Popov et al. (2004), Khersonian after Palcu et al. (2021), Maeotian after Palcu et al. (2019).

that may have been at work, at least additionally, during the MBEE related to the deterioration of the deep-water habitat for fishes. In larger parts of the Central Paratethys, the MBBE of deep-water fishes may have been related to the Middle Badenian Salinity Crisis. The Eastern Paratethys was separated from the Central Paratethys during the Chokrakian, becoming isolated from the world

ocean. According to the model developed by Mikerina and Pinchuk (2014), desalination spread across the basin from the northern periphery during the late Chokrakian and encompassed the entire basin during the Karaganian. Reduced water circulation led to an anoxic development in the deeper part of the sea and pushed the fish fauna into the upper brackish layers of the pelagic zone.

During the early late Badenian, short-lived marine reconnections occurred at the western-most region of the Central Paratethys (Bartol et al. 2014) that allowed some Mediterranean biota to reenter the Central Paratethys and potentially then reconnected the Eastern Paratethys (Kovać et al. 2007). Such remigration, however, was likely restricted to shallow-water fishes, either due to the shallow-water nature of the ephemeral connection to the Mediterranean or to the continuation of a layered water column by which the deep-water environments remained in a low-oxygen zone unsuitable for deep-water fishes (Harzhauser & Piller 2007).

The Konkian deposits studied from Mangyshlak, Kazakhstan, by Bratishko et al. (2015) have shown a significant increase of endemic fish elements. Assumed primary endemisms have been observed in at least 14 fish families out of 27 (i.e., slightly more than half of the entire fauna) (Fig. 19). A look into the species level of the predominant group, the Gobiidae, reveals that taxa with Atlanto-Mediterranean affinities still prevailed (17 species) during the Konkian. In contrast, the amount of clear Ponto-Caspian endemic lineages was still in its early generating phase (five species) (Fig. 20–21). Other persistent fish groups in the Paratethys reveal prevailing endemic evolution in the Gadidae, Atherinidae, and Bothidae, while more persistent taxa are seen in the Soleidae (Fig. 22). A recently described late Badenian otolith association from a back-reef environment of a short-lived barrier reef in western Ukraine has elucidated a rich and diverse fauna, again dominated by the Gobiidae but of a different composition (Schwarzhans et al. 2022). This otolith-based fish fauna from western Ukraine is characterized by several supposedly reef-adopted endemic species that are thought to have derived from earlier stenohaline marine Middle Miocene stocks. Relatives of the Ponto-Caspian stock are absent from that community.

The Badenian-Sarmatian boundary marks the largest faunal turnover in the history of the (Central) Paratethys, the so-called Badenian-Sarmatian extinction event (BSEE; Harzhauser & Piller 2007; Palcu et al. 2015). The faunistic turnover was originally thought to be related to reduced salinity in the Sarmatian Sea (Papp 1956 and literature cited in Piller & Harzhauser 2005), but in more recent literature, the water chemistry has been considered as "highly supersaturated in respect to calcium carbonate and probably also with high alkalinity" (Pisera 1996; Piller & Harzhauser 2005). Thus, during the Sarmatian s.s. in the Central Paratethys and in the early and middle Sarmatian s.l. in the Eastern Paratethys, fully marine conditions may have prevailed with increased alkalinity (Piller & Harzhauser 2005), which herein is called "restricted marine" as opposed to "brackish marine" (see Müller et al. 2007). Harzhauser and Piller (2007; p. 20) noted 588 last occurrence dates (LOD) for gastropods and 121 for foraminifers at the BSEE. Furthermore, they observed that most Badenian gastropod species and most long-ranging species with Early Miocene roots became extinct in the Paratethys. However, they also commented that the trigger mechanism for the BSEE is unresolved. In teleost fishes, most families of the original Atlanto-Mediterranean composition also disappear at the BSEE, with the possible exception of a few sciaenids and a few gobiids. In contrast, the vast majority of lineages exhibit an accelerated endemic evolution. The presumably forced endemic evolution is evident, for example, in the Gadidae, Gobiidae, Mugilidae, Atherinidae, Bothidae, Soleidae, Callionymidae, Serranidae, Sciaenidae, Sparidae, and Caproidae (Figs. 19-22). The two remaining endemic mesopelagic species of the Myctophidae became extinct with the BSEE, and the number of represented teleost families was reduced to 19 of the total 67 families in Jurkine (28%).

Today, most of the fish families that underwent endemic evolution during the Sarmatian contain exclusively or predominantly stenohaline marine taxa. The evolution of the various lineages in the family Gobiidae are of particular interest because of their extreme diversity in the Sarmatian of the Paratethys and the presence of both stenohaline and euryhaline lineages (Figs. 20–21). Three phases of endemic pulses have thus far been observed in that time interval (Fig. 20–21). First, an initial endemic pulse occurred in the Konkian of the Eastern Paratethys that gave rise to some early members of what now forms the Ponto-Caspian goby stock

Genus	Provenance		
	Primary endemic	Atlantic-Mediter.	Indo-Pac. (exotic)
Alosa		X	
†*Maeotichthys*	X		
†*Palimphemus*		X	
Enchelyopus		X	
Onogadus		X	
Mesogobius	X		
Neogobius	X		
Zosterisessor	X		
†*Pontogobius*	X		
†*Globogobius*	X		
Amblyeleotris			X
Hyrcanogobius	X		
†*Paroxymetopon*			X[1]
Chelon		X	
Atherina		X	
†*Paramacroramphosus*		X[2]	
Arnoglossus		X	
Aseraggodes			X
Dicologlossa		X	
†*Parasolea*	X		
Callionymus		X	
Scomber		X	
Trachurus		X	
Pseudanthias			X
Congiopodus			(X)
Diplodus		X	
†*Pshekharus*	X		
†*Pontosciaena*	X		
Capros		X	
Totals	**10**	**14**	**4 (+1)**
% of specimens	**44.27%**	**45.57%**	**10.16%**

Tab. 5 - Biogeographic relationships of the otolith-based taxa in Jurkine.
Extant genera related to and used for fossil genera in table:
    X1 from *Oxymetopon.*
    X2 from *Macroramphosus.*

(Bratishko et al. 2015). In the late Badenian of the Central Paratethys, gobiid taxa of Atlanto-Mediterranean origin continued to prevail, including specialized adaptations to reefal environments (Schwarzhans et al. 2020b, 2022). A second endemic pulse led to increased diversity during the early Sarmatian (Volhynian) in the Central and Eastern Paratethys. Interestingly, this second pulse affected not only lineages leading to the current Ponto-Caspian gobies (Schwarzhans et al. 2017c), but also the *Aphia* lineage ("*Lesueurigobius* look-alikes"; Reichenbacher & Bannikov 2021). In the Ponto-Caspian stock, the earliest representatives of the *Benthophilus* Group have been identified, as have the Ponto-Caspian lineages of the *Pomatoschistus* Lineage (Fig. 21). Only few gobiid taxa of Atlanto-Mediterranean origin persisted seemingly unaltered in the Sarmatian s.s. (Volhynian) of the Central Paratethys (Schwarzhans et al. 2020b). The third endemic pulse in gobiid evolution appears to have been largely confined to the Eastern Paratethys and is primarily evidenced

in the fauna from Jurkine. This phase contains the first records of the Ponto-Caspian goby genera *Mesogobius, Zosterisessor* and *Hyrcanogobius*, as well as extinct putative genera of the *Benthophilus* Group (*Pontogobius*) and a last pulse in speciation of steno-haline gobies. This last pulse includes the extinct "*Lesueurigobius* look-alike" *Globogobius* and species of *Aphia* and *Amblyeleotris* (Fig. 20–21). The high degree of Bessarabian endemism in the fish fauna of Jurkine is also highlighted in the gadids, bothids, and soleids (Fig. 22) and correlates with a similarly strong endemic evolutionary pulse in other biota, such as mollusks and foraminifers (see above).

The boundary of the Sarmatian s.s. and the Pannonian marks the Sarmatian-Pannonian extinction event (SPEE) in the Central Paratethys (Harzhauser & Piller 2007). This event is thought to be related to the separation of the Central Paratethys from the Eastern Paratethys and its change to the brackish water body of Lake Pannon. The otolith-based teleost fauna from the Pannonian of the Central Paratethys is still insufficiently known and appears to be dominated by euryhaline endemisms (Weinfurter 1953 as revised by Nolf 2013).

As already indicated above and witnessed by the fauna from Jurkine, the marine endemic evolution continued in the Eastern Paratethys through the middle Sarmatian s.l. (Bessarabian) (i.e., the early Tortonian of the international time scale). We interpreted the entire otolith-based teleost fauna from Jurkine as endemic at a species level. The high degree of new species (24, corresponding to 66.7% of the total species in the assemblage; Table 1) in Jurkine expressed the accelerated endemic evolution during the Bessarabian of the Eastern Paratethys. Species of the original early Badenian Atlanto-Mediterranean composition were no longer present (Fig. 19). Even at the genus level, 10 genera representing 44.27% of the specimens in Jurkine are thought to be primary endemics of the Eastern Paratethys (Table 5). Six of those are now extinct, while the remaining four belong to endemic Ponto-Caspian goby genera.

The late Sarmatian s.l. (Khersonian) was a time of rapidly changing sea levels and water chemistry. The details of the water level draw-downs and environmental implications are currently a matter of intense research and discussion (Popov et al. 2019; Palcu et al. 2017, 2021; Šujan et al. 2022), but the biota in the Eastern Paratethys were indisputably ex-

posed to considerable ecological stress. Mollusks and foraminfera indicate a widespread suboxic sea bottom environment (see above) that would have been detrimental for many demersal fishes. Our data on otoliths from the Khersonian and subsequent Maeotian are sparse (Pobedina 1954, 1956; Suzin 1968; Djafarova 2006; Schwarzhans et al. 2017c, 2020a), and some data require revision. However, the currently available data point to a massive decrease of diversity in the fish fauna and most likely a complete loss of stenohaline marine endemic elements during the Khersonian (Fig. 19–23). In the Eastern Paratethys, we interpret this event as one of the most fundamental changes in the composition of the fish fauna, for which we propose the term "late Sarmatian s.l. extinction event" (LSEE) (Fig. 23). We postulate that only euryhaline fishes survived this event in the Sarmatian Sea and that later occurrences of marine fishes of the Atlanto-Mediterranean provenance during Maeotian and Dacian represent renewed immigration events (Bannikov et al. 2018; Schwarzhans et al. 2020a). The exact timing of the event remains uncertain from a perspective of the fish fauna, and the analysis of other biota in the Jurkine section (mollusks and foraminifers; see above) indicate a gradual depletion of faunal diversity during the late Bessarabian. The current understanding on the critical and primary turning points in the evolution of the fish fauna during the Middle and Late Miocene as reconstructed from otoliths as discussed above is summarized in Figure 23.

Fishes that aren't

Despite the rich otolith assemblage in Jurkine, certain lineages we would have expected to be present were missing, such as lineages that have been identified in the Konkian and/or Volhynian, those that are known to have occurred in the post-Bessarabian strata of the Eastern Paratethys, and those that belong to persistent endemic Ponto-Caspian groups. Such gaps occurred primarily in two families: Gadidae and Gobiidae.

Gadidae: *Paratrisopterus caspius* (Bogatshov, 1929) is an endemic Paratethyan species known from skeletons with otoliths in situ from the Volhynian (Schwarzhans et al. 2017b) and from many isolated otolith records since late Badenian. This species was possibly even present in the Chokrakian of Azerbaijan (Djafarova 2006 as *Macrurus* sp.) and at least until the Bessarabian of the Caspian

Basin (Pobedina 1956; Djafarova 2006). This species may have existed through the Maeotian and even Pontian considering that Djafarova's mention of Ot. (Macruridarum) *minusculus* likely represented the species. This explanation would be consistent with the sudden occurrence of the species in the late Tortonian/Messinian equivalent in the North Sea Basin (Schwarzhans et al. 2017b), which may have resulted from emigration from the Euxinic Basin during a short-lived connection with the eastern Mediterranean during the early Maeotian (Popov. et al. 2019).

Paratrisopterus rumanus (Weiler, 1943) is well known from the late Badenian and Sarmatian s.s. of the Central Paratethys (Weiler 1943; Schwarzhans et al. 2017b), as well as the middle Sarmatian s.l. from the Eastern Paratethys (Suzin 1968) as Ot. (Gadidarum) *labiatiformis*. However, it has not been recorded from Jurkine. A record of the species also exists from the pre-evaporitic Messinian of the Aegean Sea from Skyros, Greece (Schwarzhans et al. 2020a), which was under Paratethyan and Mediterranean influence during the time (Popov et al. 2006). *Paratrisopterus* species presumably entertained an epipelagic lifestyle (Schwarzhans et al. 2017b), and their otoliths are common and ubiquitous where species of *Paratrisopterus* occurred. Therefore, their absence in Jurkine remains unresolved.

Gobiidae: In gobies, species of the Ponto-Caspian genera *Economidichthys, Knipowitschia, Benthophilus, Poterorhinus,* and *Ponticola* are not represented in Jurkine, but are known from Volhynian rocks and post-Bessarabian strata. A species of *Ponticola* is also known from the transitional marine-brackish environment of the Bessarabian of Mykhailivka (Bratishko et al. 2017). The most likely cause for these species' absence in Jurkine may indeed be that they were already adapted to reduced salinities, as they are currently, which would also favor their survival during the Khersonian Crisis.

"Exotic" fishes and their origins (Tab. 5)

Ten of the 29 genera recognized from otoliths in Jurkine represent primary endemics (44.27% of the specimens), and 14 genera have Atlanto-Mediterranean affinities (45.57% of the specimens). The identified species of the latter were also endemic to the Eastern Paratethys (Table 5). Thus, five genera (10.16% of the specimens) are associated with some type of outside and perhaps unexpected re-

lationship (Table 5); four are placed in groups currently found in the Indo-Pacific, and one is placed in the southern temperate zone.

Amblyeleotris is a gobiid genus that lives commensally with alpheid shrimps. Many of its species are found in the tropical to subtropical waters of the Indo-Pacific (Thacker & Roje 2011; Agorreta et al. 2013). The genus has been known in the fossil record since late Burdigalian (from India; Carolin et al. 2022) and from the Paratethys since the Langhian (early Badenian) (Schwarzhans et al. 2020b).

The extinct genus *Paroxymetopon* of the family Microdesmidae is an unexpected and rare find in the Bessarabian of Jurkine, but another microdesmid, *Microdesmus paratethycus* Schwarzhans, 2017, was found in the Konkian of Bulgaria. Microdesmids are stenohaline marine fishes, and *Oxymetopon*, the putatively closest relative of the fossil *Paroxymetopon*, has been associated with reefs in the West Pacific (Froese & Pauly 2021).

The soleid *Aseraggodes* is another case of an Indo-Pacific clade represented in Jurkine, as is the serranid *Pseudanthias*. The latter is the only exotic find that has a relatively common occurrence. Like the two gobioids mentioned above, it is a reef-associated fish group. However, the generic allocation of *Pseudanthias obrotchishtensis* remains tentative because of the limited knowledge of the many extant fishes with look-alike otolith morphologies.

In any case, these four fish clades could have had a wider geographic distribution in the past when the Mediterranean (and Paratethys) was still connected to the Indian Ocean and its environment was suitable for such fishes. They are all considered herein as migrants from the Indo-Pacific during Early to Middle Miocene times that became trapped in the Eastern Paratethys after its separation and became extinct when the sea was no longer suitable for stenohaline marine fishes with tropical to subtropical affinities.

A completely different case is the single otolith of *Congiopodus*? *inopinatus*. The Congiopodidae are a family currently restricted to the temperate to cool waters of the southern hemisphere (Froese & Pauly 2021), and an occurrence of this fish in the Paratethys cannot be readily explained. Therefore, we attributed the otolith in question only tentatively to this family as we could not find a more satisfactory taxonomic identification. However, it is also possible that *Congiopodus*? *inopinatus* may represent

an extinct group entirely unrelated to the Congiopodidae, and of which otoliths are not yet known. Therefore, we refrain from any far-reaching interpretation of this singular find.

Summary of fish evolution in the Eastern Paratethys during the Middle and Late Miocene as based on otoliths (Fig. 19, 23)

The Neogene history of the Paratethys is complex and characterized by phases of separation and connectivity as well as changing environmental settings and water chemistry. These characteristics greatly affected the biota living in the Paratethys and its subbasins and are the subject of a large body of research work accumulated over many years (see Popov et al, 2004, 2006, and 2019 for syntheses). Bony fishes are capable of reacting to waterway connections, endemic evolution, and adaptation to changing environments in various ways, but a data base has not yet been established on these fish to the extent that has been achieved, for example, for mollusks or foraminifers. Articulated skeletons are relatively well documented from the Early to Middle Miocene—less so in younger strata (see Bannikov 2010 and Schultz 2013 for syntheses)—but overall remain dependent on specific Lagerstätten that are favorable for their preservation. Otoliths are much more common and occur in a larger variety of taphocoenoses. They have been studied extensively in the Central Paratethys (e.g., Radwańska 1992; Brzobohatý et al. 2007; Nolf & Brzobohatý 2009; Schwarzhans 2017; Brzobohatý & Nolf 2018; Schwarzhans et al. 2020b), but otolith assemblages from the Eastern Paratethys are still severely understudied (see Bratishko et al. 2015, 2017; Schwarzhans et al. 2020a, 2022). Nevertheless, with the mentioned publications, the fauna from Jurkine described herein, and a tentative review of certain data published by Pobedina (1954, 1956), Suzin (1968), and Djafarova (2006), we feel able to make a preliminary attempt to outline the evolution of teleost fishes in the Eastern Paratethys since Badenian, as reconstructed from otoliths (Figs. 19, 23).

During the Tarkhanian/early Badenian, the Paratethys was connected to the Mediterranean in the west and the Indian Ocean in the east (Rögl 1999; Popov et al. 2004; Sant et al. 2017; Palcu et al. 2019). During this time, the Paratethys recruited a fully marine fauna ranging from shallow-water environments through meso- and bathypelagic com-

munities and including bathydemersal fishes. The otolith-based fish fauna from the Central Paratethys is particularly well known (see references above), and the deep-water fish communities in the area exhibit strong continuity since the Karpatian (e.g., Brzobohatý et al. 2003; Brzobohatý & Stránik 2012; Brzobohatý & Nolf 2018; Schwarzhans & Radwanska 2022). Limited coeval data from the Eastern Paratethys are consistent with the rich fauna known from the Central Paratethys. Carolin et al. (2022) studied otoliths from southern India, which stem from slightly earlier strata dating from the late Burdigalian, and indicate a relatively limited faunal influence from the Indian Ocean in the Paratethys (e.g., the *Asterropteryx* lineage of the Gobiidae). According to Sun et al. (2021), the Tethyan Seaway had become a restricted marine environment in the area of the closure (central Iran and southeastern Turkey) during the time, which likely limited the faunal exchange.

Following the separation of the Eastern Paratethys from the Central Paratethys during the Chokrakian, as well as its complete separation during the Karaganian, all deepwater fish became extinct during the Karaganian Crisis. This was also the case of deepwater fish from the Central Paratethys following the MBEE, except for two endemic *Diaphus* species that may have been able to adapt to reduced oxygen levels and survive in some deeper regions of the basins. The cause for the depletion of the deepwater fish fauna is seen in the development of a layered water column, hypersaline in the Central Paratethys, and dysoxic at depth in the Eastern Paratethys. In the Eastern Paratethys, fishes survived in the freshwater and brackish water epipelagic and coastal zones. Clupeidae developed endemics during that time (Baykina & Schwarzhans 2017). Pobedina (1954, 1956) and Strashimirov (1981a) showed otoliths pertaining to the Gobiidae, Bothidae, Gasterosteidae, and Mullidae from the Karaganian, which, however, require review.

Connection of the Central and Eastern Paratethys was re-established during the Konkian and to the Mediterranean in the west during the early Konkian (Popov et al. 2004; Kovać et al. 2007; Bartol et al. 2014). The extent of a possible, brief reconnection to the Indian Ocean in the east is under debate (compare Rögl 1999 and Popov et al. 2006), and according to the reconstruction by Sun et al. (2021), this reconnection would likely represent the final opportunity for any migration from the east into the Eastern Paratethys. In any case, we interprete the rich Konkian otolith-based fishes fauna in the Paratethys as new recruits in part from the Mediterranean and possibly also from the Indian Ocean (see also the discussion in Bratishko et al. 2015). Some of the exotic fishes occurring in the Bessarabian of Jurkine may be descendants of immigrants from the Indian Ocean during that time. Bratishko et al. (2015) also demonstrated the presence of a considerable number of endemic bony fishes in the Konkian of Kazakhstan. Similarly, the short-lived Medobory barrier reef in western Ukraine represented a flourishing environment for an endemic evolution of its associated fish fauna (Schwarzhans et al. 2022). No deepwater fish re-emigrated into the Paratethys, either because the gateways were too shallow to be navigated or because the layered water column persisted and prohibited repopulation of the deep Paratethyan Sea.

The beginning of the Sarmatian marked a major change in the Paratethyan biota due to a major extinction event (BSEE). In the Central Paratethys, the BSEE is considered to represent the largest faunal turnover in its history (Harzhauser & Piller 2007). Regarding the fish fauna, the last remaining mesopelagic fishes disappeared in the Central Paratethys, and most of the stenohaline fishes of Atlanto-Mediterranean origin disappeared in the Central and Eastern Paratethys or evolved endemically. The early and middle Sarmatian s.l. (Volhynian and Bessarabian) was a time of accelerated forced endemic evolution of the fish fauna in the Eastern Paratethys, and this evolution occurred in open marine environments like Jurkine as well as in transitional marine-brackish environments. The Konkian, Volhynian, and Bessarabian mark three pulses of endemic speciation events; a fact that is particularly evident in the evolution of the Gobiidae in the Eastern Paratethys (Figs. 20–21). The endemic marine evolution ended in the Central Paratethys with the Sarmatian-Pannonian extinction event (SPEE), while in the Eastern Paratethys, the marine endemic evolution continued for about two more million years until at the least the middle of the Bessarabian. The evolution of the stenohaline endemic fish fauna terminated with the LSEE shortly after the fish fauna documented in Jurkine and a possible depletion period during the terminal Bessarabian with the onset of the Khersonian Crisis.

The causes of the Khersonian Crisis in the Eastern Paratethys are currently the subject of intense research and debate (compare Palcu et al. 2021 and Šujan et al. 2022). These causes involve periods of drought with sea-level draw-downs, periods of high meteoric water influx, establishment of suboxic bottom-water generation, and formation of brackish water in the shallow parts of the basin (Popov et al. 2019; Palcu et al. 2021; Šujan et al. 2022). These environmental and hydrological fluctuations must have severely impacted the fish fauna of the Eastern Paratethys, both demersal fish (because of the suboxic bottom conditions) and nectonic fish (caused by the brackish water influx). Otoliths from the Khersonian (see above) are not well known, but most marine endemic fishes seem to have become extinct with the LSEE, except for a few that may have been able to adapt to reduced salinity and rapidly changing environmental conditions. Among them may have been gadids, macroramphosids, and serranids (Fig. 19). Euryhaline endemics, such as clupeids, gobiids, atherinids, and bothids, survived and, in the case of gobiids and clupeids, possibly benefited from the environmental change. In the Gobiidae, the stenohaline marine endemics of the *Aphia* and *Asterropteryx* lineages became extinct, as did *Pontogobius,* which is believed to belong to the *Benthophilus* group (Fig. 21).

Only 12% of the original composition of bony fishes at the family level from the early Badenian have been identified by otoliths in the Maeotian (Fig. 19). This fish fauna included potential new immigrants (*Bregmaceros*) from the Mediterranean during a postulated connection through the Aegean region (Popov et al. 2019). Conversely, there are indications of Paratethyan gobiid migrants into the Mediterranean during that time (Schwarzhans et al. 2020a). Currently, only two families have survived from the original Paratethyan stock in the Ponto-Caspian Basin, the Gobiidae and the Clupeidae (Fig. 19), both of which have a multitude of endemic species primarily in the Caspian Sea but also in the rivers discharging into the Black Sea and the riverine-marine transition zones.

BIOSTRATIGRAPHIC CONSIDERATIONS OF THE OTOLITH ASSOCIATION

Findings regarding the evolution of bony fish assemblages in the Paratethys could be useful for biostratigraphic purposes, particularly the accelerated endemic evolution of the many gobiid lineages. However, these gobiid lineages are highly environmentally dependent and therefore difficult to assess in a wider stratigraphic context. More promising are certain gadid, bothid, and soleid species, which have the benefit of being common, being widely distributed, and having evolved endemically in the Paratethys. In addition, the disappearance of certain common and widespread species over the course of the extinction events may represent useful markers.

In gadids, the species of *Palimphemus* are most useful because of their abundance, easy identification, and as far as the endemic species in the Paratethys (*P. macropterygius* and *P. cimmerius*) are concerned, their restricted stratigraphic range. During the early Badenian, the genus *Palimphemus* was represented in the Paratethys by *P. anceps* Kner, 1862, a long-ranging species from late Oligocene to early Pliocene in other European seas (e.g., the North Sea Basin). In the Central Paratethys, *P. anceps* was still present in the late Badenian, but it disappeared in the Sarmatian s.s. In the Eastern Paratethys, it terminated with the Karaganian Crisis and was no longer present in the Volhynian. *Palimphemus macropterygius* (Kramberger-Gorjanovic, 1883) was common in the Konkian/late Badenian and Sarmatian s.s. (Volhynian) throughout the Paratethys. It likely represents already an endemic Paratethyan evolution that derived from *P. anceps,* likely in the Eastern Paratethys. *Palimphemus cimmerius* clearly derived from *P. macropterygius* and was widespread in the marine Bessarabian of the Eastern Paratethys, where it has been found in Jurkine and Zavetnoe on the Kerch Peninsula (the latter unpublished material). This lineage terminates with the LSEE. The endemic Paratethyan species of *Paratrisopterus* have a longer stratigraphic range and are therefore of less stratigraphic value.

In bothids, *Arnoglossus bassanianus* (Kramberger, 1883) is a common species in the Konkian/late Badenian and Sarmatian s.s. (Volhynian) throughout the Paratethys. Records of *Rhombus corius* Chalilov, 1946 in the Karaganian by Strashimirov (1981a) and Pobedina (1954, 1956), as well as those of *Rhombus altus* Pobedina, 1954, possibly represent a different species of *Arnoglossus.* No Karaganian otoliths have been available for review. In the Bessarabian of the Eastern Paratethys, the two species, *A. kerichensis* and *A. scitulus,* replaced

A. bassanianus. In soleids, the widespread but relatively uncommon *Dicologlossa patens* (Bassoli, 1906) was replaced by the endemic descendant *D. postpatens* in the Bessarabian. *Dicologlossa patens* is known through the Middle and Upper Miocene of Italy and the Badenian and Konkian of the Paratethys, but a recording gap remains for the Sarmatian s.s./Volhynian.

The MBEE is best characterized by the disappearance of most myctophid otoliths in the Central Paratethys (they have yet to be found in the Tarkhanian and Chokrakian of the Eastern Paratethys), particularly the common species *Diaphus austriacus* (Koken, 1891) and *Diaphus kokeni* (Procházka, 1893). In the Eastern Paratethys, the disappearance of gonostomatid otoliths, particularly *Gonostoma*? *cyclomorphum* (Weiler, 1950), is the most useful marker for the MBEE. The BSEE, which is prominent in mollusks and foraminifers, is less clear in fish otoliths. In the Central Paratethys, the best indicator of the BSEE is the disappearance of the remaining myctophids. In the Eastern Paratethys, the best indicator may be the disappearance of species of the gobiid genus *Lesueurigobius*.

Highly characteristic and common gobiids occurring first in the Bessarabian are the *Pontogobius, Globogobius,* and *Hyrcanogobius* species. The first two also appear to terminate at the LSEE and may give a good marker for that event. Other groups that apparently became extinct at the LSEE in the Eastern Paratethys are the Gaidropsaridae and Soleidae.

RESULTS AND OUTLOOK

The otolith assemblage from the Bessarabian of Jurkine, Kerch Peninsula, Crimea, is an important cornerstone for unraveling the evolution of fishes in the Paratethys during the Neogene. It is the richest fauna of that interval that has been investigated thus far. The Jurkine assemblage illuminates the amount and speed in which the forced endemic evolution occurred in the Sarmatian Sea of the Eastern Paratethys, particularly in gobies. It further witnesses the presence of a diverse stenohaline marine fish fauna at that time. Not a single common otolith-based species was found between Jurkine and any other basin in western Europe, clearly demonstrating that no faunal exchange through any marine gateway had occurred during that time. The Bessarabian fauna from Jurkine

is a logical descendant from the earlier Volhynian fauna of the Paratethys. However, it also seems to represent the terminal stage for many of the stenohaline faunal elements prior to the Khersonian Crisis.

The Jurkine otolith assemblage also demonstrates the value otolith studies can deliver for evaluating past fish faunas, as well as the sometimes twisted path evolution may take. The present faunal composition is a random piece of this path. Regarding the evolution of fishes in the Paratethys, particularly the Eastern Paratethys, more studies of other time intervals and environmental settings, particularly the Khersonian and younger strata, are required before a contingent picture can be created. The Kerch and Taman peninsulas are prime candidates for such studies but may be difficult to access. We nevertheless hope that the results from Jurkine presented herein will inspire colleagues to collect otoliths when opportunities arise in the future.

REFERENCES

Agorreta A., San Mauro D., Schliewen U., Van Tassell J.L., Kovačić M., Zardoya R. & Rüber L. (2013) - Molecular

phylogenetics of gobioidei and phylogenetic placement of European gobies. *Molecular Phylogenetics and Evolution*, 69: 619-633.

Andrusov N.I. (1893) - Geotektonika Kerchenskogo polyostrova (Geotectonics of the Kerch Peninsula). Typography of the Imperial Academy of Science, St. Petersburg: 1-271. [in Russian].

Anistratenko V.V. (2004) - Phylogenetic relationships of *Coelacanthia* and *Archaschenia*, two spinose rissoids (Mollusca, Gastropoda) from the Micoene of the Eastern Paratethys. *Vestnik zoologii*, 38(2): 3-12.

Anistratenko V.V. (2005) - Morphology and taxonomy of late Badenian to Sarmatian *Mohrensternia* (Gastropoda: Rissoidea) of the Central Paratethys. *Acta Geologica Polonica*, 55: 371-392.

Antunes M.T., Legoinha P., Cunha P.P. & Pais J. (2000) - High resolution stratigraphy and Miocene facies correlation in Lisbon and Sétubal Peninsula (Lower Tagus Basin, Portugal). *Ciências da Terra (UNL)*, 14: 183-190.

Archangelsky A.D. (Ed.) (1940) - Stratigraphiya SSSR. Tom 12: Neogen SSSR (Stratigraphy of the USSR. Vol. 12: Neogene USSR). AN SSSR, Moskva, Leningrad, 687 p. [in Russian].

Arkhangelsky A.D., Blokhin A.A., Menner V.V., Osipov S.S., Sokolov M.I. & Chepikov K.R. (1930) - Kratkiy ocherk geologicheskogo stroeniia i neftianyh mestorozhdeniy Kerchenskogo poluostrova (A short review of the Geological structure and oil deposits of the Kerch Peninsula). *Transaction of the Geological and Prospecting Service of USSR*, 13: 1-146. [in Russian].

Baciu D.-S., Bannikov A.F. & Tyler J.C. (2009) - Revision of the fossil fishes of the family Caproidae (Acanthomorpha). *Miscellanea paleontologica, Studie recerche sui giacimenti terziari di Bolca XI*, 8: 7-74.

Bannikov A.F. (2009) - On early Sarmatian fishes from the Eastern Paratethys. *Paleontological Journal*, 43: 569-573.

Bannikov A.F. (2010) - Fossil Acanthopterygian fishes (Teleostei, Acanathopterygii). In: Tatarinov L.P., Vorobeyva E.I. & Kurochkin E.N. (Eds.) - Fossil vertebrates of Russia and adjacent countries. GEOS, Moscow: 1-243.

Bannikov A.F. & Kotlyar A.N. (2015) - A new genus and species of Early Sarmatian porgies (Perciformes, Sparidae) from the Krasnodar region. *Paleontological Journal*, 49: 627-635.

Bannikov A.F., Schwarzhans W. & Carnevale G. (2018) - Neogene Paratethyan croakers (Teleostei, Sciaenidae). *Rivista Italiana di Paleontologia e Stratigrafia*, 124: 535-571.

Bartol M., Mikuž V. & Horvat A. (2014) - Palaeontological evidence of communication between the Central Paratethys and the Mediterranean in the late Badenian/early Serravallian. *Palaeogeography, Palaeoclimatology, Palaeoecology*, 394: 144-157.

Bassoli G. (1906) - Otoliti fossili terziari dell' Emilia. *Rivista Italiana di Paleontologia*, 12: 36-61.

Baykina E.M. & Schwarzhans W.W. (2017) - Review of "*Clupea humilis*" from the Sarmatian of Moldova and description of *Moldavichthys switshenskae* gen. et sp. nov. *Swiss Journal of Palaeontology*, 136: 141-152.

Belokrys L.S. (1962) - Stratygrafichnyi podil sarmatskyh vidkladiv Borysfenskoi zatoky za faunoiu moluskiv (Stratigraphical subdivision of Sarmatian of Borysthenes Bay based on mollusk fauna). *Dopovidi akademii nauk Ukrainskoi radianskoi socialistychnoi respubliky*, 8: 1089-1092. [in Ukrainian].

Belokrys L.S. (1963) - Ob evolutsii sarmatskih maktrid v Borisfenskom zalive (About the evolution of the Sarmatian Maktridae in the Borysphen Bay). *Paleontologicheskiy Journal*, 1: 13-34. [in Russian].

Belokrys L.S. (1976) - Sarmat uga USSR (The Sarmatian of the South of the Ukrainian SSR). In: Barg I.M. & Nosovskiy M.F. Stratigraphy of the Northern Black sea region and the Crimea, Dnepropetrovsk: 3-21. [in Russian].

Bialik O.M., Frank M., Betzler C., Zammit R. & Waldmann N.D. (2019) - Two-step closure of the Miocene Indian Ocean Gateway to the Mediterranean. *Scientific Reports*, 9:8842: 1-10.

Bogdanowich A.K. (1952) - Miliolody i Peneroplidy (Miliolidae and Peneropliidae). *Proceedings of VNIGRI*, 64, 338 p. [in Russian].

Bogdanowich A.K. (1965) - Stratigraphicheskoye I fatsialnoye raspredeleniye foraminifer v Miotsene Zapadnogo Predkavkaziya I voprosy ikh genezisa (The stratigraphic and facies distribution of foraminifera in the Miocene of the Western Ciscaucasia and questions of their genesis). *Trudy KFVNII*, Leningrad, 19: 300-350 [in Russian].

Bogdanovich A.K. (1974) - Indeks novykh taksonov otryada Miliolida iz Mezozoya, Kainozoya I Antroppogena SSSR za period 1850-1970 gody (Index of new taxons of the order miliolida from the Mesozoic, Cenozoic and Anthropogen of the USSR over period of 1850-1970). *Questions of micropaleontology*, 17: 155-192.

Boltovskoy E. & Totah V. (1985) - Diversity, similarity and dominance in benthic foraminiferal fauna along one transect of the Argentina shelf. *Revue de Micropaleontologie*, 28: 23-31.

Bratishko A., Schwarzhans W., Reichenbacher B., Vernyhorova Y. & Ćorić S. (2015) - Fish otoliths from the Konkian (Miocene, early Serravallian) of Mangyshlak (Kazakhstan): testimony to an early endemic evolution in the eastern Paratethys. *Paläontologische Zeitschrift*, 89(4): 839-889.

Bratishko A., Kovalchuk O. & Schwarzhans W. (2017) - Bessarabian (Tortonian, late Miocene) fish otoliths from a transitional freshwater-brackish environment of Mykhailivka, Southern Ukraine. *Palaeontologia Electronica*, 20.3.44A: 1-13.

Brzobohatý R. & Nolf D. (2018) - Revision of the middle Badenian fish otoliths from the Carpathian Foredeep in Moravia (middle Miocene, Czech Republic). *Cybium*, 42: 143-167.

Brzobohatý R. & Stráník Z. (2012) - Paleogeography of the early Badenian connection between the Vienna Basin and the Carpathian Foredeep. *Central European Journal of Geosciences*, 4: 126-137.

Brzobohatý R., Reichenbacher B. & Gregorová R. (2003) - Teleostei (otoliths, skeletons with otoliths in situ) from the

Karpatian of the Central Paratethys. In: Brzobohatý R., Cicha I., Kováč M. & Rögl F. (Eds.) - The Karpatian. A lower Miocene stage of the Central Paratethys. Masaryk University, Brno: 265-280.

Brzobohatý R., Nolf D. & Kroupa O. (2007) - Fish Otoliths from the middle Miocene of Kienberg at Mikulov, Czech Republic, Vienna Basin: their paleoenvironmental and paleogeographic significance. *Bulletin de l'Institut Royal des Sciences Naturelles de Belgique, Sciences de la Terre*, 77: 167-196

Bugrova E.M., Gladkova V.I., Dmitrieva T.V., Nevzorova L.S., Pinchuk T.V., Podobina V.M., Tverskaia L.A., Tur N.A. & Fregatova N.A. (2005). - Prakticheskoe rukovodstvo po microfaune (*Practical guide to microfauna*), 8: Foraminifery kainozoia (*Cenozoic Foraminifera*), VSEGEI, St. Petersburg: 1-323. [in Russian].

Caputo D., Carnevale G. & Landini W. (2009) - Fish otoliths from the Messinian of Strada degli Archi (Tuscany, Italy) - Taxonomy and paleoecology. *Annalen des Naturhistorischen Museums in Wien*, 111A: 257-280.

Carnevale G. & Collette B.B. (2014) - †*Zappaichthys harzhauseri*, gen. et sp. nov., a new Miocene toadfish (Teleostei, Batrachoidiformes) from the Paratethys (St. Margarethen in Burgenland, Austria), with comments on the fossil record of batrachoidiform fishes. *Journal of Vertebrate Paleontology*, 34: 1005-1017.

Carnevale G. & Harzhauser M. (2013) - Middle Miocene rockling (Teleostei, Gadidae) from the Paratethys (St. Margarethen in Burgenland, Austria). *Bulletin of Geosciences*, 88: 609-620.

Carnevale G. & Schwarzhans W. (2022) - Marine life in the Mediterranean during the Messinian Salinity Crisis: a paleoichthyological perspective. *Rivista Italiana di Paleontologia e Stratigrafia*, 128: 283-324.

Carnevale G., Bannikov A.F., Landini W. & Sorbini C. (2006) - Volhynian (early Sarmatian sensu lato) fishes from Tsurevsky, north Caucasus, Russia. *Journal of Paleontology*, 80: 684-699.

Carolin N., Bajpai S., Maurya A.S. & Schwarzhans W. (2022) - New perspectives on late Tethyan Neogene biodiversity development of fishes based on Miocene (~17 Ma) otoliths from southwestern India. *PalZ*, 1-38. https://doi.org/10.1007/s12542-022-00623-9.

Chaine J. & Duvergier J. (1934) - Recherches sur les otolithes des poissons. Etude descriptive et comparative de la sagitta des Téléostéens. *Actes de la Societé Linnéenne de Bordeaux*, 86: 5-256.

Chalilov D.M. (1946) - Kakraganskie i konkskie sloi severo-vostochnogo Azerbaijana (Karaganian and Konkian Beds of northeastern Azerbaijan). *Doklady Akademii Nauk Azerbaijanskoy SSR*, 2: 275-277. [in Russian].

Chanet B. & Guintard C. (2019) - The absence of gas bladder in the Atlantic mackerel *Scomber scombrus* Linnaeus, 1758 (Actinopterygii : Teleostei : Scombridae). A review. *Cahiers de Biologie Marine*, 60: 299-302.

Conversani V.R.M., Brenha-Nunes M.R., Santificetur C., Giaretta M.B., Siliprandi C.C. & Rossi-Wongtschowski C.L. (2017) - Atlas of marine bony fish otoliths (sagittae) of southeastern-southern Brazil part VII: Atheriniformes, Beloniformes, Beryciformes, Zeiformes, Syngnathiformes, Scorpaeniformes and Tetraodontiformes. *Brazilian Journal of Oceanography*, 65: 400-447.

Didkovskiy D. Ya. (1964) Biostratigrafiia neogenovyh otlozheniy uga Russkoi platformy po faune foraminifer (Biostratigraphy of the Neogene deposits in the south of the Russian platform based on the foraminiferal fauna). Dr. geol. and mineral. sci. diss., Kiev: 1-40 [in Russian].

Dizaj L.P., Esmaeili H.R. & Teimori A. (2020) - Comparative otolith morphology of clupeids from the Iranian brackish and marine resources (Teleostei: Clupeiformes). *Acta Zoologica*, 103: 29-47 (online 2020, printed 2022).

Djafarova J.D. (2006) - Otolity neogena Azerbaidjana (Neogene otoliths of Azerbaijan). Baku, Nafta: 1-167. [in Russian].

Folliot M., Pujol C., Cahuzac B. & Alvinerie J. (1993) - Nouvelles données sur le Miocène moyen marin ("Sallomacien") de Gironde (Basin d'Aquitaine-France). Approche des paléoenvironments. *Ciêncas da Terra* (UNL), 12: 117-131.

Froese R., & Pauly D. (2021) - FishBase. *World Wide Web electronic publication*. Accessed December 2021. https://www.fishbase.se/search.php

Girone A., Nolf D. & Cavallo O. (2010) - Fish otoliths from the pre-evaporitic (early Messinian) sediments of northern Italy: their stratigraphic and palaeobiogeographic significance. *Facies*, 56: 399-432.

Goncharova I.A., & Rostovtseva Y.V. (2009) - Evolution of organic carbonate buildups in the middle through late Miocene of the Euxine-Caspian Basin (Eastern Paratethys). *Paleontological Journal*, 43: 866-876.

Gorjanovic-Kramberger D. (1891) - Palaeoichthyolozki prilozi. (Collectae palaeoichthyologicae.) Dio 11. *RAD, Jugoslavenske Akademije znanosti i umjetnosti*, 106: 59-129.

Guenser P., Ginot S., Escarguel G. & Goudemand N. (2022) - When less is more and more is less: the impact of sampling effort on species delineation. *Palaeontology*, e12598: 1-18.

Harzhauser M. & Piller W.E. (2007) - Benchmark data of a changing sea – palaeogeography, palaeobiogeography and events in the Central Paratethys during the Miocene. *Palaeogeography, Palaeoclimatology, Palaeoecology*, 253: 8-31.

Harzhauser M., Kranner M., Mandic O., Strauss P., Siedl W. & Piller W.E. (2020) - Miocene lithostratigraphy of the northern and central Vienna Basin (Austria). *Austrian Journal of Earth Sciences*, 113: 169-200.

Hedgpeth J.W. (1957) - Chapter 6 Classification of Marine Environments. In: Treatise on marine ecology and paleoecology, Volume 2, Paleoecology. H.S. Ladd (Ed.). The Geological Society of America, Memoir 67: 93-100. DOI: https://doi.org/10.1130/MEM67V2

Hohenegger J., Ćorić S. & Wagreich M. (2014) - Timing of the middle Miocene Badenian Stage of the Central Paratethys. *Geologica Carpathica*, 65: 55-66.

Iljina L.V. (2006) - Morphogenesis of Rissoidae in the inland basins of the Eastern Paratethys. *Paleontological Journal*,

40: 404-414.

Jonet S. (1973) - Etude des otolithes des téléostéens (Pisces) du Miocène des environs de Lisbonne. *Communiçaoes dos Serviços Geologicos de Portugal*, 56 : 107-294.

Kaiho K. (1994) - Benthic foraminiferal dissolved-oxygen index and dissolved-oxygen levels in the modern ocean. *Geology*, 22: 719-722. https://doi.org/10.1130/0091-7613(1994)022<0719:BFDOIA>2.3.CO;2

Kaiho K. (1999) - Effect of organic carbon flux and dissolved oxygen on the benthic foraminiferal oxygen index (BFOI). *Marine Micropaleontology*, 37: 67-76.

Kner R. (1863) - Über einige fossile Fische aus den Kreide- und Tertiärschichten von Comen und Podsused. *Akademie der Wissenschaften, Mathematisch- Naturwissenschaftliche Classe, Abt. 1*, 48: 126-148.

Koiava K. (2006) - Biostratigraphiya sarmatskikh otlozheniy Bostochnoi Gruzii po foraminiferam (Biostratigraphy of the Sarmatian deposits of the Eastern Georgia based on foraminifera). Abstract of Ph. D. thesis, Tbilisi [in Georgian and Russian].

Kolesnikov (1935) - Sarmatskie molluski. Paleontologiia SSSR (The Sarmatian moluscs. Paleontology of the USSR)*,* 10(2), The Academy of Science USSR Press, Leningrad: 1-507. [in Russian].

Kolesnikov et al. (1940) - Neogen SSSR. Stratigrafia SSSR (Neogene USSR. Stratigraphy of the USSR), 12, The Academy of Science USSR Press, Moscow, Leningrad: 1-687. [in Russian].

Koken E. (1884) - Über Fisch-Otolithen, insbesondere über diejenigen der norddeutschen Oligocän-Ablagerungen. *Zeitschrift der Deutschen Geologischen Gesellschaft*, 36: 500-565.

Koken E. (1891) - Neue Untersuchungen an tertiären Fisch-Otolithen. II. *Zeitschrift der Deutschen Geologischen Gesellschaft*, 43: 77-170.

Kováč M., Andreyeva-Grigorovich A., Bajraktarević Z., Brzobohatý R., Filipescu S., Fodor L., Harzhauser M., Nagymarosy A., Oszczypko N., Pavelić D., Rögl F., Saftić B., Sliva L. & Studencka B. (2007) - Badenian evolution of the Central Paratethys Sea: paleogeography, climate and eustatic sea-level changes. *Geologica Carpathica*, 58: 579-606.

Kováč M., Halásová E., Hudáčková N., Holcová K., Hyžný M., Jamrich M. & Ruman A. (2018) - Towards better correlation of the Central Paratethys regional time scale with the standard geological time scale of the Miocene Epoch. *Geologica Carpathica*, 69: 283-300.

Kramberger-Gorjanovic D. (1882) - Die jungtertiäre Fisch-fauna Kroatiens. 1.Theil. *Beiträge zur Paläontologie Oester-reich-Ungarns und des Orients*, 2: 86-135.

Kramberger-Gorjanovic D. (1883) - Die jungtertiäre Fisch-fauna Kroatiens. 2. Theil. *Beiträge zur Paläontologie Oester-reich-Ungarns und des Orients*, 3: 65-85.

Lanckneus J. & Nolf D. (1979) - Les otolithes des téléos-téens Redoniens de Bretagne (Nèogéne de l'ouest de la France). *Bulletin de l'Institut de Géologie du Bassin d'Aqui-taine*, 25 : 83-109.

Lin C.-H. & Chang C.-W. (2012) - Otolith atlas of Taiwan

fishes. *National Museum of Marine Biology and Aquarium*, 12: 1-415.

Lin C.-H., Girone A. & Nolf D. (2015) - Tortonian fish oto-liths from turbiditic deposits in Northern Italy: Taxo-nomic and stratigraphic significance. *Geobios*, 48: 249-261.

Lin C.-H., Brzobohatý R., Nolf D. & Girone A. (2017) - Tor-tonian teleost otoliths from northern Italy: taxonomic synthesis and stratigraphic significance. *European Journal of Taxonomy*, 322: 1-44.

Loeblich A.R.J. & Tappan H. (1988) - Foraminiferal genera and their classification, Van Nostrand Reinhold Compa-ny, New York: 1-1694.

Lombarte A., Chic Ò., Parisi-Baradad V., Olivella R., Piera J. & García-Ladona E. (2006) - A web-based environment from shape analysis of fish otoliths. The AFORO data-base. *Scientia Marina*, 70: 147-152. http://isis.cmima.csic.es/aforo/index.jsp

Longhurst A.R. (2007) - Ecological geography of the sea. El-sevier Science: 1-560. https://doi.org/10.1016/B978-0-12-455521-1.X5000-1

Lueger J.P. (1981) - Die Landschnecken im Pannon und Pont des Wiener Beckens. I. Systematik. II. Fundorte, Stratigra-phie, Faunenprovinzen. Österreichische Akademie der Wissenschaften, mathematisch-naturwissenschaftliche Klasse, Denkschriften, 120: 1-152.

Lukeneder S., Zuschin M., Harzhauser M. & Mandic O. (2011) - Spatiotemporal signals and palaeoenvironments of en-demic molluscan assemblages in the marine system of the Sarmatian Paratethys. *Acta Palaeontologica Polonica*, 56: 767-784.

Maissuradze L.S. (1971) - Foraminifery sarmata Zapadnoi Gruzii (Foraminifera of the Sarmatian of the Western Georgia). Tbilisi, 120 pp. [in Russian].

Maissuradze L.S. (1980) - K paleobiologicheskoi istorii fora-minifer pozdnego miocena Chernomorsko-Kaspiiskogo basseina (About the paleobionomics history of the Late Miocene of the Black Sea-Caspian basin), *Metsniereba*, Tbilisi, 107 po.

Maissuradze L. & Koiava K. (2011) - Biodiversity of Sarma-tian Foraminifera of the Eastern Paratethys. *Bulletin of the Georgian National Academy of Sciences*, 5: 143-151.

Mikerina T.B. & Pinchuk T.N. (2014) - Distribution and source of dispersed organic matter in the Karaganian-Konki-an-Sarmatian deposits of the Eastern Paraethys. *Geology, Geography and global Energy*, 4: 20-33. [in Russian].

Müller P., Geary D.H. & Magyar I. (2007) - The endemic mol-luscs of the late Miocene Lake Pannon: their origin, evolution, and family-level taxonomy. *Lethaia*, 32: 47-60.

Muratov M.V. & Nevesskaya L.A. (Eds.) (1986) - Stratigraphy of the USSR. Neogene System [Stratigraphiya SSSR. Neogenovaya sistema] Moskva, Semivol. 1, 420 pp. [in Russian].

Murray J.W. (2006) - Ecology and Applications of Benthic For-aminifera. *Cambridge University Press*. 426 p. https://doi.org/10.1017/CBO9780511535529

Nelson J.S., Grande T.C. & Wilson M.V.H. (2016) - Fishes of the world. 5th ed. John Wiley and Sons, Hoboken:

1-707.

Nevesskaya L.A., Bogdanovich A.K., Vyalov O.S., Zhizhchenko B.P., Il'ina L.B. & Nossovskiy, M.F. (1975) - A stage stratigraphic scale of Neogene deposits for the South USSR [Yarusnaya shkala neogenovyih otlozheniy yuga SSSR]. In: Senes, J. (ed), *Proceedings of the VIth Congress of the Regional Committee on Mediterranean Neogene Stratigraphy* (RCMNS), Bratislava I, pp. 267-289.

Nolf D. (1973) - Deuxième note sur les téléostéens des Sables de Lede (Eocène belge). *Bulletin de la Société belge de Géologie, de Paléontologie et d'Hydrologie*, 81: 95-109.

Nolf D. (2013) - The diversity of fish otoliths, past and present. Operational directorate "Earth and History of Life" of the Royal Belgian Institute of Natural Sciences, Brussels, Belgium: 1-581.

Nolf D. (2018) - Otoliths of fishes from the North Sea and the English Channel. Royal Belgian Institute of Natural Sciences: 1-277.

Nolf D. & Brzobohatý R. (2009) - Lower Badenian fish otoliths of the Styrian and Lavanttal basins, with a revision of Weinfurter´s type material. *Annalen des naturhistorischen Museums in Wien*, 111 A: 323-356

Nolf D. & Cavallo O. (1994) - Otolithes de poissons du Pliocène Inférieur de Monticello de Alba (Piemont, Italie). *Rivista Piemontese di Storia Naturale*, 15: 11-40.

Nolf D. & Steurbaut E. (1979) - Les otolithes de téléostéens des faluns sallomaciens d'Orthez et de Sallespisse (Miocène moyen d'Aquitaine méridionale, France). *Palaeontographica* A, 164: 1-23.

Palcu D.V., Tulbure M., Bartol M., Kouwenhoven T.J. & Krijgsman W. (2015) - The Badenian–Sarmatian extinction event in the Carpathian foredeep basin of Romania: paleogeographic changes in the Paratethys domain. *Global and Planetary Change*, 133: 346-358.

Palcu D.V., Golovina L.A., Vernyhorova Y.V., Popov S.V. & Krijgsman W. (2017) - Middle Miocene paleoenvironmental crises in Central Eurasia caused by changes in marine gateway configuration. *Global and Planetary Change*, 158: 57-71.

Palcu D.V., Popov S.V., Golovina L.A., Kuiper K.F., Liu S. & Krijgsman W. (2019) - The shutdown of an anoxic giant: Magnetostratigraphic dating of the end of the Maikop Sea. *Gondwana Research*, 67: 82–100.

Palcu D.V., Patina I.S., Șandric I., Lazarev S., Vasiliev I., Stoica M. & Krijgsman W. (2021) - Late Miocene megalake regressions in Eurasia. *Scientific Reports*, 11:11471.

Papp A. (1951) - Das Pannon des Wiener Beckens. *Mitteilungen der Geologischen Gesellschaft in Wien*, 39-41: 99-193.

Papp A. (1956) - Fazies und Gliederung des Sarmats im Wiener Becken. *Mitteilungen der Geologischen Gesellschaft in Wien*, 47: 1-97.

Paramonova N.P. (1994) - Istoriya sarmatskih i akchagylskih dvustvorchatyh molluskov (History of Sarmatian and Akchagylian Bivalves). *Transactions of the Palaeontological Institute*, 260: 1-212. [in Russian].

Paramonova N.P. & Belokrys L.S. (1972) – Ob obieme sarmatskogo yarusa. (Stratigraphical volume of the Sarmatian). *Bulletin Moskovskogo obchsestva ispytateley prirody,*

otdelenie geologii, 47 (3): 35-46. [in Russian].

Piller W.E. & Harzhauser M. (2005) - The myth of the brackish Sarmatian Sea. *Terra Nova*, 17: 450-455.

Pisera A. (1996) - Miocene reefs of the Paratethys: a review. *SEPM, Concepts in Sedimentology and Paleontology*, 5: 97-104.

Pobedina V.M. (1954) - Iskopaemye otoly ryb miocenovyh otlozheniy Azerbaijana i ih stratigraficheskoe znachenie (Fossil fish otoliths from the Miocene deposits of Azerbaijan and their stratigraphical significance). *Izvestia Akademii Nauk Azerbaidjanskoy SSR*, 10: 23-37. [in Russian].

Pobedina V.M. (1956) - In: Pobedina V.M., Voroshilova A.G., Rybina O.I. & Kuznetsova Z.V. (Eds) - Spravochnik po mikrofaune sredne– i verkhnemiocenovykh otlozhenii Azerbaidjana (Handbook about microfauna middle and upper Miocene deposits of Azerbaijan). *Baku: Azerbaidjanskoe gosudarstvennoe izdatelstvo neftyanoi nauchno-tekhnicheskoy literatury*: 21-179. [in Russian].

Popov S.V., Rögl F., Rozanov A.Y., Steininger F.F., Shcherba I.G. & Kovač M. (Eds.) (2004) - Lithological-paleogeographic maps of Paratethys. 10 maps late Eocene to Pliocene. *Courier Forschungs-Institut Senckenberg*, 250: 1-46.

Popov S.V., Shcherba I.G., Ilyina L.B., Nevesskaya L.A., Paramonova N.P., Khondakarian S.O. & Magyar I. (2006) - Late Miocene to Pliocene palaeogeography of the Paratethys and its relation to the Mediterranean. *Palaeogeography, Palaeoclimatology, Palaeoecology*, 238: 91-106.

Popov S.V., Rostovtseva Y.V., Pinchuk T.N. & Patina I.S. (2019) - Oligocene to Neogene paleogeography an depositional environments of the Euxinian part of Paratethys in Crimean - Caucasian junction. *Marine and Petroleum Geology*, 103: 163–175.

Procházka V.J. (1893) - Das Miozän von Seelowitz in Mähren und dessen Fauna. *Rozpravy* České *Akademie Císaře Františka Josefa pro Vědy, Slovesnost a Umění v Praze*, 2: 65-88.

Radionova E., Golovina L., Filippova N., Trubikhin V., Popov S., Goncharova I., Vernigorova Y. & Pinchuk T. (2012) - Middle- Upper Miocene stratigraphy of the Taman Peninsula, Eastern Paratethys. *Central European Journal of Geosciences* 4(1): 188–204.

Radwańska U. (1992) - Fish otoliths in the middle Miocene (Badenian) deposits of southern Poland. *Acta Geologica Polonica*, 42: 141-328.

Raffi I., Wade B.S. & Pälike H. (2020) - The Neogene Period. In: Gradstein F.M., Ogg J.G., Schmitz M.D. & Ogg G.M. (Eds.) - Geologic Time Scale 2020, Elsevier: 1141-1215.

Reichenbacher B. & Bannikov A.F. (2021) - Diversity of gobioid fishes in the late middle Miocene of northern Moldova, Eastern Paratethys - part I: an extinct clade of *Lesueurigobius* look-alikes. *PalZ*, 96: 67-112 (online 2021, printed 2022).

Reichenbacher B. & Bannikov A.F. (2022) - Diversity of gobioid fishes in the late middle Miocene of northern Moldova, Eastern Paratethys - part II: description of *Moldavigobius helenae* gen. et sp. nov. *PalZ*, https://doi.org/10.1007/s12542-022-3229 00639-1.

Reichenbacher B. & Weidmann M. (1992) - Fisch-Otolithen aus der oligo-/miozänen Molasse der West-Schweiz und

der haute-Savoie (Frankreich). *Stuttgarter Beiträge zur Naturkunde, Serie B (Geologie und Paläontologie)*, 184: 1-83.

Reichenbacher B., Filipescu S. & Miclea A. (2018) - A unique middle Miocene (Sarmatian) fish fauna from coastal deposits in the eastern Pannonian Basin (Romania). *Palaeobiodiversity and Palaeoenvironments*, 99: 177-194.

Rögl F. (1999) - Mediterranean and Paratethys. Facts and hpyotheses of an Oligocene to Miocene paleogeography (short overview). *Geologica Carpathica*, 50: 339-349.

Rosoff D.B. & Corliss B.H. (1992) - An analysis of Recent deep-sea benthic foraminiferal morphotypes from the Norwegian and Greenland seas. *Palaeogeography, Palaeoclirnatology, Palaeoecology*, 91:13-20. https://doi.org/10.1016/0031-0182(92)90028-4

Rückert-Ülkümen N. (1996) - Weitere Beiträge zur Otolithenfauna von Avcılar W Küçükcekmece See (Thrakien, Türkei). *Mitteilungen der Bayerischen Staatssammlung für Paläontologie und historische Geologie*, 36: 117-133.

Rückert-Ülkümen N., Kaya O., & Hottenrott M. (1993) - Neue Beiträge zur Tertiär-Stratigraphie und Otolithenfauna der Umgebung von Istanbul (Küçükçekmece- und Büyükçekmece See), Türkei. *Mitteilungen der Bayerischen Staatssammlung für Paläontologie und historische Geologie*, 33: 51-89.

Sant K., Palcu D.V., Mandic O. & Krijgsman W. (2017) - Changing seas in the Early-Middle Miocene of Central Europe: a Mediterranean approach to Paratethyan stratigraphy. *Terra Nova*, 29: 273-281.

Schubert R.J. (1906) - Die Fischotolithen des österr.-ungar. Tertiärs. III. Macruriden und Beryciden. *Jahrbuch der Kaiserlich-Königlichen Geologischen Reichsanstalt, Wien*, 56: 623-706.

Schubert R.J. (1912) - Die Fischotolithen der ungarischen Tertiärablagerungen. *Mitteilungen aus dem Jahrbuch der Königlichen ungarischen geologischen Reichsanstalt*, 20: 115- 139.

Schultz O. (2013) - Catalogus Fossilium Austriae. Band 3. Pisces. Verlag der Österreichischen Akademie der Wissenschaften, Wien: 1-576.

Schwarzhans W. (1978) - Otolith-morphology and its usage for higher systematical units with special reference to the Myctophiformes s.l. *Mededelingen van de Werkgroep voor Tertiaire en Kwartaire Geologie*, 15: 167-185.

Schwarzhans W. (1994) - Die Fisch-Otolithen aus dem Oberoligzän der Niederrheinischen Bucht. Systematik, Palökologie, Paläobiogeographie, Biostratigraphie und Otolithen-Zonierung. *Geologisches Jahrbuch*, A, 140: 3-248.

Schwarzhans W. (1999) - A comparative morphological treatise of recent and fossil otoliths of the order Pleuronectiformes. *Piscium Catalogus, Otolithi Piscium*, 2: 1-391.

Schwarzhans W. (2007) - The otoliths from the middle Eocene of Osteroden near Bramsche, north-western Germany. *Neues Jahrbuch Geologie und Paläontologie Abhandlungen*, 244: 299-369.

Schwarzhans W. (2008) - Otolithen aus küstennahen Sedimenten des Ober-Oligozän der Niederrheinischen Bucht (Norddeutschland). *Neues Jahrbuch Geologie und Paläontologie Abhandlungen*, 248: 11-44.

Schwarzhans W. (2010) - The otoliths from the Miocene of

the North Sea Basin. Backhuys Publishers, Leiden & Margraf Publishers, Weikersheim, Germany, 352 pp.

Schwarzhans W. (2014) - Otoliths from the middle Miocene (Serravallian) of the Karaman Basin, Turkey. *Cainozoic Research*, 14: 35-69.

Schwarzhans W. (2017) - A review of otoliths collected by W. Weiler from the Badenian of Romania and by B. Strashimirov from Badenian equivalents of Bulgaria. *Cainozoic Research*, 17: 167-191.

Schwarzhans W. (2019) - Reconstruction of the fossil marine fish fauna (Teleostei) from the Eocene to Pleistocene of New Zealand by means of otoliths. *Memorie della Società Italiana di Scienze Naturali e del Museo di Storia Naturale di Milano*, 46: 3-326.

Schwarzhans W. & Carnevale G. (2017) - Otoliths in situ from Sarmatian (middle Miocene) fishes of the Paratethys. Preface: a first attempt to fill the gap between the otolith and skeletal records of teleost fishes. *Swiss Journal of Palaeontology*, 136: 1-6.

Schwarzhans W. & Nielsen S.N. (2021) - Fish otoliths from the early Miocene of Chile: A window into the evolution of marine bony fishes in the Southeast Pacific. *Swiss Journal of Palaeontology*, 140: 1-62.

Schwarzhans W. & Radwańska U. (2022) - A review of lanternfish otoliths (Myctophidae, Teleostei) of the early Badenian (Langhian, middle Miocene) from Bęczyn, southern Poland. *Cainozoic Research*, 22: 9-24.

Schwarzhans W. & Wienrich G. (2009) - Otolithen. In: Wienrich G. (Ed.). Die Fauna des marinen Miozäns von Kevelaer (Niederrhein). Backhuys Publishers, Leiden: 959-1185.

Schwarzhans W., Carnevale G., Bratishko A., Japundžić S. & Bradić K. (2017a) - Otoliths in situ from Sarmatian (middle Miocene) fishes of the Paratethys. Part II: Gadidae and Lotidae. *Swiss Journal of Palaeontology*, 136: 19-43.

Schwarzhans W., Ahnelt H., Carnevale G., Japundžić S., Bradić K. & Bratishko A. (2017b) - Otoliths in situ from Sarmatian (middle Miocene) fishes of the Paratethys. Part III: tales from the cradle of the Ponto-Caspian gobies. *Swiss Journal of Palaeontology*, 136: 45-92.

Schwarzhans W., Carnevale G., Japundžić S. & Bradić-Milinović K. (2017c) - Otoliths in situ from Sarmatian (middle Miocene) fishes of the Paratethys. Part V: Bothidae and Soleidae. *Swiss Journal of Palaeontology*, 136: 109-127.

Schwarzhans W., Agiadi K. & Carnevale G. (2020a) - Late Miocene-Early Pliocene evolution of Mediterranean gobies and their environmental and biogeographic significance. *Rivista Italiana di Paleontologia e Stratigrafia*, 126: 657-723.

Schwarzhans W., Brzobohatý R. & Radwańska U. (2020b) - Goby otoliths from the Badenian (middle Miocene) of the Central Paratethys from the Czech Republic, Slovakia and Poland: a baseline for the evolution of the European Gobiidae (Gobiiformes; Teleostei). *Bolletino della Società Palaeontologica Italiana,* 59: 125-173.

Schwarzhans W., Klots O., Ryabokon, T. & Kovalchuk O. (2022) - A rare window into a back-reef fish community from the Middle Miocene (late Badenian) Medobory

Hills barrier reef in western Ukraine, reconstructed by means of otoliths. *Swiss Journal of Palaeontology*, 141:18: 1-35. https://doi.org/10.1186/s13358-022-00261-3.

Smale M.J., Watson G. & Hecht T. (1995) - Otolith atlas of southern African marine fishes. *J.L.B. Smith Institute of Ichthyology, Ichthyological Monographs*, 1: 1-402.

Steurbaut E. (1984) - Les otolithes de téléostéens de l'Oligo-Miocène d'Aquitaine (Sud-Ouest de la France). *Palaeontographica*, A, 186: 1-162.

Steurbaut E. & Jonet S. (1981) - Revision des otolithes de téléostéens du Miocène Portugais. *Bulletin de la Société belge de Géologie*, 90: 191-229.

Strashimirov B. (1972) - Otolity ot tarkhana na Severoistochna Bulgaria. *Annuaire de l'Ecole Supérieure des Mines et de Geologie*, Sofia 18: 301-313.

Strashimirov B. (1980) - Otolithes du Tchokrakien de la Bulgarie nordorientale. *Geologica Balcanica*, 10: 61-70.

Strashimirov B. (1981a) Otolity ot karagana na Severoistochna Bulgaria. *Palaeontology, Stratigraphy and Lithology*, 14: 19-28.

Strashimirov B. (1981b) - Otolity ot konka na Severoistochna Bulgaria. *Palaeontology, Stratigraphy and Lithology*, 15: 52-65.

Strashimirov B. (1984) - Otolity ot dolnia sarmat na Severnaia Bulgaria. *Palaentology, Stratigraphy and Lithology*, 20: 15-41.

Strashimirov B. (1985) - Otolity ot srednia sarmat na Severnaia Bulgaria. *Annual of the Highest Institute of Mining and Geology Sofia*, 31: 7-20.

Šujan M., Hudáčková N. & Magyar I. (2022) - How to drain a megalake: Comments on a study by Palcu et al. (2021) *Scientific Reports*, 11, Art. Nr.: 11471. https://doi.org/10.31223/X5865V (preprint).

Sun J., Sheykh M., Ahmadi N., Cao M., Zhang Z., Tian S., Sha J., Jian Z., Windley B.F. & Talebian M. (2021) - Permanent closure of the Tethyan Seaway in the northwestern Iranian Plateau driven by cyclic sea-level fluctuations in the Middle Miocene. *Palaeogeography, Palaeoclimatology, Palaeoecology*, 564:110172: 1-18.

Suzin A.V. (1968) - Otoliths. In: Zhizhchenko, B.P. (Ed.). Micropaleontologicheskie metody stratigraficheskih postroeniy v neftegazonosnyh oblastiah (Micropalaeontological methods of stratigraphical research in the oil-and-gas bearing region). Nedra, Moscow: 74-77. [in Russian].

Sytchevskaya E.K. & Prokofiev A.M. (2007) - A dragonet (Perciformes: Callionymidae) from the Middle Miocene of southern Russia. *Voprosy Ikhtiologii,* 47: 750-756.

ter Borgh M., Stoica M., Donselaar M.E., Matenco L. & Krijgsman W. (2014) - Miocene connectivity between the Central and Eastern Paratethys: Constraints from the western Dacian Basin. *Palaeogeography, Palaeoclimatology, Palaeoecology*, 412: 45-67.

Thacker C.E. (2009) - Phylogeny of Gobioidei and placement within Acanthomorpha, with a new classification and investigation of diversification and character evolution. *Copeia*, 2009: 93-104.

Thacker C.E. & Roje D.M. (2011) - Phylogeny of Gobiidae and identification of gobiid lineages. *Systematics and Biodiversity*, 9: 329-347.

Torfstein A. & Steinberg J. (2020) - The Oligo-Miocene closure of the tethys Ocean and evolution of the proto-Mediterranean Sea. *Scientific Reports*, 10:13817: 1-10.

Trabelsi R., Elloumi J., Hamza A., Ayadi N., Zghal I. & Ayadi H. (2017) - Variability of foraminifera associations in seagrass ecosystems in shallow water during winter (Kerkennah – Southern Tunisian coasts). *Journal of the Marine Biological Association of the United Kingdom*, 98 , Special Issue 8: Special Section: European Marine Biology Symposium Papers 2018: 1945-1954. DOI: https://doi.org/10.1017/S0025315417001667

Veis O.B. (1988) - The bryozoans from the Miocene of the Northern Caucasus and the Crimea, Proceedings of the Paleontological Institute, Moscow, Vol. 232, 102 pp. [in Russian].

Vernyhorova Y.V. (2014) – Lito- i biofatsialni osoblyvosti neogenovyh vidkladiv Kerchenskogo pivostrova (Lytho- and biofacies features of the Neogene deposits of the Kerch Peninsula). *Collection of scientic works of the Institute of Geological Sciences NAS of Ukraine*, 7: 126-171. [in Ukrainian].

Vernyhorova Y.V. (2016) - Stratygrafichna shema neogenovyh vidkladiv Krymskogo pivostrova (Stratigraphic scheme for the Neogene deposits of the Crimean Peninsula). *Stratigraphy and Paleontology, Heolohiia ta Rudonosnist Ukrainy*, 2: 59-106. [in Ukrainian].

Vernyhorova Y.V., Fikolina L.A. & Obsharskaya N.N. (2012) - Strukturno-fatsyalnoe raionirovanie neogenovyh otlozheniy Kerchenskogo polyostrova (Structural and facies zonation of the Neogene deposits of the Kerch Peninsula). *Geological Journal*, 3: 74-94. [in Russian].

Weiler W. (1943) - Die Otolithen aus dem Jungtertiär Süd-Rumäniens; 1. Buglow und Sarmat. *Senckenbergiana Lethaea*, 26: 87-115.

Weiler W. (1950) - Die Otolithen aus dem Jung-Tertiär SüdRumäniens, 2. Mittel-Miozän, Torton, Buglow und Sarmat. *Senckenbergiana Lethaea*, 31: 209-258.

Weinfurter E. (1954) - Pisces. In: Papp A. & Thenius E. (Eds.) - Vösendorf - ein Lebensbild aus dem Pannon des Wiener Beckens. *Mitteilungen der Geologischen Gesellschaft in Wien*, 46: 30-41.